Optimising Energy Efficiency and Spectral Efficiency in Multi-Tier Heterogeneous Networks: Performance and Tradeoffs

by

Haris Bin Pervaiz

A thesis submitted in partial fulfillment for the
degree of Doctor of Philosophy

in the

Faculty of Science and Technology
School of Computing and Communications

Declaration of Authorship

I, Haris Bin Pervaiz, declare that this thesis titled, **"Optimising Energy Efficiency and Spectral Efficiency in Multi-Tier Heterogeneous Networks: Performance and Tradeoffs"** and the work presented in it are my own. I confirm that:

- Where I have consulted the published work of others, this is always clearly attributed.
- Where I have quoted from the work of others, the source is always given. With the exception of such quotations, this thesis is entirely my own work.
- I have acknowledged all main sources of help.
- Where the thesis is based on work done by myself jointly with others, I have made clear exactly what was done by others and what I have contributed myself.
- Detailed breakdown of the publications is presented in the first chapter of this thesis.

Signed:

Date:

"If we did all the things we are capable of, we would literally astound ourselves."

Thomas A. Edison

Abstract

The exponential growth in the number of cellular users along with their increasing demand of higher transmission rate and lower power consumption is a dilemma for the design of future generation networks. The spectral efficiency (SE) can be improved by better utilisation of the network resources at the cost of reduction in the energy efficiency (EE) due to the enormous increase in the network power expenditure arising from the densification of the network. One of the possible solutions is to deploy Heterogeneous Networks (HetNets) consisting of several tiers of small cell BSs overlaid within the coverage area of the macrocells. The HetNets can provide better coverage and data rate to the cell edge users in comparison to the macrocells only deployment. One of the key requirements for the next generation networks is to maintain acceptable levels of both EE and SE. In order to tackle these challenges, this thesis focuses on the analysis of the EE, SE and their tradeoff for different scenarios of HetNets.

First, a joint network and user adaptive selection mechanism in two-tier HetNets is proposed to improve the SE using game theory to dynamically re-configure the network while satisfying the user's quality-of-service (QoS) requirements. In this work, the proposed scheme tries to offload the traffic from the heavily loaded small cells to the macrocell. The user can only be admitted to a network which satisfies the call admission control procedures for both the uplink and downlink transmission scheme.

Second, an energy efficient resource allocation scheme is designed for a two-tier HetNets. The proposed scheme uses a low-complexity user association and power allocation algorithm to improve the uplink system EE performance in comparison to the traditional cellular systems. In addition, an opportunistic joint user association and power allocation algorithm is proposed in an uplink transmission scheme of device to device (D2D) enabled HetNets. In this scheme, each user tries to maximise its own Area Spectral Efficiency (ASE) subject to the required Area Energy Efficiency (AEE) requirements. Further, a near-optimal joint user association and power allocation approach is proposed to

investigate the tradeoff between the two conflicting objectives such as achievable throughput and minimising the power consumption in two-tier HetNets for the downlink transmission scheme.

Finally, a multi-objective optimization problem is formulated that jointly maximizes the EE and SE in two-tier HetNets. In this context, a joint user association and power allocation algorithm is proposed to analyse the tradeoff between the achievable EE and SE in two-tier HetNets. The formulated problem is solved using convex optimisation methods to obtain the Pareto-optimal solution for the various network parameters.

Acknowledgements

First of all I would like to thank Allah Almighty for His immense blessings and help throughout the duration of PhD studies. I would also like to sincerely thank my supervisors Professor Qiang Ni and Dr Leila Musavian for their continuous guidance and encouragement throughout the PhD. I would also like to thank my supervisors for their critical reading and language corrections of my manuscripts. Finally, I want to thank my wife Aleena Mohyuddin for her continuous encouragement, support and bearing with me for my negligence towards her during this journey and my parents for their infinite affection, patience and love.

Contents

List of Figures

List of Tables

List of Algorithms

List of Symbols

θ_{ij}	denotes the preference indicator of network j to serve user i
co_{ij}	denotes the connectivity status between user i and network j
σ_{ij}	denotes whether user i lies within the coverage area of network j
λ_{ij}	denotes the quality of wireless link between user i and network j
m_{ij}	denotes the mobility support provided to user i by network j
γ_j	denotes the coverage area of network j
C	denotes the comparison matrix
y	small bold-faced letter defines an eigenvector of a matrix C
ε	defines an eigenvalue of a matrix C
$\varepsilon_{\max}$	defines the largest eigenvalue of a matrix C
I	defines an identity matrix
$c_{i,k}$	denotes the (i,k)-th entry of a matrix C
n_k	denotes the index of attribute k
p	denotes the payment plan
$z_s^{(l)}$	denotes the proportion of users choosing strategy s in service area l
$N^{(l)}$	denotes the total number of users in service area l
$\pi_{i,j}^{(l)}$	denotes the payoff of user i associated with network j in service area l
π_j^{hom}	denotes the homogeneous payoff of network j
$\bar{\pi}^{\text{hom}}$	denotes the average homogeneous payoff
Cap_j^{avail}	denotes the available capacity of network j
Cap_j	denotes the total capacity of network j
β_j^{adj}	denotes the network adjustment factor of network j

R_{ho}	denotes the radius of the Handover threshold
R_{RoI}	denotes the radius of the Region of Interest threshold
ΔD	denotes the considered region for RoI based evolutionary game
pi	denotes the pricing coefficient or respective price per user
m	denotes the index set of the networks
n	denotes the index set of all users
k	denotes the index set of all subcarriers
$a_{m,n}$	denotes the association of user n with network m
$\gamma_{k,n}^{(m)}$	denotes the SNR of user n on subcarrier k associated with network m
$r_{k,n}^{(m)}$	denotes the achievable rate of user n on subcarrier k associated with network m
$p_{k,n}^{(m)}$	denotes the optimal power allocation to user n on subcarrier k associated with network m
R_n	denotes the total achievable rate of user n
$\sigma_{k,n}^{(m)}$	denotes the subcarrier allocation indicator of user n on subcarrier k associated with network
BEE	denotes the backhaul energy efficiency
α	denotes the tradeoff biasing factor
B_k	denotes the bandwidth available to each subcarrier k
N_0	denotes the noise spectral density
m_n	denotes the binary variable to represent the communication mode of user n
$P^{\max}$	denotes the maximum transmission power
$R_n^{\min}$	denotes the minimum rate requirement of user n
η_{EE}	denotes the energy efficiency
η_{AEE}	denotes the area energy efficiency normalised by the total area
η_{SE}	denotes the spectral efficiency
η_{ASE}	denotes the area spectral efficiency
η_n^{req}	denotes the required area energy efficiency threshold
α_{ASE}	denotes the ASE gain rate
α_{AEE}	denotes the AEE loss rate
P_{C}	denotes the circuit power consumption
ω	denotes the different rate fairness levels

For/Dedicated to/To my. . .

Chapter 1

Introduction

In the first section of this chapter, the importance of the energy efficiency challenge in the design of next generation wireless communication systems are discussed. The second section describes the direction and focus of this thesis. The research contributions of this thesis are outlined in the third section. The fourth section describes the outline of this thesis. The final section highlights the author's publication in various conferences and journals during the tenure of his PhD studies.

1.1 Thesis Context

According to one of the recent reports from Cisco [1], the monthly global mobile data traffic is expected to reach 24.3 exabytes by end of 2019, wherein 75% of the total monthly mobile traffic will be video. Almost 80% of the total video based monthly data traffic will originate from indoors. The traditional cellular deployment consisting of macrocell cannot cope with this ever increasing data traffic demands. Dense deployment of macrocells in order to enhance the coverage area and increased number of mobile

subscribers are not feasible due to their high deployment costs [2]. Due to this fact, a paradigm shift is required for the next generation communication networks.

One of the emerging paradigms proposed for the next generation communication networks is the fifth Generation (5G) network to provide 1000 times more capacity along with the data rates in range of 1 Giga bits per second (Gbps), end-to-end delay of 1 milli second (ms) and 100 times less energy consumption in comparison to the current cellular networks [2]. The promising seven enabling technologies for 5G networks are identified as [3] 1) heterogeneous networks (HetNets), 2) device-to-device (D2D) communication, 3) massive multiple-input multiple-output (MIMO), 4) millimeter wave (mmWave) communications technologies, 5) full duplex communication, 6) energy-aware communication and energy harvesting, 7) cloud-based radio access network (C-RAN) and virtualisation of network resources.

One of the promising solutions is HetNets promising solutions include providing a better coverage at the cell edge and higher data rates as enabling technology for the future generation networks. The HetNets include low-power overlaid BSs (or small cells), e.g., microcell, picocells, and femtocells, within the macrocell geographical area, deployed by either the user or the network operator who share the same spectrum with the macrocells [4]. The purpose of HetNet is to allow the user equipments (UEs) to access the small cells that overlap geographical coverage areas even though the UEs are within the macrocell [5]. The deployment of small cells has a great potential to improve the spatial reuse of radio resources and also to enhance the transmit power efficiency [6], and in turn, the network EE.

Device-to-Device (D2D) communication is a promising technique which can be integrated by cellular network providers to fulfil the spectral and energy efficiency requirements for the future 5G wireless networks [7]. D2D communication can significantly improve the resource utilisation due to the hop gain, the proximity gain and the reuse gain. Each promising solution alone is unlikely to meet the QoS and throughput requirements for 5G [2]. One of the promising solution is a hierarchical HetNets in which the above mentioned technologies such as HetNets and D2D can coexist in parallel to improve the network performance.

EE is, in fact, one of the key performance indicators for the next generation wireless communication systems. The motivation behind the EE arises due to the current energy cost payable by operators for running their access networks as a significant factor of their operational expenditures (OPEX). Hence, green networking paradigm, which focuses on the means to reduce the energy consumption in the wireless access networks, has received alot of attention [8]. One of the fundamental system design requirements for the future generation networks, such as the Fifth generation (5G) networks is to jointly optimise contradicting objectives, e.g., to provide reliable coverage with higher SE and lower energy consumption and cost per information transfer requirements [9].

1.2 Objective and Scope of this Thesis

The main objective of this thesis is to analyse the EE , SE and their tradeoff in a two-tier HetNet consisting of a macrocell and pico BSs. The focus of this thesis has been on the design parameters and deployment strategies of HetNets that will allow us to achieve

the required QoS for the next generation networks while maintaining an acceptable EE. In this context, the trade-off between the conflicting objectives of improving the SE and reducing the power consumption in different HetNet deployment scenarios have been addressed. The main objectives of this thesis are outlined as follow:

Chapter 2:

1. To develop an accurate and tractable user centric network selection scheme in a two-tier HetNet.

2. To investigate the impact of proposed user churning selection mechanism subject to the network re-configuration and pricing mechanisms on the achievable SE of a two-tier HetNet.

3. To propose a low complexity dynamic contextual user centric network selection scheme with faster convergence to the near optimum achievable SE.

   Chapter 3:

4. To propose a energy efficient deployment model to improve the achievable EE of two-tier HetNets. The objective of this deployment is to improve the performance of cell edge users by deploying pico BSs at the edge of macrocell coverage area.

5. To investigate the effect of the number of D2D pairs on the performance of both EE and SE, in a traditional macrocell-only network and a HetNet consisting of macrocell and pico BSs.

6. To investigate the effect of pico BSs deployed both randomly and at the cell edge within the macrocell coverage area on the achievable EE.

7. To investigate the achievable EE of the access and backhaul links by incorporating the deployment of pico BSs in areas with poor signal strength from the serving macrocell.

   Chapter 4:

8. To study the interrelationship between the achievable EE and SE of two-tier HetNets

9. To investigate the performance gains in terms of the achievable EE and SE in the HetNets consisting of a macrocell and pico BSs in comparison to a traditional macrocell only network.

10. To investigate the effect of the densification of pico BSs on the achievable EE and SE of the two-tier HetNets.

11. To obtain the optimum number of pico BSs that maximises achievable EE and SE for the two-tier HetNets

1.3 Thesis Contributions

The open challenges regarding user association and power allocation mechanisms in multi-tier HetNets are highlighted, which sheds lights on the research direction. The contributions of the thesis are summarised as follows:

In chapter 2, a joint network and user adaptive selection mechanism is proposed in two-tier HetNets to maximise the SE using game theory to dynamically re-configure the network while satisfying the user's QoS requirements. The network selection problem

is formulated using evolutionary game theory where the multi criteria decision making (MCDM) mechanisms are utilised to define the utility function. The formulated game is solved using replicator dynamics and an evolutionary equilibrium is considered as an optimal solution where no user is willing to deviate from its chosen strategy. In addition, an evolutionary game with the reduced complexity is also developed which achieves similar system performance with better computational efficiency in comparison to the previously proposed approach.

In chapter 3, an energy efficient resource allocation scheme is designed for two-tier HetNets. In this proposed scheme, a low-complexity user association and power allocation algorithm is proposed to improve the uplink system EE performance in comparison to the traditional cellular systems. In addition, an opportunistic joint user association and power allocation algorithm is proposed in an uplink transmission scheme of device to device (D2D) enabled HetNets in which each user tries to maximise its own Area Spectral Efficiency (ASE) subject to the required Area Energy Efficiency (AEE) requirements. In order to address the fairness issues among the users, a near-optimal joint user association and power allocation approach is proposed for the downlink transmission scheme. In this proposed approach, a multi objective optimisation problem is formulated to investigate the tradeoff between the two conflicting objectives such as achievable throughput and minimising the power consumption in two-tier HetNets for different weighting coefficients and fairness levels.

In chapter 4, a multi-objective optimization problem using weighted sum method is formulated to jointly maximize the achievable EE and SE in two-tier HetNets. In this

context, a joint user association and power allocation algorithm is proposed to achieve the tradeoff between the achievable EE and SE. The formulated problem is solved using convex optimisation methods to obtain the Pareto-optimal solution for the different network parameters.

1.4 Thesis Outline

This thesis is organized into 5 chapters.

Chapter 1 provides an introduction to the thesis and presents the motivation for the proposed research.

Chapter 2 describes the evolutionary game theoretic approach to model the network selection from both user's and network's perspective.

Chapter 3 proposes different energy efficient resource allocation schemes are proposed for multi-tier HetNets.

Chapter 4 investigates the EE-SE tradeoff as a multi-objective optimisation problem in two-tier HetNets.

Chapter 5 concludes the thesis and also provides possibilities for future work.

1.5 Author's Publication

Many of the results presented in the thesis are based on the following papers in various journals and conferences.

Journal Papers

1. **Haris Pervaiz**, Leila Musavian, Qiang Ni and Zhiguo Ding, "Energy and Spectrum

Efficient Transmission Techniques Under QoS Constraints Toward Green Heterogeneous Networks," in IEEE Access Special Section on Ultra-Dense Cellular Networks, vol.3, pp.1655-1671, Sept. 2015

2. **Haris Pervaiz**, Qiang Ni and Charilaos C Zarakovitis, " User adaptive QoS aware selection method for cooperative heterogeneous wireless systems: A dynamic contextual approach", in Elsevier Journal on Future Generation Computer Systems, Vol. 39, Pages:75-87, Oct. 2014. [Impact Factor: 2.64]

Conference Papers

1. Hamnah Munir, Syed Ali Hassan, **Haris Pervaiz** and Qiang Ni, "A Game Theoretical Network-Assisted User-Centric Design for Resource Allocation in HetNets ", accepted in 83rd IEEE Vehicular Technology Conference (VTC2016-Spring)-First IEEE International Workshop on User-Centric Networking for 5G and Beyond, Nanjing, China, 15-18th May 2016.

2. **Haris Pervaiz**, Zhengyu Song, Leila Musavian, Qiang Ni and Xiaohu Ge, "Throughput and Backhaul Energy Efficiency Analysis in two-tier HetNets: A Multi-Objective Approach", 20th IEEE International Workshop on Computer Aided Modelling and Design of Communication Links and Networks (CAMAD 2015), Guildford, UK, 07th-09th Sept. 2015.

3. **Haris Pervaiz**, Leila Musavian and Qiang Ni, "Area Energy and Area Spectrum Efficiency Trade-off in 5G Heterogeneous Networks", IEEE ICC 2015- Workshop on 5G and Beyond, London, UK, 08th-12th June 2015.

4. **Haris Pervaiz**, Leila Musavian and Qiang Ni, "Energy and Spectrum Efficiency Trade-off for Green Small Cell Networks", IEEE International Conference on Communications (ICC 2015), London, UK, 08th-12th June 2015.

5. **Haris Pervaiz**, Leila Musavian and Qiang Ni, "Joint User Association and Energy-Efficient Resource Allocation with Minimum-Rate Constraints in Two-Tier HetNets", 24th IEEE International Symposium on Personal Indoor and Mobile Radio Communications (PIMRC), London, UK, 08th-11th September 2013.

6. **Haris Pervaiz** and Qiang Ni, "User Preferences-Adaptive Dynamic Network Selection Approach in Cooperative Wireless Networks: A Game Theoretic Approach", 11th IEEE International Conference on Trust, Security and Privacy in Computing and Communications (TrustCom), Liverpool, UK, 25th-27th June 2012.

Chapter 2

User Centric Game Theoretic based Network Selection in Cooperative 5G Heterogeneous Networks[1]

This chapter proposes an adaptive realistic mechanism for joint network and user selection in cooperative wireless networks. We present a novel utility optimization method to incorporate the quality-of-service (QoS) dynamics of the available networks along with heterogeneous attributes of each user. The joint network and user selection method is modelled by an evolutionary game theoretical approach by combining both self-control of users' preferences and self-adjustment of networks' parameters. The replicator dynamic is then solved to seek an optimal stable solution. The simulation results demonstrate that the inverse cumulative ranking scheme significantly improves the overall QoS

[1]The work presented in this chapter has been published in Elsevier Journal on Future Generation Computer Systems, Vol. 39, Pages:75-87, Oct. 2014 [Impact Factor: 2.64] and a shorter version has been published in 11th IEEE International Conference on Trust, Security and Privacy in Computing and Communications (TrustCom) held at Liverpool, UK in June 2012.

performance and system parameters as compared to current available solutions in literatures, e.g., [10–12]. The simulation results also show that by incorporating the Region of Interest (RoI) scheme, the complexity of the evolutionary game, with or without network re-configuration, can be reduced by 23% and 58%, respectively.

2.1 Related Work

A key role of resource management in wireless networks is to provide the highest possible measures of QoS exploitation according to the users' requirements while maintaining the high utilization of network resources. A major challenge arising nowadays is that multiple networks coexist and are to be integrated with different properties, e.g., coverage area, mobility support, QoS and price [13]. In such cases, the overall system is heterogeneous by its nature. Such heterogeneity requires that the integration of various access technologies is to be coordinated by effective network selection algorithms. However, existing network selection solutions present pros and cons regarding their performances on various issues, e.g., optimality, complexity and convergence. Some network selection algorithms for integrated Wireless Local Area Networks (WLAN) and cellular network environments are presented in [14–16] . Specifically [15] proposes a methodology that combines the Analytic Hierarchy Process (AHP) and the Grey Relational Analysis (GRA) to compare networks on an end-to-end QoS level. Additionally, [16] provides an example about how these methods can be applied and combined.

Another interesting topic in this research direction is to utilize evolutionary game theory in cognitive radios. The idea is to allocate users between different available primary

networks and to optimally select spare spectrum for secondary users. The corresponding network selection issue is modelled in [10] using a payoff function combining both linear pricing mechanism and allocated bandwidth to each user. Authors use replicator dynamics to identify whether it is profitable for a user to change network and use random selection approaches to churn the users among different systems. On the other hand, [11] considers a system with multiple access points, where each mobile user chooses the most efficient access point according to its requirements. In this case, a continuous-time Markov chain model is developed to represent the arrival/departure processes as well as the rational/irrational churning behaviours of users. By introducing an evolutionary equilibrium solution, [11] investigates cooperative and non-cooperative pricing schemes that aim at maximising the individual and total revenue of users and service providers, respectively. Furthermore, authors in [12] consider incomplete information exchange between users to model the network selection problem as a Bayesian game. The optimal solution is then given by a Bayesian Nash equilibrium mapped with the equilibrium distribution of the aggregate dynamics. The study in [17] introduces the Y-Comm interworking architecture; a layered approach that supports both reactive and proactive handovers. Y-Comm framework uses a Stream Bundle Management layer [18] to handle downward QoS residing in the QoS plane of a mobile node. The layer collects context information from the network, client and application domains to make intelligent choices in network selection and QoS management.

The task of establishing trust and reputation becomes more challenging when the nodes

are mobile. An in-depth information about trust and reputation as well as their application in Wireless Sensor Networks (WSN) is presented in [19] which also describes the components required to build Trust and Reputation Monitoring (TRM) systems. Other related approaches on joint energy-efficient and QoS issues for heterogeneous networks can be found in [20–23]

In most of the existing dynamic network selection schemes [10–12], when utilising evolutionary game theory, all users lying within a geographic area are treated the same, regardless of their locations and the offered QoS levels. This do not comply with the realistic wireless environment. In contrast to the existing approaches, we propose a novel joint network and user selection approach modelling realistic cooperative wireless environments to search for evolutionary-equilibrium-driven optimal solutions. In this work, the initial partition is computed using the AHP-based utility function in comparison to the randomly chosen values which is considered in most of the current literature.

2.2 Chapter Organisation

The rest of this chapter is organized as follows. Section 2.3 describes the system model. Section 2.4 describes the user preference model. Section 2.5 presents the formulation of joint network and user selection based evolutionary game. Section 2.6 explains our proposed iterative methods to find an optimal solution to the network selection problem modelled as an evolutionary game. Section 2.7 presents the simulation results. Section 2.8 concludes the chapter.

2.3 System Model

We consider a heterogeneous wireless access environment consisting of a macrocell overlaid with a small cell (e.g., pico BS) as shown in Fig. 2.1. The coverage area of the macro-cell is the service area (1) and (2), and that of small cell is the service area (1). The interaction area, that is, the service area (1), is the region where Network A is completely covered by Network B, and is the main focus of this work. In this setting, Network A is a small cell network that lies within the geographic region of a macro-cell, i.e., Network B. This work assumes that the channel is ideal (no fading is assumed) and that the only loss is due to the propagation.

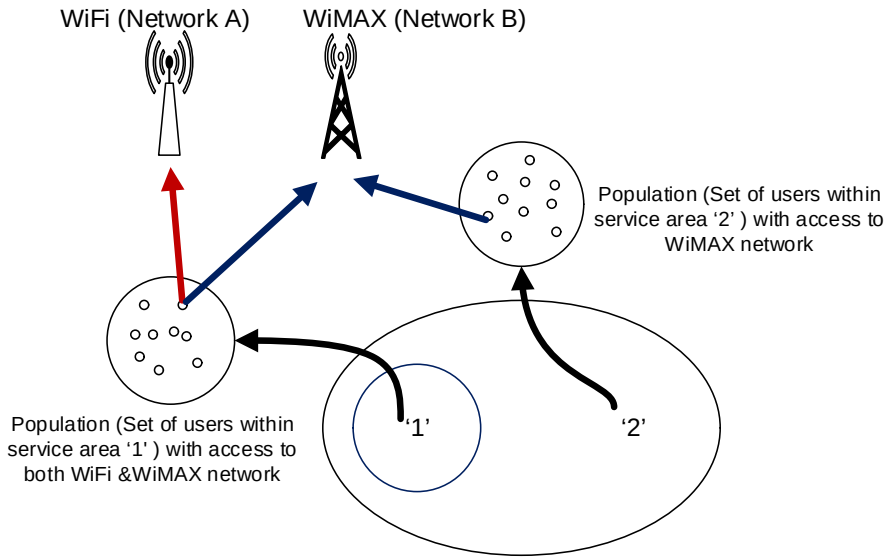

FIGURE 2.1: System Model of Cooperating Heterogeneous Wireless Networks

The handovers as classified as upward or downward. Upward handovers are considered for users that move from a small coverage and high bandwidth network to a large coverage and low bandwidth network. Correspondingly, downward handovers apply to users that move from a large coverage and low bandwidth network to a small coverage and high

bandwidth network. In other words, the users of Network B coming into Network A's range perform alternative downward handovers, while users of Network A coming into Network B's range perform upward handovers.

In this Section, we introduce a set of network selection terms defining the concept of coverage area as the region where signals from an Access Point (AP), or a Base station (BS), can be detected. The signals are assumed unreliable when users move on the boundary points of the coverage area. Another assumption is that signals cannot be detected beyond the coverage area.

In order to reduce the number of handovers, we define two thresholds; the handover threshold represented by a circle with the corresponding radius R_{ho} and the Remaining Time in Network (RTiN) threshold represented by T_{RTiN}, which is dependent on the velocity of the user. If T_{RTiN} is larger or equal than the RTiN threshold for pedestrian users, i.e., 20 secs, then the handover is completed before the handover threshold boundary is reached. This indicates that the mobile users who move with high speed need to initiate the handover process early. Later, we will incorporate a straightforward mathematical handover reduction technique along with the game theoretical network selection mechanisms to derive an intelligent and adaptive decision making process.

2.3.1 Mathematical Notations

Each network j has an associated capacity Cap_j which shows the maximum number of users that network j can serve. From the network selection and handover perspective, it is an optimal strategy to serve the users with no mobility by the pico BS. It can provide better QoS due to the smaller coverage area; on the other hand, mobile will be better

off to be served by a macrocell so that we can avoid frequent handovers. Following this concept, we define θ_{ij} as the preference variable to indicate the degree of preference that a network j would prefer to serve user i. For example, the static users are preferred by pico BS than macrocell and this relationship is represented by $\theta_{ij}^{\text{static}}$ such that $x_j^{\text{sta}} > y_j^{\text{sta}}$ so $x_j^{\text{sta}} + y_j^{\text{sta}} = 1$ as follows:

$$\theta_{ij}^{\text{static}} = \begin{cases} x_j^{\text{sta}}, \text{ if } j \text{ is a picoBS.} \\ y_j^{\text{sta}}, \text{ if } j \text{ is a macrocell.} \end{cases} \tag{2.1a}$$

On the other hand, pedestrian users are preferred by macrocells more than pico BSs and are represented by $\theta_{ij}^{\text{pedestrian}}$ such that $x_j^{\text{ped}} > y_j^{\text{ped}}$ so $x_j^{\text{ped}} + y_j^{\text{ped}} = 1$ as follows:

$$\theta_{ij}^{\text{pedestrian}} = \begin{cases} x_j^{\text{ped}}, \text{ if } j \text{ is a picoBS.} \\ y_j^{\text{ped}}, \text{ if } j \text{ is a macrocell.} \end{cases} \tag{2.1b}$$

Let us also define $co_{ij} \in \{0, 1\}$ that shows the status of connection between user i and network j, i.e.,

$$co_{ij} = \begin{cases} 1, & \text{if user } i \text{ is connected to network } j, \\ 0, & \text{otherwise.} \end{cases} \tag{2.1c}$$

The status of connectivity is also defined in terms of the coverage area with $\sigma_{ij} \in \{0, 1\}$ according to

$$\sigma_{ij} = \begin{cases} 1, & \text{if user } i \in \text{coverage of network } j, \\ 0, & \text{otherwise.} \end{cases} \tag{2.1d}$$

Another important considered parameter for the optimal decision is the quality of the wireless link λ_{ij} represented in terms of the offered bit rate by network j b_{ij}, i.e.,

$$\lambda_{ij} = \begin{cases} \sigma_{ij} \times b_{ij} > 0, & \text{if } b_{ij} \geq b_k^{req}, \\ 0, & \text{otherwise,} \end{cases} \tag{2.1e}$$

where b_k^{req} denotes the minimum required bit rate dependent on the application type k of

any user. In addition, the coverage area of network j is denoted with γ_j and the distance between user i and the BS or AP of the network j is defined by d_{ij}. Finally, the mobility support is denoted by m_{ij} which can be formulated as

$$m_{ij} = \begin{cases} 1 - \frac{d_{ij}}{\gamma_j}, & \text{if } d_{ij} < \gamma_j. \\ 0, & \text{otherwise.} \end{cases} \tag{2.1f}$$

2.3.2 Problem Formulation

This Subsection describes the proposed network selection problem formulated as a Multi-Criteria Decision Making (MCDM) problem [24]. AHP is a structured and efficient mathematical technique to analyze and solve complex decision problems with multiple criteria. It decomposes a decision problem into three types of elements; the goal, the n attributes and the v alternatives. It then chooses the best alternative by measuring the weight of each alternative against the attributes and ultimately the goal. The element "goal" is introduced to select an optimal network. The n attributes i.e., n=4, are price (denoted by n_1), reliability (denoted by n_2), offered bit rate (denoted by n_3) and mobility support (denoted by n_4). The v alternatives are the macrocell or pico BS available to the users i.e., v=2. The optimal selection hierarchy for our proposed scheme is demonstrated in Fig. 2.2.

Fig. 2.3 illustrates the three main stages of our proposed scheme: the formulation of network selection (steps 1-3), the user model (steps 4-5), and the network model (steps 6-7), where d = 1, 2..., 7 stands for the step number. In this work, AHP is used to calculate the relative weights for each attribute. It is worthwhile to mention that deleting the alternatives might change the ranking of the remaining alternatives and lead to undesired

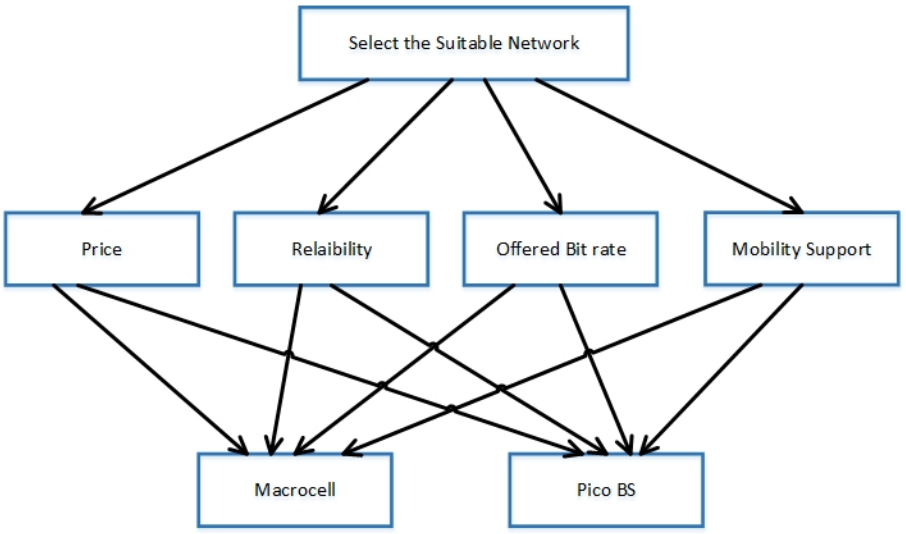

FIGURE 2.2: Network Selection Hierarchy

outcomes. This is commonly referred to rank reversal problem[ref]. In this work, the rank preservation is not enforced on the alternatives.

2.4 User Preference Model

Each user expresses its preferences for the following attributes: reliability, offered bit rate, price and mobility support. Users that request voice applications are classified into four types of payment plans: pay as you go, pay monthly, business and default. In default payment plan, the user gives equal importance to all the attributes. In this Section, the user preference model consisting of three steps are detailed in the following Subsections 2.5.1-2.5.3.

2.4.1 Defining User's Preferences

To meet the specific needs of different types of user profiles, the preference model includes a set of pre-defined payment plans p as shown in Table 2.I. Each attribute is

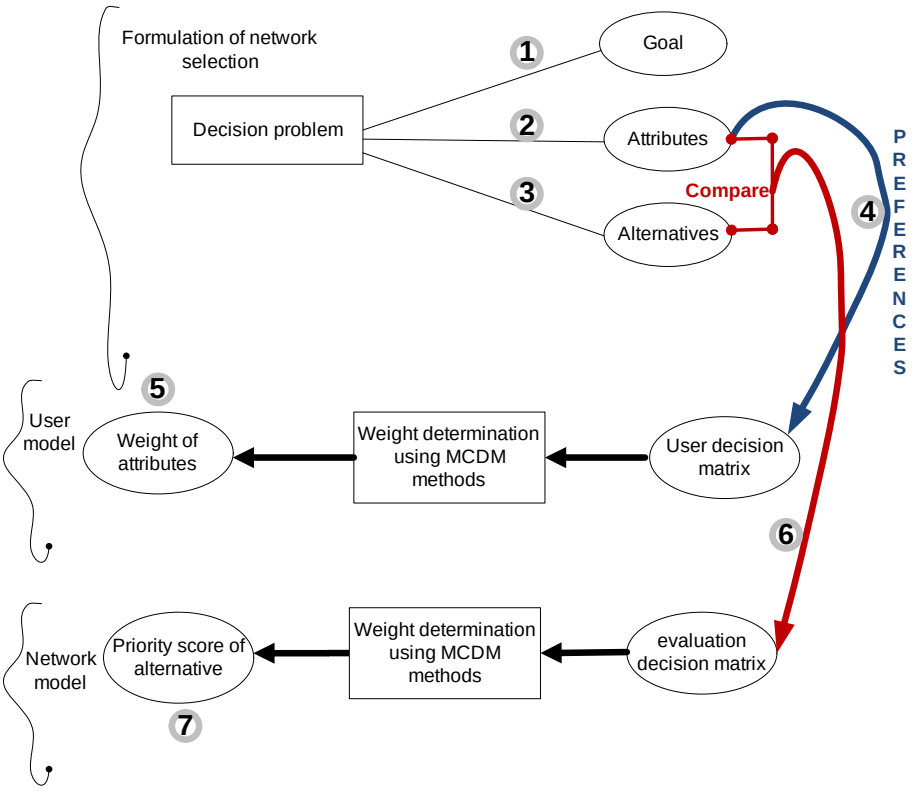

FIGURE 2.3: Main Stages of our Proposed Network Selection Model

ordered according to its relative importance for the goals of each user payment plan as demonstrated in Table 2.II.

TABLE 2.I: User Payment Plan Goals

User Profile	**Defining Objective**
Pay as You Go	Low price, acceptable QoS
Pay Monthly	Good QoS, Fixed price
Business	Excellent QoS, price within budget

Based on the order of attributes for voice application with a particular payment plan, the most preferred choice is assigned by a lowest score of scale '1', while the least preferred choice is assigned by a highest score of scale '9'. The scores are equally spaced integers

TABLE 2.II: Order of Network Attributes for Each Plan

User profile	**Order of Network Attributes**
Pay-as-You-Go	Price; Reliability; Bit rate; Mobility support
Pay-Monthly	Reliability; Bit rate; Mobility support; Price
Business	Bit rate; Price; Reliability; Mobility support

with the space gap defined as [25]

$$G = \frac{S_h - S_l}{N_c},$$

where N_c is the number of attributes and S_h, S_l denote the highest and the lowest possible scores i.e., 9 and 1, respectively. In other words, G represents the numeric space gap between two subsequent scores and it is rounded to the next integer, e.g., when $N_c = 3$, $S_h = 9$ and $S_l = 1$ give $G = \frac{9-1}{3} = 2.666 \approx 3$.

Throughout this chapter, the scores of attributes of each user payment plan for voice application are shown in Table 2.III in order to provide examples for our model's dynamics.

TABLE 2.III: Attribute Scores per Payment Plan for Voice Application

Score	**Pay as you go**	**Pay Monthly**	**Business**
1	Price	Reliability	Bit rate
3	Reliability	Bit rate	Price
5	Bit rate	Mobility support	Reliability
7	Mobility support	Price	Mobility support

2.4.2 Deriving Pair-Wise Comparison Matrix

In the second step, we build a matrix $C_{\mathrm{n}\times\mathrm{n}}$ for pair-wise comparisons to calculate the weights of the considered n attributes and v alternatives. Let C be n×n square matrix, its eigenvalue equation is given as:

$$C\mathbf{y} = \varepsilon\mathbf{y}, \tag{2.2}$$

where $\boldsymbol{y}$ is a non-zero vector called eigenvector and ε is an Eigenvalue of C. The vector $\boldsymbol{y}$ contains the weight of each attribute. The above relation can also be written as

$$(C - \varepsilon I)\,\mathbf{y} = 0, \tag{2.3}$$

where I *is* the $n \times n$ identity matrix. In order for a non-zero vector $\mathbf{y}$ to satisfy the above relation, $C - \varepsilon I$ must not be invertible. The determinant of $C - \varepsilon I$ must be equal to 0. For this reason, the lower triangular elements of $C_{n\times n}$ comparison matrix will be the reciprocal of the upper triangular elements.

Pair-wise comparisons describe the relative importance among the n attributes. As the attribute cannot be compared with itself, all the diagonal elements of the comparison matrix should be equal to 1. The relative importance of each attribute can be decided by comparing each attribute with all others using the aforementioned 1 to 9 score scales. For example, If $s_{ip}(n_1)$ and $s_{ip}(n_2)$ represent the scores of attributes n_1 and n_2 of user i for the payment plan p, respectively, then each user can perform pair-wise comparisons by

computing the relative score $c_{ip}(n_1,n_2)$ as follows:

$$c_{ip}(n_1,n_2)=\left(1-\frac{s_{ip}(n_1)}{s_{ip}(n_2)}\right)\times 10\ ,\ s_{ip}(n_1)< s_{ip}(n_2), \tag{2.4}$$

$$\frac{1}{c_{ip}(n_1,n_2)}=\left(1-\frac{s_{ip}(n_2)}{s_{ip}(n_1)}\right)\times 10\ ,\ s_{ip}(n_1)>s_{ip}(n_2), \tag{2.5}$$

$$c_{ip}(n_1,n_2)=1\ ,\ s_{ip}(n_1)=s_{ip}(n_2). \tag{2.6}$$

Based on the scores of four considered attributes for each payment plan p as mentioned in Table 2.III, the relative score between two attributes can be computed by using equations (2.4), (2.5) and (2.6). In total, four different payment plans are considered which in result require four comparison matrices, i.e.,$C^{v,payg}$, $C^{v,payM}$, $C^{v,Business}$ and$C^{v,Default}$. As the constructing method is the same for each matrix, for brevity the computation of the comparison matrix $C^{v,payg}$ for the pay-as-you-go plan (denoted by payg) with voice applications is only shown. All the diagonal elements of the matrix $C^{v,payg}$ equal to 1, with its upper triangular elements to be calculated as

$$c_{ipayg}(n_1,n_2)=\left(1-\frac{1}{3}\right)\times 10=\frac{20}{3}\approx 7,\quad c_{ipayg}(n_1,n_3)=\left(1-\frac{1}{5}\right)\times 10=8,$$

$$c_{ipayg}(n_1,n_4)=\left(1-\frac{1}{7}\right)\times 10=\frac{60}{7}\approx 9,\quad c_{ipayg}(n_2,n_3)=\left(1-\frac{3}{5}\right)\times 10=4,$$

$$c_{ipayg}(n_2,n_4)=\left(1-\frac{3}{7}\right)\times 10=\frac{40}{7}\approx 6,\quad c_{ipayg}(n_3,n_4)=\left(1-\frac{5}{7}\right)\times 10\approx 3,$$

Its lower triangular elements are reciprocal of its upper triangular elements, i.e.,

$$c_{ipayg}(n_2,n_1)=\frac{1}{c_{ipayg}(n_1,n_2)}=\frac{1}{7}\ ,\ c_{ipayg}(n_3,n_1)=\frac{1}{c_{ipayg}(n_1,n_3)}=\frac{1}{8},$$

$$c_{ipayg}(n_4,n_1)=\frac{1}{c_{ipayg}(n_1,n_4)}=\frac{1}{9}\ ,\ c_{ipayg}(n_3,n_2)=\frac{1}{c_{ipayg}(n_2,n_3)}=\frac{1}{4},$$

$$c_{ipayg}(n_4,n_2)=\frac{1}{c_{ipayg}(n_2,n_4)}=\frac{1}{6},\ c_{ipayg}(n_4,n_3)=\frac{1}{c_{ipayg}(n_3,n_4)}=\frac{1}{3},$$

Consequently, $C^{v,payg}$ is defined as

$$C^{v,payg}=\begin{bmatrix} 1 & c_{ipayg}(n_1,n_2) & c_{ipayg}(n_1,n_3) & c_{ipayg}(n_1,n_4) \\ c_{ipayg}(n_2,n_1) & 1 & c_{ipayg}(n_2,n_3) & c_{ipayg}(n_2,n_4) \\ c_{ipayg}(n_3,n_1) & c_{ipayg}(n_3,n_2) & 1 & c_{ipayg}(n_3,n_4) \\ c_{ipayg}(n_4,n_1) & c_{ipayg}(n_4,n_2) & c_{ipayg}(n_4,n_3) & 1 \end{bmatrix}=$$

$$\begin{bmatrix} 1 & 7 & 8 & 9 \\ \frac{1}{7} & 1 & 4 & 6 \\ \frac{1}{8} & \frac{1}{4} & 1 & 3 \\ \frac{1}{9} & \frac{1}{6} & \frac{1}{3} & 1 \end{bmatrix}. \tag{2.7}$$

A matrix C is said to be consistent if every element of the matrix satisfies the constraints, $c_{ij}\times c_{ji}=1$ and $c_{ik}\times c_{kj}=c_{ij}$. As the users preferences are based on random judgements, the comparison matrices are often inconsistent. The judgement errors in the users

preferences can be determined by a Consistency Ratio (CR) according to:

$$\mathrm{CR} = \frac{\mathrm{CI}}{\mathrm{RI}} = \frac{(\varepsilon_{\max} - n)}{(n-1) \times \mathrm{RI}}, \tag{2.8}$$

where $\varepsilon_{\max}$ is the largest Eigen value of comparison matrix C, n is the size of comparison matrix C and RI values are shown in Table 2.IV. The errors in judgements of users preferences are considered tolerable when $\mathrm{CR} \leq 0.1$ otherwise, the pairwise comparisons need to be adjusted.

TABLE 2.IV: Consistency Index (CI)

n	1.2	3	4	5	6	7	8	9	$\cdots$
Random Consistency Index(RI)	0	0.58	0.9	1.12	1.24	1.32	1.41	1.45	$\cdots$

2.4.3 Computing Corresponding Weights for Each Attribute

As mentioned in Section 2.4.2, the variable n represents the number of attributes, i.e., n=4, while $n_k \in \{n_1, n_2, n_3, n_4\}$ represent the index of each attribute, i.e. price, reliability, bit rate and mobility support, respectively. We will continue our modeling by computing the weight $\mathrm{w_{ip}}(n_k)$ of the n_k attributes for each user i that belong to payment plan p through applying the geometric mean method [26], [27]. More precisely, we will calculate the k^{th} element of eigenvector $\overline{\mathrm{w}}_{\mathrm{ip}}$ denoted by $\overline{\mathrm{w}}_{\mathrm{ip}}(n_k)$ of attribute n_k using the relative scores as

$$\overline{\mathrm{w}}_{\mathrm{ip}}(\mathrm{n_k}) = \sqrt[\mathrm{n}]{c_{ip}(n_k, n_1) \times c_{ip}(n_k, n_2) \times c_{ip}(n_k, n_3) \times c_{ip}(n_k, n_4)}, \; n_k \in \{n_1, n_2, n_3, n_4\} \tag{2.9}$$

Upon normalization of the $\overline{\mathrm{w}}_{\mathrm{ip}}(n_k)$ for each of the n_k attributes, we determine the corresponding weight $\mathrm{w}_{\mathrm{ip}}(n_k)$ as:

$$w_{ip}(n_k) = \frac{\overline{w}_{ip}(n_k)}{\sum_{n_k=n_1}^{n_4} \overline{w}_{ip}(n_k)} \quad n_k \in \{n_1, n_2, n_3, n_4\} \tag{2.10}$$

2.5 Proposed Evolutionary Game Theoretic Network Selection Framework

In this Section, we describe the formulation of evolutionary game to model the dynamic behaviour of the joint network and user selection problem. The replicator dynamics are utilised to capture the dynamics of strategy adaptation subject to the user's diverse preferences. The evolutionary equilibrium is considered to be the solution of the evolutionary game. A distributed user centric network assisted selection mechanism is proposed on the replicator dynamics. The optimal and stable solution is achieved by obtaining the evolutionary equilibrium of the replicator dynamics.

2.5.1 Formulation of Evolutionary Game

Some fundamental notations of evolutionary game theory are detailed as follow:

- As shown in Fig. 2.1, any user lying within the service area (1) and (2) is a player of the game.
- The strategy available to each player, i.e., a potential user, within the service area (1) is to choose a suitable network. Accordingly, the strategy set can be denoted by $S = \left\{\text{macrocell}, \text{pico BS}\right\}$ which corresponds to the selection of macrocell and

pico BS, respectively.

- The set of players which have same strategy set S constitutes the population in an evolutionary equilibrium. As shown in Fig. 2.1, all the users lying within service area (1) constitute one population whereas all the users lying within the service area (2) constitute another population.
- The number of users (or players) choosing the strategy $s \in S$ in population (or service area) l is denoted by $N_s^{(l)}$. The partition (or population share) of strategy s in population l can be then computed as $z_s^{(l)} = \dfrac{N_s^{(l)}}{N^{(l)}}$ where $z_s^{(l)} \in \big[0,1\big]$.
- The partition for all two available strategies within the population l constitute the population state denoted by a vector $z^{(l)} = \big[z_{macrocell}^{(l)}\ z_{picoBS}^{(l)}\big]^T$ such that $z_{macrocell}^{(l)} + z_{picoBS}^{(l)} = 1$.
- The payoff measures the satisfaction level of a user selecting a strategy s given the population state $z^{(l)}$. The payoff utility function is defined considering the strategies of all users within the same population as well as the offered QoS to the users by the network in terms of the network modulation scheme, load and available spectrum. More details can be found in Section 2.5.3.

The assumptions considered in our evolutionary game are as follow:

- Users have no influence on the decision of other users and choose their strategy independently.
- The rational behaviour of a user is to choose the wireless network with the highest payoff.

- Upward handovers is only considered i.e. churning of users from pico BS to macro-cell.
- As seen from Fig. 2.1, users can be grouped into two populations. Users within the same population have similar behavior. Without loss of generality, from now onwards, we will focus on the population of users lying within the service area (1) and the same analysis can be applied to the population of users lying within the service area (2).
- The proposed evolutionary game is distributed in nature and the average payoff can be calculated by the network itself and broadcast back periodically to all potential users as shown below:

$$\overline{\pi}^{hom}(\mathrm{N}^{(1)}) = \left(z^{(1)}_{picoBS} \times \pi^{\mathrm{hom}}_{\mathrm{picoBS}}\left(\mathrm{N}^{(1)}\right) + z^{(1)}_{macrocell} \times \pi^{\mathrm{hom}}_{\mathrm{macrocell}}\left(\mathrm{N}^{(1)}\right)\right)$$

- The evolutionary equilibrium is a solution or Evolutionary Stable Strategy (ESS)[2] to an evolutionary game and is defined as the stable fixed point of replicator dynamics (defined in (2.17)) such that the population state will not change. Hence, the rate of strategy adaptation will be zero, formulated as $\dot{z}^{(1)}_{\mathrm{j}} = 0 \quad \forall j \in v$.
- Once the Evolutionary equilibrium is achieved, no user will be willing to change its strategy since its payoff is equal to the average payoff of the population $\pi^{\mathrm{hom}}_{\mathrm{j}}\left(\mathrm{N}^{(1)}\right) = \overline{\pi}^{hom}(\mathrm{N}^{(1)}) \quad \forall j \in v$.

[2]It is also Nash Equilibrium due to it being best response to itself and it provides a strong refinement of NE

2.5.2 Adaptive vs Non-Adaptive User Preferences Model

To consider accurate system conditions, users' preferences can be classified as either *non-adaptive* or *adaptive*. For example, in the non-adaptive case, all users with a pay-as-you-go payment plan who requesting voice application will have identical preferences. On the other hand, in the adaptive approach, all users with a pay-as-you-go payment plan requesting voice application, can have different preferences. In reality, even though different users may request the same application type, they often have different preferences. Considering such pragmatic conditions, we will carry out the user survey to determine the preferences of users that request voice application with a particular payment plan for the n attributes. In our user adaptive approach, the relative scores for the n attributes are given by user feedbacks utilising the conducted user survey and constituting the comparison matrices $C^{v,payg}$, $C^{v,payM}$, $C^{v,Business}$ and $C^{v,Default}$. The examples of user profiles for both non-adaptive and adaptive approaches for the pay-as-you-go payment plan are shown in Table 2.V.

TABLE 2.V: Example of User Profiles in Non-Adaptive and Adaptive Approaches for Pay As You Go Payment Plan

c_{ip} Models	c_{12}	c_{13}	c_{14}	c_{31}	c_{32}	c_{42}
Non-Adaptive	7	8	9	1/8	1/4	1/6
Adaptive	1	1	5	1	9	1/7
	1/9	1/7	1/5	7	5	1/5
	⋮	⋮	⋮	⋮	⋮	⋮
	5	5	5	1	1/5	5

2.5.3 Formulation of Payoff Function

An AHP-based utility function is utilised to obtain the payoff in order to quantify user's QoS constraints. In the following Subsection, we present the details on how to compute the payoffs . To approach our modeling with a realistic view, we consider two different notions of payoff to be computed by each user i; the heterogeneous and homogeneous payoffs.

2.5.3.1 Heterogeneous Payoff

Considering price, reliability, bit rate and mobility support parameters, the heterogeneous payoff $\pi_{ij}^{(1)}$of the user i in the network j within the service area (1) is computed using an AHP-based utility function as

$$\pi_{ij}^{(1)} = \sum_{n_k=n_1}^{n_4} (w_{ip}(n_k) \times a_{ij}(n_k)), \tag{2.11}$$

where $a_{ij}(n_k)$ represents the relative quality level offered to the user i by the network j for n attributes. The attribute can be classified as positive, i.e., the larger the better, or negative, i.e., smaller the better. The calculation of $a_{ij}(n_k)$ are dependent on the type of attribute such that

Positive attribute: $a_{ij}(n_k) = \dfrac{a_{ij}^*(n_k)}{max_{j \in v}\, a_{ij}^*(n_k)}$

Negative attribute: $a_{ij}(n_k) = \dfrac{min_{j \in v}\, a_{ij}^*(n_k)}{a_{ij}^*(n_k)}$

where $a_{ij}^*(n_k)$ represents the quality level for attribute n_k offered to user i by network j. More details about the computation of quality level for each considered attribute can be found in Section 2.5.3.3.

Once $\pi_{ij}^{(1)}$ is calculated for each candidate network, each user chooses the network that offers the maximum heterogeneous payoff. Going through all of the users $\mathrm{N}^{(1)}$ within service area (1), we define the partition $z^{(1)}=z_{\text{picoBS}}^{(1)} \cup z_{\text{macrocell}}^{(1)}$, where $z_{\text{picoBS}}^{(1)}$ and $z_{\text{macrocell}}^{(1)}$ represent the set of users that prefer pico BS or macrocell connections, respectively.

2.5.3.2 Homogeneous Payoff

Furthermore, homogeneous payoff is used to satisfy the assumptions of population in an evolutionary game, where all users within a population are treated the same [10]. The homogeneous payoff $\pi_{\mathrm{j}}^{\mathrm{hom}}(\mathrm{N}^{(1)})$ for any of the users in network j within service area (1) is defined as [10]

$$\pi_{\mathrm{j}}^{\mathrm{hom}}\left(\mathrm{N}^{(1)}\right) = mean\ R_j^{(1)}, \tag{2.12}$$

where $\mathrm{R}_{\mathrm{j}}^{(1)}$ represents the set of heterogeneous payoffs of all the $\mathrm{N}^{(1)}$users within the service area (1) choosing network j, i.e., $\mathrm{R}_{\mathrm{j}}^{(1)}=\left\{\pi_{1\mathrm{j}}^{(1)}, \pi_{2\mathrm{j}}^{(1)}, \ldots., \pi_{\mathrm{Nj}}^{(1)}\right\}$. The logic behind (2.12) is that since the $\pi_{\mathrm{j}}^{\mathrm{hom}}\left(\mathrm{N}^{(1)}\right)$ payoffs are the same for all users $\mathrm{N}^{(1)}$ within the service area (1), the payoffs homogeneity can be considered as the mean of the set with the heterogeneous payoffs $\mathrm{R}_{\mathrm{j}}^{(1)}$.

2.5.3.3 Offered Quality level for each Attribute subject to User Specific QoS Constraints

Each user defines its minimum QoS thresholds $a_{ij}^{*}(n_2)$, $a_{ij}^{*}(n_3)$ and $a_{ij}^{*}(n_4)$ based on reliability n_2, offered bit rate n_3 and mobility support n_4, respectively, i.e.,

$$a_{ij}^{*}(n_2, static) = \begin{cases} \theta_{ij}^{static} & if\ j \in \text{pico BS} \\ 1-\theta_{ij}^{static} & \text{otherwise} \end{cases} \tag{2.13a}$$

$$a^*_{ij}(n_2, pedestrian) = \begin{cases} \theta^{ped}_{ij} & if\ j \in \text{macrocell} \\ 1-\theta^{ped}_{ij} & \text{otherwise} \end{cases} \tag{2.13b}$$

$$a^*_{ij}(n_3) = \begin{cases} b_{ij} & if\ \lambda_{ij} > 0 \\ 0 & \text{otherwise} \end{cases} \tag{2.13c}$$

$$a^*_{ij}(n_4) = \begin{cases} m_{ij}\ \ T^{ped}_{RTiN} \geq 20\text{sec or}\ \ T^{static}_{RTiN} \geq 0 \\ 0 \quad \text{otherwise} \end{cases} \tag{2.13d}$$

Equations (2.13a)- (2.13d) denote that the optimal network selection is dependent on users' preferences and networks' quality levels and it should also satisfy users' minimum QoS constraints for the considered attributes n_2, n_3 and n_4. This approach provides flexibility to users to evolve from one network to another satisfying the service specific QoS constraints and achieving higher payoffs.

2.5.4 Proposed User Churning Selection Mechanism

The churning of users between networks is dependent on users' relative ranks at their previous networks. The ranks are decided considering users' heterogeneous payoffs by an Inverse Cumulative Ranking (IAR) mechanism. IAR inverts the heterogeneous payoff of each user and normalises it over the cumulative heterogeneous payoffs of all users within the same network. Then users are sorted in ascending order with the probability of selection proportional to their relative rank. In addition, a random number lies within a specific region to decide which user will shift from one network (e.g. j) to another (e.g.$\widehat{j}$). Pseudo code can be found in the following Algorithm 2.1.

Algorithm 2.1 Inverse Cumulative Ranking based User Churning Selection Algorithm

Initialization of variables:

$\pi_{ij}^{(1)}$ = indicates the heterogeneous payoff of user i in network j within service area(1)

$\pi_{i\widehat{j}}^{(1)}$ = indicates the heterogeneous payoff of user i in network $\widehat{j}$ within service area(1)

$\pi_{\mathrm{j}}^{\mathrm{hom}}\left(\mathrm{N}^{(1)}\right)$= indicates the homogeneous payoff of users for network j within service area(1)

$\overline{\pi}^{hom}(\mathrm{N}^{(1)})$= indicates the average homogeneous payoff of all users within service area(1)

M = indicates the available networks

For $j \in M$

Each user i computes its inverse rank $T_i = \frac{1}{\pi_{ij}^{(1)}+1}$

Each user i computes its inverse cumulative rank $r_i = \frac{T_i}{\sum_{i=1}^{N} T_i}$

If $\pi_{\mathrm{j}}^{\mathrm{hom}}\left(\mathrm{N}^{(1)}\right) < \overline{\pi}^{hom}(\mathrm{N}^{(1)})$ then

If $rand() \in r_i$ then

If $\pi_{ij}^{(1)} > \pi_{i\widehat{j}}^{(1)}$ then

User i choose network j

Else

User i choose network $\widehat{j}$

End If

End If

End If

End For

2.5.5 Network Adjustment and Re-configuration

The policy aims to increase the system performance by defining the benefit (or utility value) of the network $j \in v$ for serving a particular user i. The overall benefit of a network is dependent on the location of the user, the ideal modulation scheme for the user, the transmitting power and the current traffic load of the network. The network adjustment factor β_j^{adj} for network j is represented as

$$\beta_j^{adj} = \left(1 - \frac{Cap_j^{avail}}{C_{apj}}\right) \times \frac{d_{ij}}{\gamma_j} \tag{2.14}$$

Variables Cap_j^{avail} and Cap_j represent the available and total capacity of network j, respectively. The physical meaning of the network adjustment factor β_j^{adj} is that users closer to the base station or access point are more beneficial for the network[3]. Accounting β_j^{adj} we can compute the modified payoff $\widetilde{\pi}_{ij}^{(1)}$ for each user i in network j within the service area (1) satisfying the conditions mentioned in (2.13a) to (2.13d) as

$$\widetilde{\pi}_{ij}^{(1)} = \left(\sum_{n_k=n_1}^{n_4} (w_{ip}(n_k) \times a_{ij}(n_k)) \right) - \beta_j^{adj}. \tag{2.15}$$

From (2.15) it is straightforward that the payoffs (or utility values) of the users within the service area (1) are dependent on the network configuration. This means that network re-configuration can enhance the quality level offered by the *re-configured* network for n attributes.

In our system, users evolve by changing their context to prefer the macrocell instead of the pico BS; this can be achieved by re-configuring the macrocell by tilting or shaping the antenna to increase its transmission power. The macrocell coverage is then re-assessed until either all the users attain a satisfactory QoS or there are no payoff improvements upon potential strategy alternatives.

2.6 Proposed Iterative Solutions

In this Section, an optimal solution to the user adaptive network selection is provided.

[3]Network providers can change the value of β_j^{adj} by configuring the antennas of the base stations [28]. However, we omit such an option from our modeling as it is out of our research subject.

2.6.1 Dynamic Contextual Network Selection Approach

In dynamic contextual approach, the optimal network selection is performed based on user's preferences and service specific QoS threshold constraints. In particular, the benefit of network j to serve user i depends on the context of user in terms of how far the user is away from the base station or directly analogous to the transmitted power. Such benefit is considered in the modified payoff calculation $\widetilde{\pi}_{ij}^{(1)}$ in (2.15). However, to measure the exact performance of the dynamic contextual approach as a solution to the user adaptive selection, we consider two different approaches; the *Full Evolution* and the *Region of Interest (RoI)*.

In the *Full Evolution approach,* we model the optimal network selection problem as an evolutionary game which considers all users within service area (1). On the other hand, in our proposed *RoI* approach, we define a RoI threshold represented by a circle with its corresponding radius R_{RoI} for pico BS as shown in Fig. 2.4 to focus on users that lie closer to the cellular coverage boundary. More specifically, the optimal network selection problem is now modeled as a *RoI-based Evolutionary* game, which only considers the users within the service area (1) lying outside the RoI threshold circle and inside the Handover threshold circle resulting in a considered region ΔD defined as:

$$\Delta D = R_{ho} - R_{RoI} \tag{2.16}$$

In each iteration, the *RoI* threshold circle R_{RoI} is iteratively reduced by step size Δd which in result increases ΔD. After each iteration cycle, the updated *RoI* threshold can be then calculated by $R'_{RoI} = R_{RoI} - \Delta d$ to define the updated considered region $\Delta D'$ as

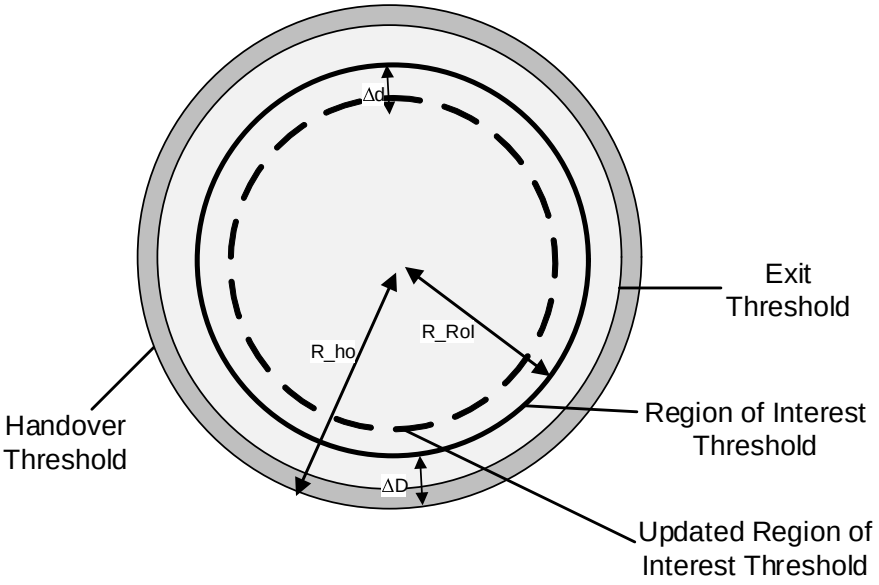

FIGURE 2.4: Region of Interest Concept

$\Delta D^{'} = R_{ho} - R^{'}_{RoI}$. The stopping criterion of the proposed iterative *RoI* approach is set to iteratively change the the RoI threshold circle until an optimal point after which no user is willing to change its strategy.

2.6.2 Solution to the Proposed Evolutionary Game

At each iteration, the macrocell reconfigures itself by changing its transmission power to provide enhanced modulation schemes, i.e. improved offered bit rate, to users within the service area (1). Also, each user observes the payoffs of other users to adopt a more profitable strategy resulting in a higher payoff. To decide whether it is profitable for a user to change its strategy to move from its current network to another, we utilise the concept of replicator dynamics to define the evolutionary equilibrium $\dot{z}_{\mathrm{j}}^{(1)}$ as follow [29]:

$$\dot{z}_{\mathrm{j}}^{(1)} = \sigma z_{\mathrm{j}}^{(1)} \left(\pi_{\mathrm{j}}^{\mathrm{hom}} \left(\mathrm{N}^{(1)} \right) - \sum_{\mathrm{j}} (z_{\mathrm{j}}^{(1)} \times \pi_{\mathrm{j}}^{\mathrm{hom}} \left(\mathrm{N}^{(1)} \right)) \right), \forall j. \tag{2.17}$$

Variable $\sigma > 0$ in (2.17) denotes the gain for the rate of strategy adaptation and controls the speed of user in observing and adapting to the network selection. The evolutionary equilibrium $\dot{z}_{\mathrm{j}}^{(1)}$ is the optimal solution of the game and can be then obtained as a fixed point of a replicator dynamic of each network j through solving (2.17) over $z_{\mathrm{j}}^{(1)}$, i.e., $\dot{z}_{\mathrm{j}}^{(1)} = 0 \; \forall \; j$. The physical meaning of such equilibrium is that no user wants to change strategy or network because all users' payoffs are equal to the average payoff within the service area. Fig. 2.5 shows the flowchart of our proposed user adaptive dynamic contextual selection mechanism.

2.6.2.1 A Clarification Example

Let us consider the replicator dynamics for two users in service area (1), i.e., $\mathrm{N}^{(1)}$=2. Also, let us assume that two strategies are available to each user; either select pico BS or macrocell, i.e. v=2. Based on our aforementioned symbolization, there would be $z_1^{(1)}$ number of users that choose pico BS and $z_2^{(1)}$ number of users that choose macrocell connections. For traceability issues, we additionally admit that the payoff function is given by $\mathrm{U_j}\left(\mathrm{N}^{(1)}\right) = \mathrm{c_{j1}} z_1^{(1)} + \mathrm{c_{j2}} z_2^{(1)}$. Then we denote the payoffs through the comparison matrix $C = \begin{bmatrix} \mathrm{c_{11}} & \mathrm{c_{12}} \\ \mathrm{c_{21}} & \mathrm{c_{22}} \end{bmatrix} = \begin{bmatrix} 0 & \mathrm{a} \\ \mathrm{b} & 0 \end{bmatrix}$. The replicator equation for this case is calculated by (2.17) as follows:

$$\dot{z}_1^{(1)} = \sigma z_1^{(1)} \left[\left(c_{11} z_1^{(1)} + c_{12}\, z_2^{(1)} \right) - \left\{ z_1^{(1)} \left(c_{11} z_1^{(1)} + c_{12}\, z_2^{(1)} \right) + \; z_2^{(1)} \left(c_{21} z_1^{(1)} + c_{22}\, z_2^{(1)} \right) \right\} \right] \tag{2.18}$$

After putting the values from the comparison matrix C, (2.18) can be rewritten as:

$$\dot{z}_1^{(1)} = \sigma z_1^{(1)} \left[\left(a \times \; z_2^{(1)} \right) - \left\{ z_1^{(1)} \left(a \times z_2^{(1)} \right) + z_2^{(1)} \left(b \times z_1^{(1)} \right) \right\} \right] \tag{2.19}$$

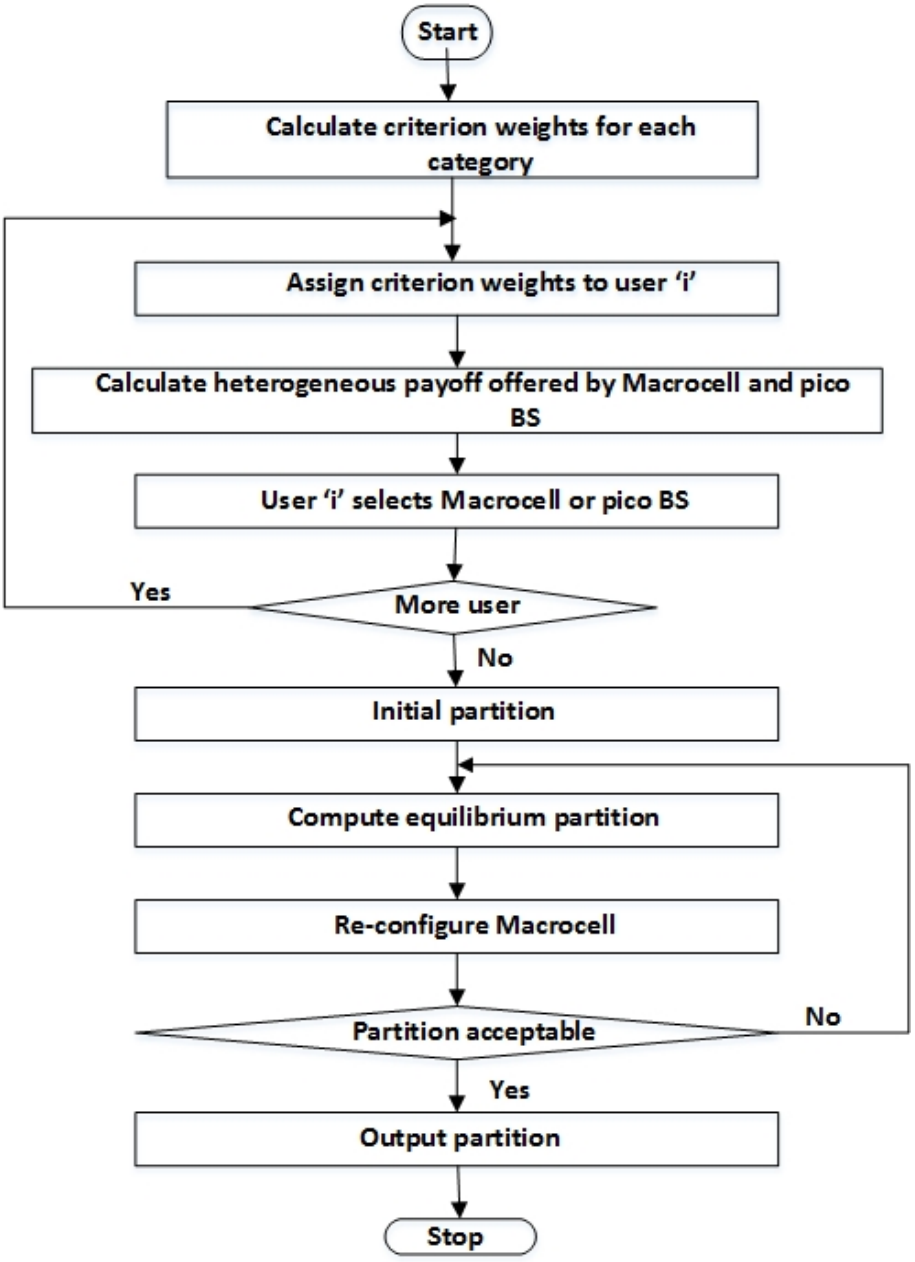

FIGURE 2.5: Flowchart of User Adaptive Dynamic Contextual Selection Algorithm

For $\sigma = 1$, we can rewrite (2.19) as follow:

$$\dot{z}_1^{(1)} = z_1^{(1)}\left[\left(a \times z_2^{(1)}\right) - \left\{z_1^{(1)}\left(a \times z_2^{(1)}\right) + z_1^{(1)}\left(b \times z_2^{(1)}\right)\right\}\right]$$

$$\dot{z}_1^{(1)} = z_1^{(1)}\left[\left(a \times z_2^{(1)}\right) - z_1^{(1)}\left(a \times z_2^{(1)}\right) - z_1^{(1)}\left(b \times z_2^{(1)}\right)\right]$$

$$\dot{z}_1^{(1)} = z_1^{(1)} z_2^{(1)} \left[a - (a+b) z_1^{(1)} \right] \tag{2.20}$$

Since $z_2^{(1)} = 1 - z_1^{(1)}$, (2.20) becomes

$$\dot{z}_1^{(1)} = z_1^{(1)} \left(1 - z_1^{(1)}\right) \left[a - (a+b) z_1^{(1)} \right] \tag{2.21}$$

Solving $\dot{z}_1^{(1)}$ over $z_j^{(1)}$ we get that

$$z_1^{(1)} \left(1 - z_1^{(1)}\right) \left[a - (a+b) z_1^{(1)} \right] = 0, \tag{2.22}$$

The fixed Evolutionary Stable Points are derived as

$z_1^{(1)} = 0, 1$ or $\frac{a}{(a+b)}$, $a, b > 0$.
$z_2^{(1)} = 1, 0$ or $\frac{b}{(a+b)}$, $a, b > 0$.

Stability of fixed Evolutionary Stable Points

To evaluate the stability at the fixed point, the eigenvalues of the Jacobian matrix corresponding to the replicator dynamics are evaluated. The fixed point is assumed stable if all eigenvalues have a negative real part [19].

2.6.3 Analysis

This Subsection focuses on the proposed distributed evolutionary game theoretic based algorithm to model the user centric network assisted selection mechanism. As explained in Section 2.1, most of the existing work in the literature on evolutionary game theory has mainly focussed on random user churning procedure as outlined in Algorithm 2.2. Initially, the users randomly select a network. In Algorithm 2.2, each user checks if its current payoff is less than the average payoff to randomly select a network such that the payoff is more than its existing payoff. This process continues until the maximum number

of iterations are reached.

In comparison to the existing approaches, our proposed Algorithm 2.3 compute the initial partition subject to user's preferences using Analytic Hierarchy Process (AHP) as mentioned earlier in Section 2.4 and 2.5. In our proposed algorithm, we utilise the user's realistic payoff to decide about the switching from a current network to another network. Our proposed user churning procedure try to increase the probability of worst users within a network to churn to another network resulting in a better benefit or payoff for both the users and networks. More details about our proposed algorithm is outlined in Algorithm 2.3.

Algorithm 2.2 Evolutionary Game Theoretic based Network Selection Algorithm

Step 1: Each user randomly chooses a network $j \in \{macro, picoBS\}$ and set $iter = 1$.
loop
Step 2: Each user i measures its average achieved data rate and compute its payoff.
Step 3: This payoff information is then sent back by each user to the network.
Step 4: The average population payoff is calculated by the network.
Step 5: Network broadcast back the average population payoff to all potential users
Step 6: At each iteration, each user checks[4]
If $(\pi_{i,j}^{\text{hom}}\left(\mathrm{N}^{(1)}\right) < \overline{\pi}^{hom}(\mathrm{N}^{(1)}))$ then
User i randomly choose network k such that $\pi_{i,k}^{\text{hom}} > \pi_{i,j}^{\text{hom}}$, where $k \neq j$
End If
Step 7: Set $iter = iter + 1$
if iter $\geq$ **Max, End loop ; otherwise goto Step 2.**

Algorithm 2.3 Proposed Evolutionary Game Theoretic based Network Selection Algorithm

Step 1: Each user give their preferences for the considered attributes.
Step 2: The comparison matrix C[5] for each user is derived as explained in Section 2.4.2.
Step 3: The comparison matrix C for each user must satisfy the Consistency Ratio (CR) as given by (2.8).
Step 4: The weight matrix W[6] for each user is computed by using (2.9) and (2.10).
Set $Iter = 1$
Step 5: Each user compute its heterogeneous payoff π_{ij} using (2.15).
Step 6: Each user chooses a network $j \in \{macro, picoBS\}$ with highest heterogeneous payoff.
Step 7: Each network j compute homogeneous payoff π_j^{hom} using (2.12) based on the heterogeneous payoff information broadcast by the users choosing network j.
Step 8: The average homogeneous payoff is computed as $\overline{\pi}^{hom} = \sum_j z_j \times \pi_j^{\text{hom}}$
Step 9: At each iteration $Iter$, call User Churning Procedure outlined in Algorithm 2.1
Step 10: Set $Iter = Iter + 1$
Step 11: Repeat Steps 5 to 10 until convergence is achieved or Iter $\geq$ Max.

[4] In Step 6, the random user selection algorithm is used to churn users from their current network to another network which is mainly used in most of the work in the literature on Evolutionary Game Theory such as [refs]

[5] The size of comparison matrix C is $n \times n$. An example of comparison matrix C is given in (2.7) where the diagonal elements represents the user preference for an attribute with itself and hence it is equal to 1. The upper triangular elements represent the user preference for an attribute with another attribute so its values are on a scale between 1 to 9 whereas the lower triangular elements are an inverse of their respective upper triangular elements

[6] The size of weight matrix W is $n \times 1$. Each element $w_i \in W$ must have a value between 0 and 1 such that $\sum_i w_i = 1$.

2.7 Results and Discussions

In this Section, the simulation configuration and results are presented. The performance comparisons between numerical and analytical methods as well as the performance of the aforementioned iterative methods are further analysed in this Section. In the following, the extended evaluations on numerous features of our proposed network selection scheme is described.

2.7.1 Simulation Setup

We consider a heterogeneous wireless network with two service areas as shown in Fig. 2.1, where all users request voice services. The number of users in the area (1) is set to $N^{(1)} = 100$, while in the area (2), it is $N^{(2)} = 100$. The pico BS uses 512 bit-size Fast Fourier Transform (FFT) Orthogonal Frequency Division Multiple Access (OFDMA) and supports the IEEE 802.16 standard with total bandwidth 7MHz. On the other hand, the WiMAX macro cell uses 512 bit-size Fast Fourier Transform (FFT) Orthogonal Frequency Division Multiple Access (OFDMA) and supports the IEEE 802.16 standard with total bandwidth 5MHz. It should be noted that WiMAX is used as a candidate air interface technology but this proposed framework can be easily extended to latest air interface technologies as well. Furthermore, the pico BS expands in a 300 meters radius coverage area covering the service area (1) and lying within the coverage area of the macrocell. The macrocell coverage has 1000 and 2000 meters minimum and maximum radius, respectively covering both areas (1) and (2). We also assume that the pricing coefficient *pi* is set to 0.005 while considering an AHP-based utility function setting $\sigma = 1$ for the replicator dynamics. The partition is defined as the proportion of the users selecting pico BS in the service area (1).

2.7.2 Comparison between Non-Adaptive and Adaptive User Preferences Model

Fig. 2.6 and Fig. 2.7 illustrate the proportion of adaptive users with four different payment plans that choose macrocell or pico BS, respectively. The corresponding proportion

of non-adaptive user preference is shown in Fig. 2.8 and Fig. 2.9, respectively. Observing the iteration numbers 1, 9, 12, 15 and 19 where users churn from pico BS to macrocell. It is observed that the adaptive scheme significantly outperforms the non-adaptive scheme. In the adaptive scheme, the users belonging to the same payment plan can have diverse preferences whereas all users belonging to the same payment plan can have identical preferences in the non-adaptive scheme. It is more practical to use adaptive scheme, and hence for brevity, the rest of the simulations are carried out for the adaptive scheme.

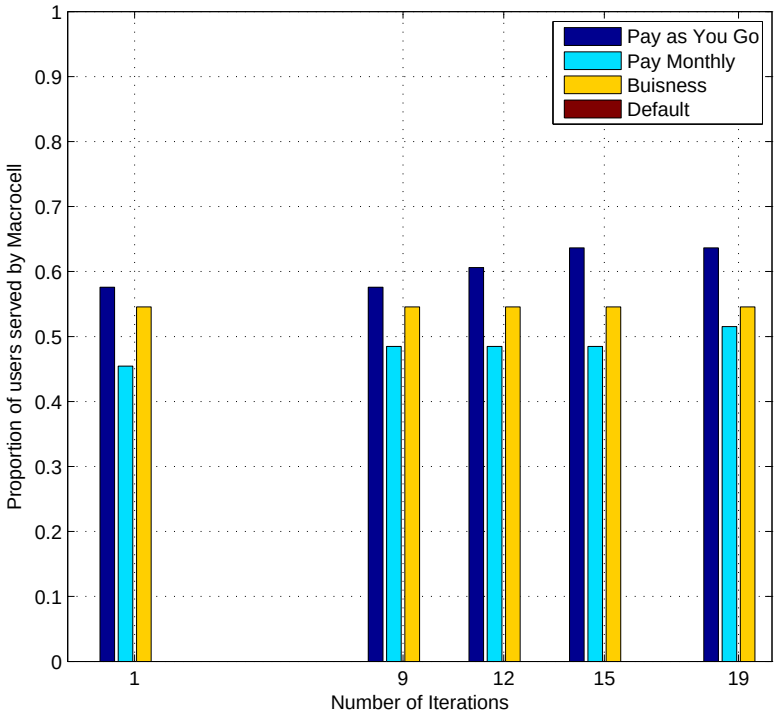

FIGURE 2.6: Proportion of Users with Adaptive Preference Model Served by macrocell

2.7.3 Impact of Pricing and Network Adjustment Mechanisms

From the network selection perspective, it is important to understand the impact of the pricing mechanism on the decision of selecting an optimal network. In this work, we

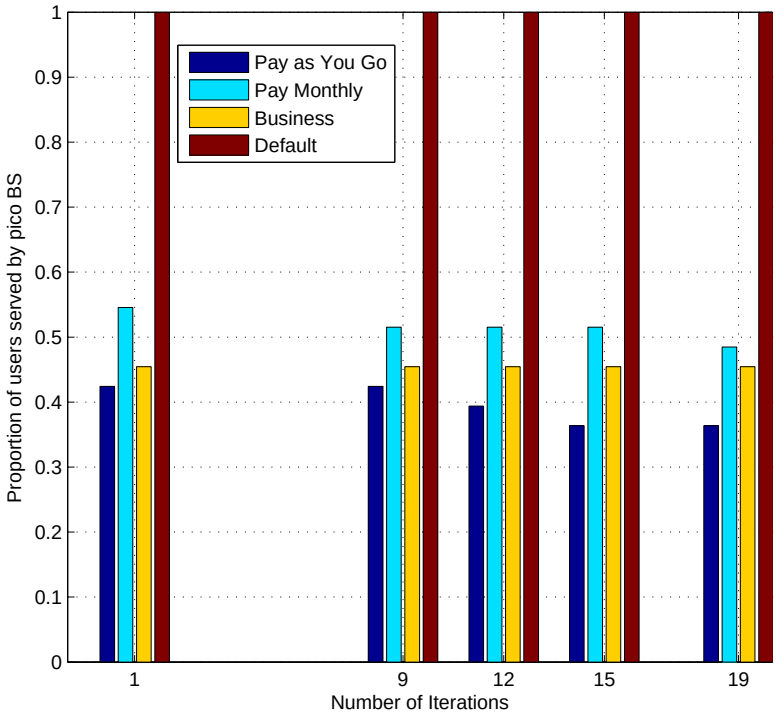

FIGURE 2.7: Proportion of Users with Adaptive Preference Model Served by pico BS

study the impact of constant and linear pricing mechanisms on the network selection. In constant pricing mechanism, the network charges a constant price from their users irrespective of their load whereas in the linear pricing mechanism the network charges a load dependent price from its users. We observe that as the number of users choosing macrocell or pico BS increases, their respective price per user also increases. In this work, the pricing co-efficient pi is set to 0.005, i.e.,$pi = 0.005$. The pricing mechanism can also be used as a load-balancing parameter.

2.7.3.1 Performance of Initial Partition using Different Allocation Strategies

In Fig. 2.10 we investigate the performance of the random and AHP-based allocation strategies by observing the initial proportion of users that choose each network. In other

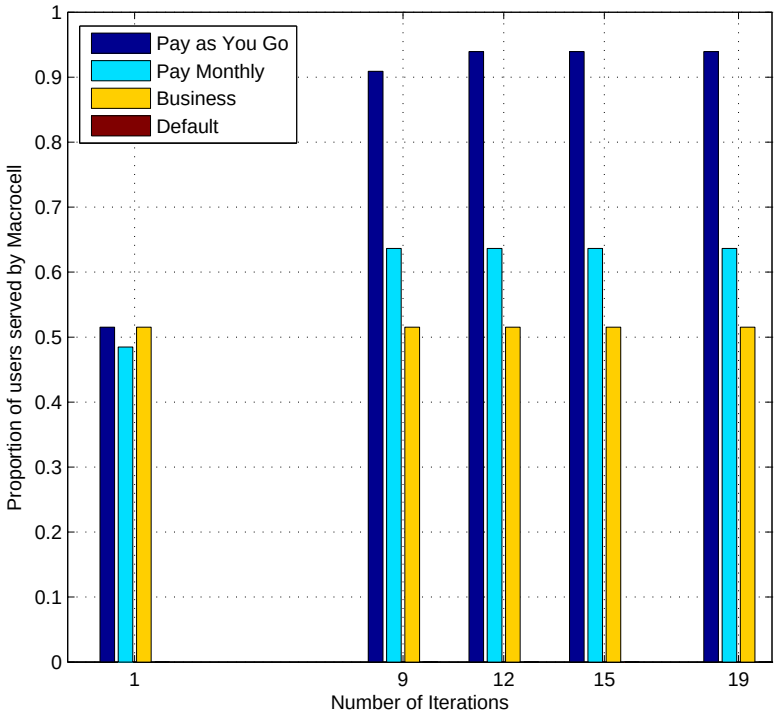

FIGURE 2.8: Proportion of Users with Non-Adaptive Preference Model Served by macrocell

words, Fig. 2.10 shows the effectiveness of the network adjustment in terms of reducing the churning of users from one network to another. Networks can make their choice on whether to consider the network adjustment or not in their utility. For this simulation, we consider three pricing scenarios: a) each network offers the same price; b) the pico BS price is lower; and c) the macrocell price is lower. In addition, two different thresholds are set for random allocations: a) $rand < 0.75$ when all users who have randomly generated number less than 0.75 to choose the pico BS; and b) $rand < 0.9$ when all users who having a randomly generated number less than 0.9 to choose pico BS. The focus is on the computation of an AHP-based allocation with and without network adjustment and re-configuration. In the case of network adjustment and re-configuration, both pico BS

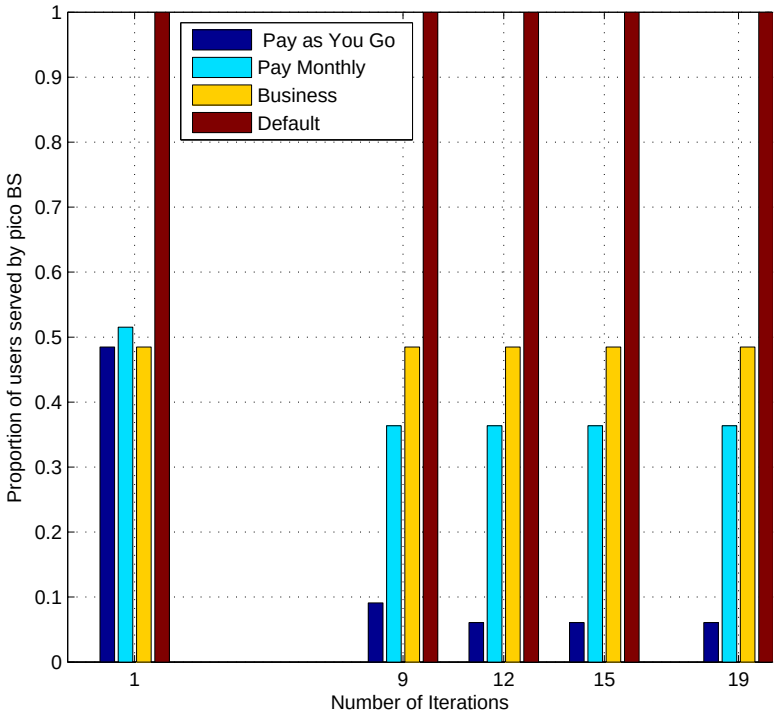

FIGURE 2.9: Proportion of Users with Non-Adaptive Preference Model Served by pico BS

and macrocell offer the same price. The proportion of the pico BS users with a constant price at the initial points is computed as $z^{(1)}_{macrocell}(0) = 0.52$ and $z^{(1)}_{picoBS}(0) = 0.48$. When network adjustment and re-configuration is not considered, the initial points for the constant price case are computed as $z^{(1)}_{macrocell}(0) = 0.24$ and $z^{(1)}_{picoBS}(0) = 0.76$. In both scenarios, the computation of the corresponding initial points are used to calculate the linear price for the next iteration, and hence, the proportion of users choosing the macrocell or the pico BS is re-computed.

From the numerical results, the impact of constant or linear pricing mechanisms, the behaviour of network adjustment, and different allocation mechanisms are observed on

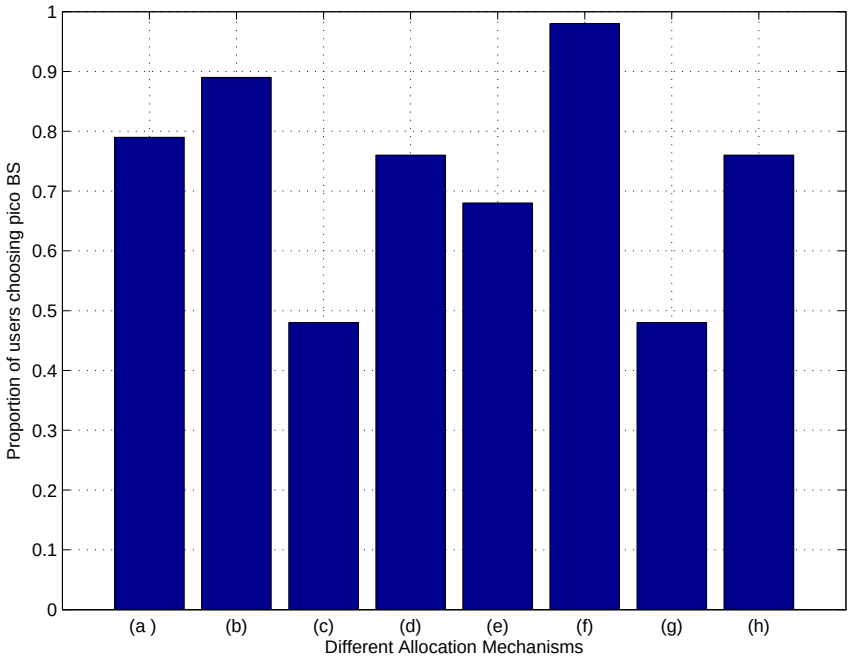

FIGURE 2.10: Initial Proportion of Users Choosing pico BS under Constant Price for Different Allocation Mechanisms; a)choose pico Bs if random no is greater than 0.75, b) choose pico Bs if random no is greater than 0.9, c) AHP based allocation with network adjustment with both networks offering same price, d)AHP based allocation without network adjustment with both networks offering same price, e)AHP based allocation with network adjustment with pico BS offering lowest price, f) AHP based allocation without network adjustment with pico BS offering lowest price, g)AHP based allocation with network adjustment with macrocell offering lowest price, h) AHP based allocation without network adjustment with macrocell offering lowest price

the user's network selection. From Fig. 2.10, it is quite evident that the AHP-based allocation with network adjustment and re-configuration using linear price mechanism provides more sensible allocations in comparison to the other allocation mechanisms. It also remarkably reduces the churning of users from one network to another one.

2.7.3.2 System Blocking Rates

In Fig. 2.11, the impact of different allocation mechanisms with or without network adjustment is investigated on the system blocking rates. The results demonstrate the effectiveness of AHP-based allocation with network adjustment in terms of reducing the

system blocking rates as compared to the case where there is no network adjustment. The results demonstrate the effectiveness of our proposed selection scheme incorporating AHP-based allocation with network adjustment for three different pricing cases of constant price outperforms in reducing the system blocking rates compared to the random allocation and AHP-based allocation without network adjustment.

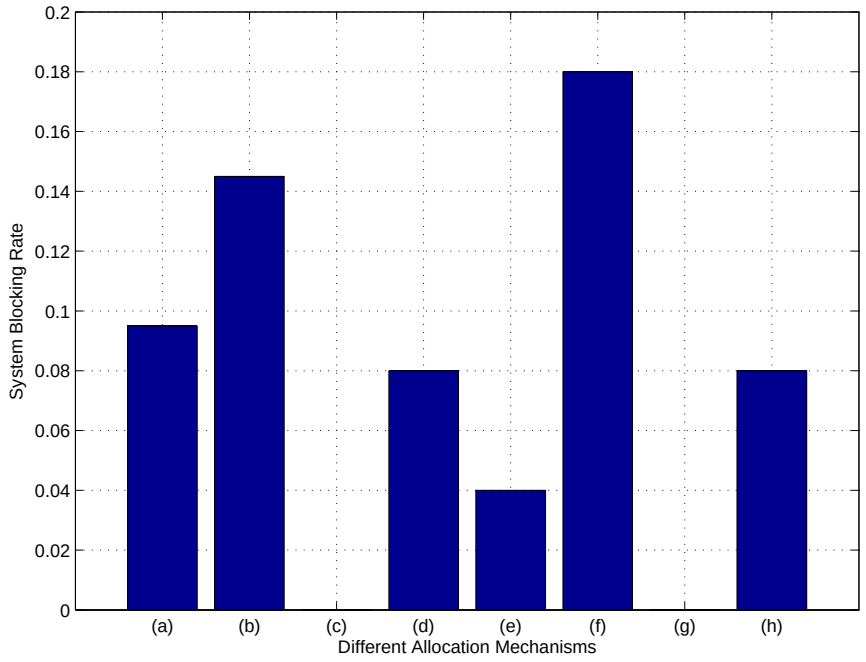

FIGURE 2.11: Initial System Blocking Rates under Constant Price for Different Allocation Mechanisms; a)choose pico Bs if random no is greater than 0.75, b) choose pico Bs if random no is greater than 0.9, c) AHP based allocation with network adjustment with both networks offering same price, d)AHP based allocation without network adjustment with both networks offering same price, e)AHP based allocation with network adjustment with pico BS offering lowest price, f) AHP based allocation without network adjustment with pico BS offering lowest price, g)AHP based allocation with network adjustment with macrocell offering lowest price, h) AHP based allocation without network adjustment with macrocell offering lowest price

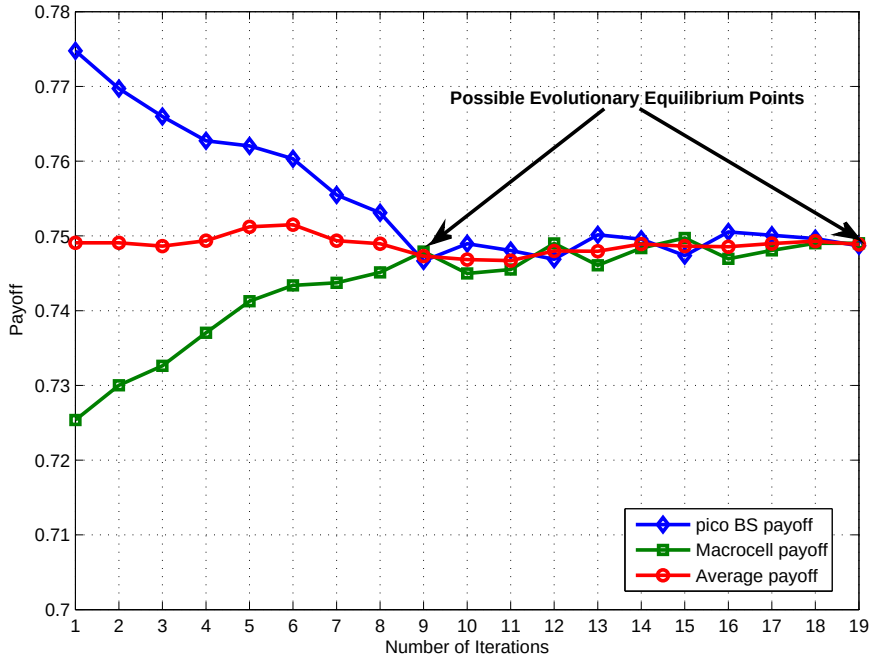

FIGURE 2.12: Allocated Payoff to Each User in AHP based Allocation using Linear Price with Network Adjustment

2.7.3.3 Convergence to Evolutionary Equilibrium

Fig. 2.12 and 2.13 present the utility values in each iteration to show the impact of churning users among networks for linear and constant pricing, respectively. For this simulation, most users in area (1) initially select the pico BS. We then reconfigure the macrocell by slowly increasing its transmission power at each iteration and observe churning of the users in area (1) from the pico BS to the macrocell. Also, as the number of users in area (1) choosing pico BS decreases, the traffic load in the macrocell increases. As a result, the allocated utility value becomes smaller for those users who choose the macrocell in area (2). Therefore in Fig. 2.12, as the number of users choosing macrocell in area (1) increases, their allocated utility value increases in each iteration for the linear price case. In the 17th iteration of Fig. 2.12, it is observed that all users, whether they choose pico

BS or macrocell, have identical utility value. In other words, Fig. 2.13 shows that the evolutionary equilibrium (where all users have chosen an optimal network and would not deviate among networks) can be achieved earlier in comparison to the linear price case.

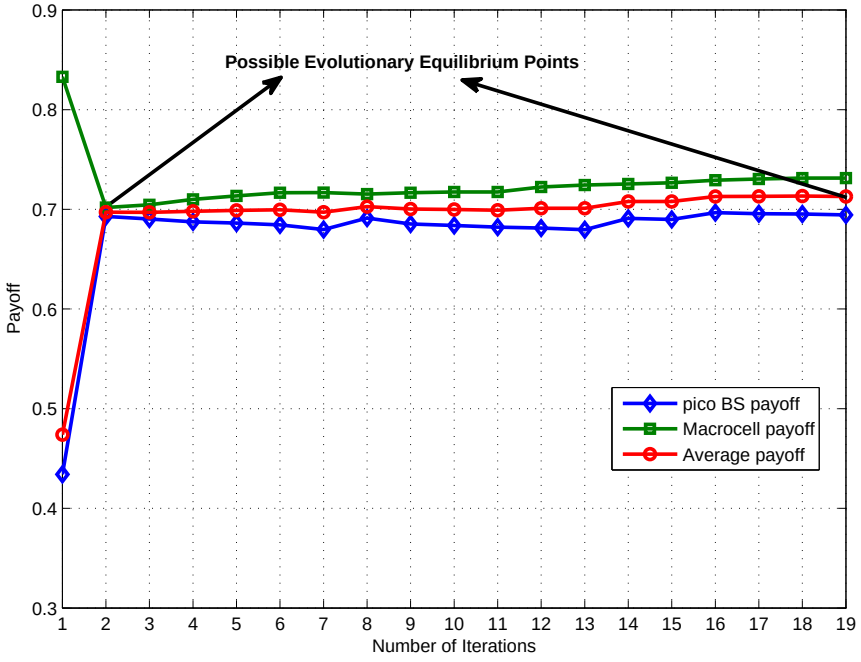

FIGURE 2.13: Allocated Payoff to Each User in AHP based Allocation Using Constant Price with Network Adjustment

2.7.3.4 Dynamics of Strategy Adaptation:

Fig. 2.14 illustrates the trajectories of strategy adaptation for AHP based allocation with and without network adjustment, for constant and linear pricing. Results demonstrate that the proposed scheme for incorporating linear price and network adjustment gives the most accurate partition which reduces the number of handovers and achieves the lowest load in the pico BS in the first iteration. This result also demonstrate the effectiveness of network adjustment for constant price case in achieving the accurate partitiion compared to the no network adjustment case.

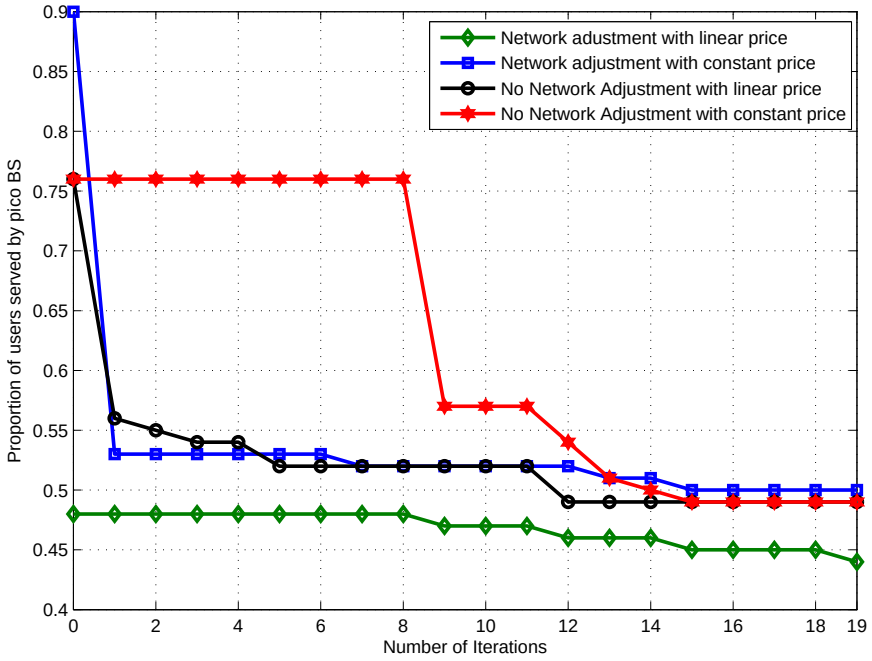

FIGURE 2.14: Trajectories of Strategy Adaptation towards Evolutionary Equilibrium

2.7.4 Performance Comparison of Full Evolution and RoI based Dynamic Contextual Approaches

Fig. 2.15 show the number of users moved from pico BS to macrocell and the number of users who need to be considered for user adaptive selection mechanism by iteratively changing the Region of Interest. Specifically, Fig. 2.15 shows that if the macrocell is not re-configured, the *RoI based Dynamic Contextual Approach* selects the optimal region $\Delta D = 0.25$. Without degrading the performance this selection reduces the number of users or players in an evolutionary game within the service area (1) required to adopt user adaptive network selection mechanism by 58% as compared to the *Full Evolution Dynamic Contextual Approach*. Fig. 2.15 also shows the case when macrocell is re-configured; the *RoI-based Dynamic Contextual Approach* selects the optimal region $\Delta D =$

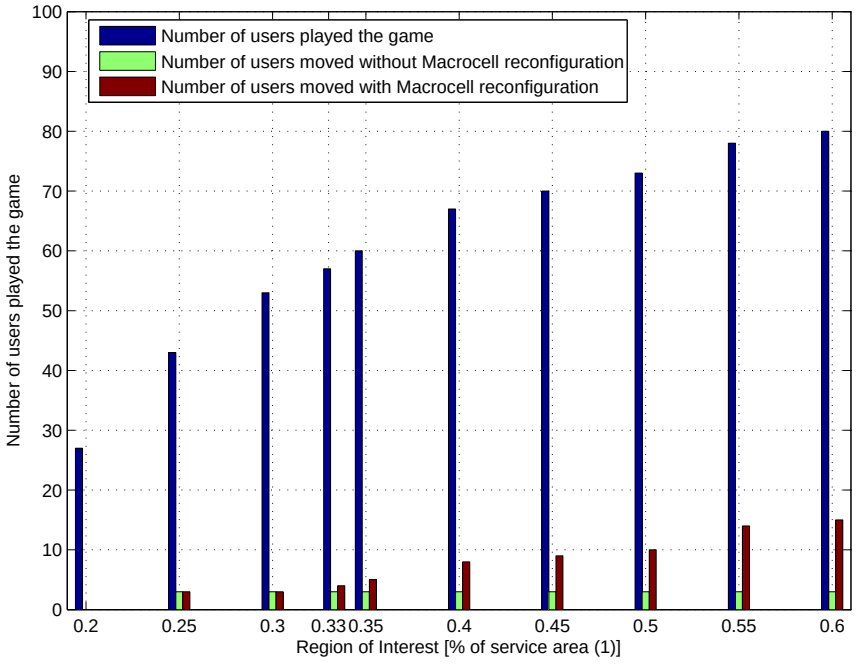

FIGURE 2.15: Performance of ROI based Dynamic Contextual Approach as Compared to the Full Evolution Dynamic Contextual Approach(i.e. ROI=1.0)

0.55 which reduces the number of users or players in an evolutionary game within the service area (1) required to adopt user adaptive network selection mechanism by 23% as compared to the *Full Evolution Dynamic Contextual Approach* without degrading the performance.

2.8 Summary

The joint network selection algorithm from both user and network perspectives are proposed in cooperative heterogeneous wireless systems. Initially, the user preferences are modelled in terms of QoS, interface preference, price and mobility support. Relying on these four preferences, an adaptive user preference model is firstly formulated, where users can change their strategy aiming to achieve better services. In particular,

the network is re-configured by iteratively controlling its transmission power and adjust its policy by introducing a utility for the service provided to the users within the coverage area. Finally, a game-theoretic approach for adaptive network selection is proposed, where an evolutionary equilibrium guarantees an optimal solution. In addition, a novel RoI-based Dynamic Contextual strategy is also proposed which significantly reduces the number of users to be considered in an evolutionary game without degrading the service. The simulation results showed that the proposed scheme outperforms the existing solutions in terms of user allocation, traffic load, blocking rates, convergence and QoS performance.

Chapter 3

Energy Efficient Resource Allocation in Heterogeneous Networks[1]

In Chapters 1 and 2, we have highlighted that the EE is considered as a key performance metric in the design of the future generation networks which requires advance techniques and algorithms to address these issues. It should be noted that the HetNets can improve the overall system coverage and throughput by deploying small cells at the edge of the macrocell coverage. This improvement is achieved by bringing the small cells closer to the users resulting in a smaller path loss and better service for the cell edge users. However, a dense deployment of these smaller cells without considering EE can result in a higher power consumption causing service degradation. The focus of Chapter 2 was to maximise the system throughput of the two-tier HetNets using the evolutionary

[1]The work presented in this chapter have been published in three IEEE conferences; 1) 24th IEEE International Symposium on Personal Indoor and Mobile Radio Communications (PIMRC), held at London, UK in September 2013; 2) 20th IEEE International Workshop on Computer Aided Modelling and Design of Communication Links and Networks (CAMAD), held at Guildford, UK in September 2015; and 3) IEEE International Conference on Communications (ICC), held at London, UK in June 2015.

game theory. In comparison to the work outlined in Chapter 2, we extend our existing system model to incorporate the energy-efficient radio resource allocation in device-to-device (D2D) enabled multi-tier HetNets subject to the minimum QoS requirement and maximum transmission power constraint. Recently, the convex optimisation methods have gained a lot of attention to address the energy-efficient radio resource allocation issues in D2D enabled multi-tier HetNets.

This chapter focuses on energy efficient resource allocation schemes in multi-tier HetNets. This chapter proposes joint user association and energy-efficient resource allocation in the uplink of multi-user two-tier Orthogonal Frequency Division Multiplexing (OFDM) Heterogeneous Networks (HetNets) subject to user's maximum transmission power and minimum-rate constraints as outlined in Section 3.4. The proposed scheme aims at achieving high rates at low powers satisfying the user's quality-of-service (QoS) constraints (in terms of minimum-rate requirements) by offloading the users with low signal to noise ratio (SNR) from macrocell to the pico base station (BS). A SNR based rate proportional resource allocation approach is proposed to transform the minimum-rate constraint into a minimum required transmission power constraint on each subcarrier. The single-user single-carrier and multi-user multi-carrier energy efficiency (EE) maximization problems are then solved under maximum and minimum power constraints using Karush-Kuhn-Tucker (KKT) conditions. The impact of users' maximum transmission power and minimum-rate requirements on EE and throughput are investigated through illustrative results. The rate-proportional approach is evaluated against the equal rate allocation approach for different user associations and various numbers of users, maximum

transmission power, and circuit powers. Significant gains in EE can be achieved for the HetNets if the path loss based user association is combined with the proposed SNR rate proportional mechanism.

A multi-tier architecture consisting of a macrocell overlaid with small cells, e.g., pico base station (BS), with provision of relays and device-to-device (D2D) communication is needed to satisfy the quality-of-service (QoS) requirements in a joint spectrum and energy efficient manner for the future Fifth generation (5G) networks. D2D communication enables the users located in close proximity to each other to communicate directly without going through the macro-cell, and hence, can be utilised to offload the traffic from the cellular infrastructure. Section 3.5 investigates the trade-off between Area Energy Efficiency (AEE) and Area Spectral Efficiency (ASE) in D2D-enabled uplink heterogeneous networks. The tradeoff is modelled as an optimization problem, in which each user wants to maximize its own ASE subject to its required AEE levels. Taking into consideration of the AEE requirement and maximum transmission power constraint, a distributed resource allocation approach is proposed to jointly optimize the mode selection, subcarrier and optimal power allocation by exploiting the properties of fractional programming. The relationship between the achievable AEE and ASE trade-off is investigated with different network parameters.

In Section 3.6, a multi-objective optimization problem (MOP) is proposed to jointly investigate the tradeoff between throughput and backhaul energy efficiency (BEE) using -fair utility function for two different backhauling technologies in downlink transmission

scheme of a two-tier HetNets. We then transform the proposed MOP into a single objective optimization problem (SOP) employing the weighted sum method to obtain the complete Pareto Frontier solution set with minimum QoS requirements and rate fairness level . The transformed SOP is solved in an iterative manner using Lagrangian Dual Decomposition (LDD) with a subgradient method providing a near-optimal solution. Simulation results demonstrate the effectiveness of our proposed approach in reducing the total area power consumption irrespective of the backhauling technology by dynamically adjusting weighting coefficient and rate fairness level . Our numerical results also demonstrate the fundamental tradeoff between throughput and BEE for different parameters such as weighting coefficient and rate fairness level .

3.1 Related Work

Recently, several works have considered throughput maximization to measure the performance in the OFDM systems for downlink [30], uplink [31] [32] [33] and joint uplink-downlink [34] transmission schemes. On the other hand, when EE is the considered performance metric, [35] proposes an EE-maximization link adaptation and resource allocation technique for an OFDMA system considering fixed circuit and transmit power by improving the mobile EE for the flat-fading OFDMA channels. Their approach is generalized to maximizing the uplink EE in frequency selective channels in [36]. A low complexity time-sharing bandwidth allocation approach to maximize the EE of a downlink flat-fading channel is proposed in [37]. Further, energy-efficient channel and power allocation problem in the uplink of an OFDM system is considered subject to maximum

transmit power constraint, based on the assumption that each user can transmit at one channel in [8], wherein two different energy scheduling algorithms were proposed. In [38], the authors investigate the tradeoff between spectral and energy efficiencies as a function of the circuit power, power amplifier (PA) efficiency and channel power gain in time-varying Rayleigh fading point-to-point channels. These works, however, do not consider the impact of users' minimum-rate requirements and the use of HetNets on EE in OFDM systems.

The major contribution of this work is to propose a joint subcarrier and power allocation technique for maximizing EE within HetNets, based on the user association when user's minimum-rate requirements are to be satisfied. Specifically, we consider the pico-BS-first user association to offload the users from macrocell to pico BS to enhance EE. Further, we propose a rate-proportional mechanism to divide the user's minimum-rate requirements in between its associated subcarriers based on the subcarriers SNRs. Specifically, when SNR of a subcarrier is higher, higher minimum-rate will be allocated to that subcarrier, and vice versa. This proposed approach is compared to the equal rate allocation approach, wherein the user's minimum-rate requirement is equally allocated among all the subcarriers [29] [33]. The minimum-rate constraint for single-user and multi-user cases is transformed into minimum power constraints on each subcarrier. The power allocation using Karush-Kuhn-Tucker (KKT) conditions are then used to compute the instantaneous subcarriers transmit powers while not violating the users' maximum transmit power constraints. Simulation results indicate that the proposed rate proportional approach enhances

the EE in the order of 10.2% as compared to the equal rate approach. Our study also reveals that EE increases with the maximum transmission power ($P_{\max}$) while on the other hand, the EE decreases with increase in minimum-rate required by the users. The EE increases with the number of users and decreases with the distance from their connecting BS.

3.2 Chapter Organisation

The rest of this chapter is organized as follows. Section 3.3 describes the system model. Section 3.4 describes the low-complexity suboptimal user association and power allocation in two-tier HetNets. Section 3.5 describes the formulation of an optimisation problem to maximise the Area Spectral efficiency (ASE) subject to the Area Energy Efficiency (AEE) requirement in multi-tier HetNets. Section 3.6 presents the multi-objective optimisation problem to optimise the conflicting objectives such as maximise the throughput and minimise the transmission power in two-tier HetNets from the fairness perspective. Section 3.7 concludes the chapter.

3.3 System Model

We consider a three-tier (or Hierarchical) HetNets as shown in Fig. 3.1 where tier-1 is modelled as macrocell, tier-2 is modelled as pico BSs and tier-3 is Device-to-Device (D2D) communication. In total, there are M BSs where BS_1 is a macrocell (Mc) and BS_m is a pico BS (PB) $(m \in \{2,3,\cdots,M\})$. The pico BS is connected to the macrocell via a high capacity wired backhaul. There are N users $(n \in \{1,2,\cdots,N\})$ randomly generated

and uniformly distributed within the coverage area of three-tier HetNets with K subcarriers ($k \in \{1,2,\cdots,K\}$). The system bandwidth B is divided equally within K subcarriers, i.e., $B_k = \frac{B}{K}$. Let $\mathcal{N}_{\mathrm{C}} = \{1,2,\cdots,C\}$ denote the set of cellular users associated with either macrocell or $M-1$ pico BS and $\mathcal{N}_{\mathrm{D}} = \{C+1, C+2, \cdots, N\}$ denote the set of potential D2D users. The set of active users in the network could be expressed as $\mathcal{N} = \mathcal{N}_{\mathrm{C}} \cup \mathcal{N}_{\mathrm{D}}$. The potential D2D users have the opportunity to select their operation mode (i.e., cellular mode or dedicated mode) as they are covered by either the macrocell or $M-1$ pico BS. It is also assumed that the user is associated to same BS for both downlink and uplink transmission scheme. It is worthwhile to mention that this model is also applicable to multi-tier HetNets consisting of multiple macrocells and different type of small cells.

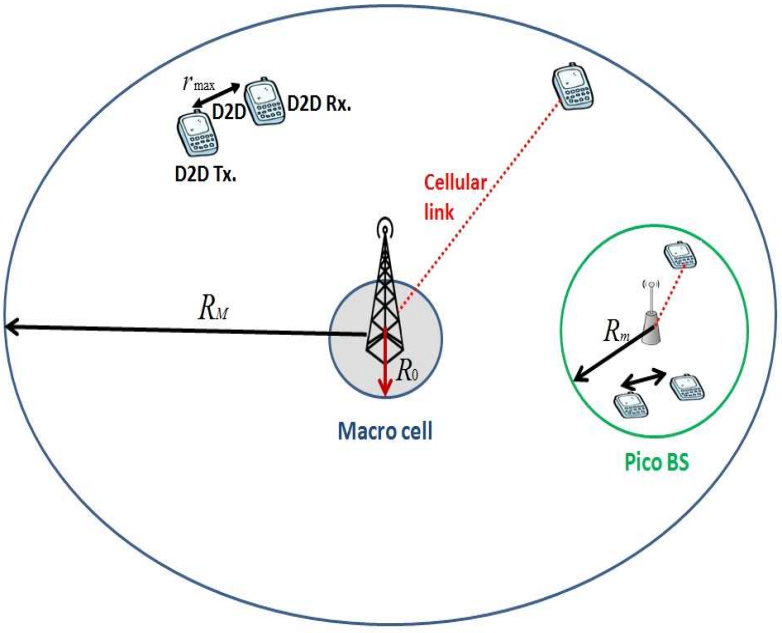

FIGURE 3.1: Three-Tier HetNets scenario

At this stage, the effect of the interference from adjacent cells is not taken into consideration. The co-channel interference between pico BS and macrocell is catered assuming that each of them communicates the usage of subcarrier with each other using Almost

Blank Frame (ABF). We consider an orthogonal subcarrier selection scheme, introduced in [39], that assigns each subcarrier exclusively to either pico BS (PB), macrocell or D2D pair at any time. Let $\sigma_{k,n}^{(\mathrm{PB})}$ and $\sigma_{k,n}^{(\mathrm{M})}$ denote the subcarrier allocation indices for pico BS and macrocell, respectively. If the subcarrier $k \in K_{\mathrm{PB}}$, for $k = \{1, \cdots, K\}$, is allocated to user n, for $n = \{1 \cdots N\}$, then $\sigma_{k,n}^{(\mathrm{PB})} = 1$, and otherwise $\sigma_{k,n}^{(\mathrm{PB})} = 0$. It is assumed that a subcarrier can only be assigned to one user in a scheduling interval. To maintain the QoS requirements, each user has a minimum-rate constraint. We assume that the minimum-rate requirement of all users are identical and is referred by $R_{\min}$.

3.3.1 Uplink System Model

The signal-to-noise-ratio (SNR) of the n-th user in D2D or cellular modes (served by either macrocell or pico BS) on subcarrier k are given as follow

$$\gamma_{k,n}^{(d)} = \frac{|h_{k,n}^{(d)}|^2}{\rho_{\mathrm{n},d}^2 \mathrm{PL}_n^{(\mathrm{d})}} \tag{3.1a}$$

$$\gamma_{k,n}^{(c)} = \frac{|h_{k,n}^{(c)}|^2}{\rho_{\mathrm{n},c}^2 \mathrm{PL}_n^{(\mathrm{c})}} \tag{3.1b}$$

$h_{k,n}^{(d)}$ represent the channel amplitude gain on subcarrier k from the n-th D2D pair to its receiver whereas $h_{k,n}^{(c)}$ represent the channel amplitude gain on subcarrier k between the n-th cellular user and the macrocell (or pico BS). The distance-based path loss for n-th user in D2D or cellular mode are denoted by $\mathrm{PL}_n^{(\mathrm{d})}$ and $\mathrm{PL}_n^{(\mathrm{c})}$, respectively. The noise power at the macrocell (or pico BS) and the D2D receiver, respectively, are given by $\rho_{\mathrm{n},d}^2 = \rho_{\mathrm{n},c}^2 = B_k N_0$, where N_0 is the noise spectral density.

The instantaneous rate achieved by user n on subcarrier k choosing either dedicated mode 'd' or cellular mode 'c' are given respectively by

$$\mathrm{r}_{k,n}^{(d)} = B_k \log_2\left(1+\gamma_{k,n}^{(d)} \times p_{k,n}^{(d)}\right), \forall k \in K_{\mathrm{d}}, \forall n \in \mathscr{N}_{\mathrm{D}} \tag{3.2a}$$

$$\mathrm{r}_{k,n}^{(c)} = B_k \log_2\left(1+\gamma_{k,n}^{(c)} \times p_{k,n}^{(c)}\right), \forall k \in K_{\mathrm{c}}, \forall n \in \mathscr{N}_{\mathrm{C}} \tag{3.2b}$$

Here, $p_{k,n}^{(d)}$ and $p_{k,n}^{(c)}$ indicate the power allocated to the user n on subcarrier k for D2D and cellular modes, respectively.

In simple terms, the potential D2D transmitter chooses a dedicated mode if $\tau_d r_{k,n}^{(d)} \geq r_{k,n}^{(c)}$, where $r_{k,n}^{(d)}$ is the achievable rate in dedicated mode, $r_{k,n}^{(c)}$ is the achievable rate in the cellular mode and τ_d is a biasing factor. In cellular mode, the D2D pair will need two subcarriers (one in uplink and one in downlink) and due to this reason $\tau_d = 2$ for the dedicated mode. To guarantee the QoS of D2D pair, both uplink and downlink SNRs should be larger than a given threshold $\gamma_{\min}$. We assume that the macrocell or pico BS can tune its transmission power to ensure that $\gamma_{k,n}^{(c,\mathrm{down})}$ is no less than $\gamma_{k,n}^{(c)}$ [40]. In order to simplify the optimisation problem, it is assumed that the subcarrier used by one D2D pair cannot be reused by any other D2D pair. Then, the achievable rate of user n on subcarrier k is

$$r_{k,n} = m_n.r_{k,n}^{(d)} + (1-m_n).r_{k,n}^{(c)}, \tag{3.3}$$

where $m_n \in \{0,1\}$ is a binary variable used to distinguish between the different modes where the cellular mode is represented by $m_n = 0$ whereas the dedicated mode is represented by $m_n = 1$. The system sum rate in an uplink transmission scheme can be expressed

as

$$R = \sum_{k=1}^{K} \sum_{n=1}^{N} r_{k,n} \tag{3.4}$$

Similarly, the transmit power of user n on subcarrier k is given by

$$p_{k,n} = m_n . p_{k,n}^{(d)} + (1 - m_n) . p_{k,n}^{(c)} \tag{3.5}$$

In practice, the transmission power available at n-th user, P_n, is limited to a maximum threshold, i.e., $P_n^{\max}$ which can be formulated as:

$$P_n = \sum_{k=1}^{K} p_{k,n} \leq P_n^{\max}, \forall n \tag{3.6}$$

Hence, the overall power consumption and the transmission power in an uplink of D2D enabled communication can be modelled as:

$$P = \varepsilon_0 P_{\mathrm{T}} + (1 + m_n) P_{\mathrm{C}}, \tag{3.7a}$$

$$P_T = \sum_{n=1}^{N} \sum_{k=1}^{K} p_{k,n} \tag{3.7b}$$

where ε_0 is an inverse of power amplifier efficiency.

Energy Efficiency (η_{EE}) is defined as the amount of data transferred per unit energy consumed by the system (usually measured in (b/J) and is defined as:

$$\eta_{\mathrm{EE}} = \frac{R}{\varepsilon_0 P_T + (1+m_n)P_{\mathrm{C}}}, \tag{3.8}$$

where R denote the total achievable data rate compromising of the achieved data rates in the macrocell, small cell and D2D communication. η_{EE} is strictly quasi-concave with respect to transmission power P_{T}. Hence, there exists one and only one optimal solution that maximises η_{EE}. η_{EE} monotonically increases with P_{T}, when $P_{\mathrm{T}} \in [0, P^*_{\eta_{\mathrm{EE}}}]$ while it monotonically decreases with P_{T}, when $P_{\mathrm{T}} \in [P^*_{\eta_{\mathrm{EE}}}, \infty)$.

3.3.2 Downlink System Model

The received downlink SNR of user n on subcarrier k associated with network m is given by

$$\gamma^{(\mathrm{m})}_{k,n} = \frac{h^{(\mathrm{m})}_{k,n}}{N_0 B_k \mathrm{PL}^{(\mathrm{m})}_n}, \tag{3.9}$$

where $h^{(\mathrm{m})}_{k,n}$ is the channel gain between network m and user n on subcarrier k, N_0 is the thermal noise at user n, $\mathrm{PL}^{(\mathrm{m})}_n$ is the pathloss between user n and network m and B_k is the subcarrier bandwidth spacing assumed to be fixed in each network m.

The instantaneous rate of user n associated with network m on subcarrier k is given as follow:

$$r^{(\mathrm{m})}_{k,n} = B_k \log_2 \left(1 + \gamma^{(\mathrm{m})}_{k,n} \times p^{(m)}_{k,n}\right), \tag{3.10}$$

The total data rate of user n is

$$R_n = \sum_{k=1}^{K} \sum_{m=1}^{M} \sigma_{k,n}^{(m)} r_{k,n}^{(m)}, \tag{3.11}$$

where $\sigma_{k,n}^{(m)}$ is the subcarrier allocation indicator such that $\sigma_{k,n}^{(m)} \in \{0,1\}$.

3.4 Optimising User Association and Power Allocation in Heterogeneous Networks

From (3.8), we can observe that improving the EE can result in reduction of the user achieved rate, and hence degrading the user's QoS. In this Section, we consider the UE minimum-rate requirement along with its maximum transmit power constraint in order to investigate the tradeoff between the achieved EE and QoS requirements.

3.4.1 Received Power based User Association

In order to avoid frequent vertical handoffs in HetNets, user association rules are defined for wireless transmission [41]. In traditional homogeneous cellular networks, the user association is based on the received signal strength [42]. One of the key issues is that all BSs within the same tier should have identical biasing factor. Unique association of users with the macrocell or pico BS is assumed. Specifically, each user can only be associated with one BS. Define the user association index for pico BS by $a_{\mathrm{PB},n}$ which is equal to 1 if the user n is associated to the pico BS and 0, otherwise. Similarly, we can define the user association index for macrocell by $a_{\mathrm{Mc},n} = (1 - a_{\mathrm{PB},n})$.

Different user association schemes for the uplink of HetNet with $N = 25$ are shown

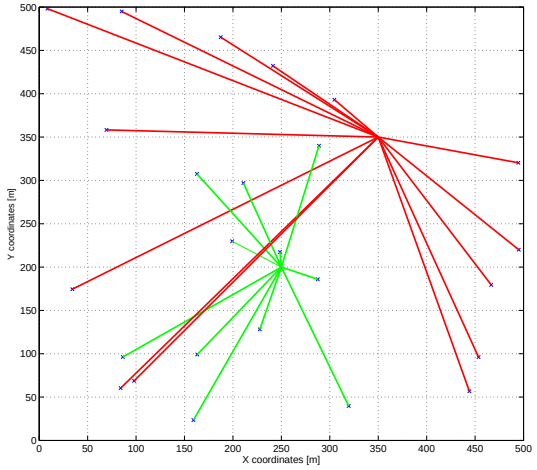

(a) Pico BS First

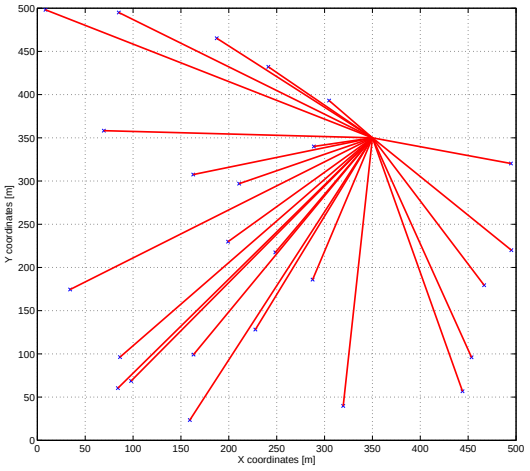

(b) Macrocell only

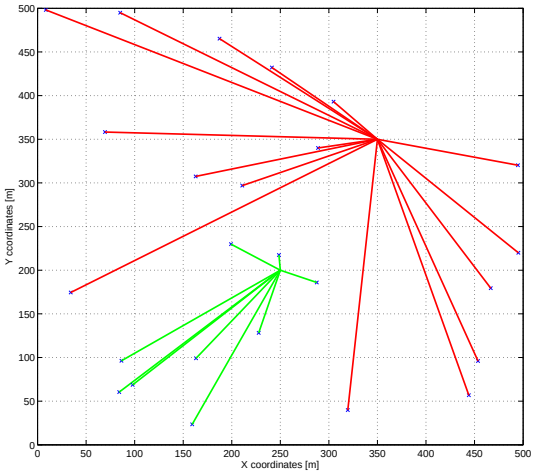

(c) Nearest BS association

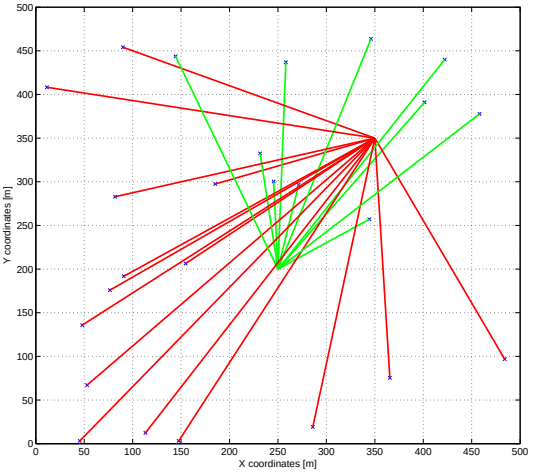

(d) Biased Received Power association with biasing factor of 10 dB

FIGURE 3.2: Different User Association Metrics

in Fig. 3.2. Fig. 3.2 depicts that pico-BS-first associates more users with pico BS as compared to the other user association techniques. In this work, we propose uplink path loss based association in which the user associates to the BS with the lowest path loss. The motivation behind using the pico-BS first [42] (or path loss) association is to associate the users with the closest BS which can help in maximizing the overall EE of the system.

3.4.2 Proposed Low Complexity Solution

Here, we consider the case of a Multi User-Multi Carrier (MU-MC) scenario with N UEs and K subcarriers in two-tier HetNets[2] subject to the maximum transmission power and minimum rate requirement constraints. In an uplink scenario, multiple users transmit data towards a BS so each communication link between user and BS introduces an individual P_C. Hence, the EE maximization problem can be formulated as:

$$\eta_{\text{EE}}^{\max} = \max \frac{\sum_{n=1}^{N} R_n + r_{k,n}}{K \times P_{\text{C}} + \sum_{n=1}^{N} P_n + p_{k,n}} \tag{3.12}$$

s.t.

$$\sum_{k=1}^{K} (\sigma_{k,n} \times p_{k,n}) \leq P^{\max}, \forall n \in \{1, \cdots, N\}$$

$$R_n \geq R_n^{\min}, \ \forall n \in \{1, \cdots, N\}$$

$$\sum_{n=1}^{N} \sigma_{k,n} = 1, \forall k \in \{1, \cdots, K\}$$

$$p_{k,n} \geq 0, \ \sigma_{k,n} \in \{0,1\}, \ \forall n,k$$

Here, σ is an $N \times K$ matrix with each element $\sigma_{k,n}$ indicating the allocation of subcarrier k to user n. Similarly, $\mathbf{P}$ is an $N \times K$ matrix with each element $p_{k,n}$ representing the allocated power to subcarrier k associated with user n. In similar manner, $\mathbf{R}$ is an $N \times K$ matrix with $r_{k,n}$ representing the allocated rate to subcarrier k associated with user n. Initially $\forall n$, R_n and P_n are set to zero.

The proposed suboptimal algorithm with low complexity consists of two stages: subcarrier allocation and power allocation. In order to maximize the EE, each subcarrier

[2] A two tier HetNet compromise of macrocell and pico BSs with no D2D pairs such that $N_C = N$ and $N_D = 0$

should be allocated to the user that can maximize the achieved rate with the minimal transmit power while satisfying the minimum-rate and maximum transmit power constraints. Once the subcarrier allocation is done, each user can calculate the optimal transmit power on its each allocated subcarrier. The solution to (3.12) can be found by taking its derivative with respect to $p_{k,n}$ and putting it equal to zero as follow:

$$\frac{\left(A+\log_2\left(1+\gamma_{k,n}{p_{k,n}}^*\right)\right)\left(1+\gamma_{k,n}{p_{k,n}}^*\right)}{\gamma_{k,n}}-B-KP_{\mathrm{C}}=0, \tag{3.13}$$

where $A=\sum_{n=1}^{N}R_n$ and $B=\sum_{n=1}^{N}P_n$. Hence, the optimal power of subcarrier k allocated to user n is given as $\min\left(P^{\max},\max\left(p^*_{k,n},p_{k,n}(R^{(k)}_{\min})\right)\right)$.

In order to find $p_{k,n}(R^{(k)}_{\min})$, the minimum-rate requirement constraint is converted into per subcarrier minimum transmission power constraint. The two different approaches are investigated namely, equal and SNR-based rate proportional allocations. In equal rate allocation approach, the minimum rate requirement $R_{\min}$ is divided equally among the subcarriers $k\in\{1,2,\cdots,|K_n|\}$ allocated to each user as follow:

$$R^{(k)}_{\min}=\frac{R_{\min}}{|K_n|}$$

The sum of the achievable rate on each subcarrier allocated to user n should be at least equal to its minimum-rate requirement according to

$$R^{(1)}_{\min}+R^{(2)}_{\min}+\cdots+R^{(|K_n|)}_{\min}\geq R_{\min}, \tag{3.14}$$

In SNR-based rate proportional mechanism, the minimum-rate constraint is distributed among the subcarriers $k \in \{1, \cdots, |K_n|\}$ allocated to user n, proportional to their respective $\gamma's$ as

$$R_{\min}^{(1)} : R_{\min}^{(2)} : \cdots : R_{\min}^{(|K_n|)} = \gamma_1 : \gamma_2 : \cdots : \gamma_{|K_n|}, \tag{3.15}$$

which can be transformed into

$$\frac{R_{\min}^{(1)}}{\gamma_1} = \frac{R_{\min}^{(2)}}{\gamma_2} = \cdots = \frac{R_{\min}^{(|K_n|-1)}}{\gamma_{|K_n|-1}} = \frac{R_{\min}^{(|K_n|)}}{\gamma_{|K_n|}}. \tag{3.16}$$

Now, by substituting (3.16) into (3.14), we get

$$\mathrm{R}_{\min}^{(|K_n|)} = \frac{R_{\min}}{\left(\frac{\gamma_1}{\gamma_{|K_n|}} + \frac{\gamma_2}{\gamma_{|K_n|}} + \cdots + \frac{\gamma_{|K_n|}}{\gamma_{|K_n|}}\right)}, \tag{3.17a}$$

$$\mathrm{R}_{\min}^{(i)} = \frac{\gamma_i}{\gamma_{i+1}} \times R_{\min}^{(i+1)},\ i = 1, 2, \cdots, |K_n| - 1. \tag{3.17b}$$

Similarly, the minimum transmission power required on each subcarrier denoted by $p_{k,n}\left(R_{\min}^{(k)}\right)$, $\forall k \in \{1, \cdots, |K_n|\}$ to satisfy the user's minimum rate requirement can be computed as:

$$p_{k,n}\left(R_{\min}^{(k)}\right) = \frac{2^{\frac{R_{\min}^{(k)}}{B_k}} - 1}{\gamma_k},\ \ \forall k = 1, 2, \cdots, |K_n|, \tag{3.18}$$

More details about the proposed algorithm can be found in Algorithms 3.1 and 3.2.

3.4.3 Simulation Results

We consider a two-tier HetNets environment with a single macrocell with 500 m radius overlaid with a pico BS with a radius of 125 m. For EE measurements, the bandwidth of

Algorithm 3.1 User Association and Energy-Efficient Resource Allocation in two-tier HetNets: A Suboptimal Approach

Initialization of variables:

N_{Total} : Total number of schedulable users in the system

$S = \{1, 2, \cdots, K\}$

$\forall n = 1$ to $N, C_n = \emptyset, P_n = 0, R_n = 0$

Step 1: User Association

Compute $\gamma_{k,n}^{(\mathrm{PB})} = \dfrac{\left|h_{k,n}^{(\mathrm{PB})}\right|^2}{\mathrm{PL}_n^{(\mathrm{PB})} N_0 B}$ and $\gamma_{k,n}^{(\mathrm{Mc})} = \dfrac{\left|h_{k,n}^{(\mathrm{Mc})}\right|^2}{\mathrm{PL}_n^{(\mathrm{Mc})} N_0 B}$

$\gamma_{k,n} = a_{\mathrm{PB},n}\gamma_{k,n}^{(\mathrm{PB})} + a_{\mathrm{Mc},n}\gamma_{k,n}^{(\mathrm{Mc})}, \forall k \in S$

Step 2: Subcarrier Allocation

For each subcarrier $k \in S$, select the user n with maximum value of $\gamma_{k,n}$

$C_n = C_n \cup \{k\}$

$S = S - \{k\}$

$\mathrm{count}_n = size\,(\mathrm{C}_n), \forall n$

Step 3: Power Allocation

If $\mathrm{count}_n = 1$,

Compute $P_n(R_{\min}) = \dfrac{2^{\frac{R_{\min}}{B_k}} - 1}{\gamma}$

Compute energy-efficient power as $\dfrac{\log_2(1+\gamma p^*)(1+\gamma p^*)}{\gamma} - P_{\mathrm{C}} = 0$

Compute optimal power as $\min\left(P_{\max}, \max\left(p^*, P_n\left(R_{\min}\right)\right)\right)$

if $P^{\max} < P_n(R_{\min})$

No Feasible Solution exists, call Algorithm 3.2

else $(\forall k \in C_n,)$

Transform R_{min} into $R_{\min,n}^{(k)}$ over the number of allocated subcarriers $k \in C_n$ to user n using (3.17a) and (3.17b)

Compute optimal power ${p_{k,n}}^*$ satisfying the power constraint for multi-user multi-subcarrier case using (3.13)

Check the maximum transmit power violation for each user otherwise call Algorithm 3.2.

end If

each subcarrier is 180 kHz. The minimum-rate requirement for each user is considered as 0.42 b/s/Hz. The maximum transmission power of macrocell and pico BS are 20 W and 200 mW respectively whereas the value of circuit power is $P_C = 100$ mW. We assume that the total number of users $N = 25$ are uniformly distributed within the simulated scenario. The path-loss model for macrocell and pico BS are given as $\mathrm{PL(dB)} = 34 + 40\log_{10}(d_n)$

Algorithm 3.2 Reallocate the Subcarriers

Step 1: U is the set of users not satisfying the minimum rate requirement

While $U \neq 0$

(a) Select a user $n \in U$

(b) Randomly select a subcarrier $k \in \{1, \cdots, K\}$ such that $k \notin C_n$

(c) Let x be an owner of subcarrier k and to check by removing k whether x can still satisfy the R_{min} constraint

If $\hat{p}_x^k(R_{\min}) \leq P_{\max}$

$C_n = C_n \cup \{k\}$

$C_x = C_x - \{k\}$

else

goto (b)

else If (no more subcarrier k)

break While;

goto (a)

end If

Compute the new minimum required power and compare it with $P_{\max}$

Remove n from U and goto (a)

Step 2:

Finally the EE of the system is given as follow:

$$\eta_{\text{total}}^* = \frac{\sum_{n=1}^{N} R^n}{\mathrm{N}_{\text{total}} \times P_{\mathrm{C}} + \sum_{n=1}^{N} P^n}$$

and $\mathrm{PL(dB)} = 37 + 30\log_{10}(d_n)$ [41], where d_n is the is the distance of a user n from the BS in km and therefore, $PL_n^M = 10^{(PL_n^M(\mathrm{dB})/10)}$ and $PL_n^P = 10^{(PL_n^P(\mathrm{dB})/10)}$. The noise spectral density is assumed to be $N_0 = -141$ dBm/Hz.

We investigate the effects of the proposed SNR-based rate proportional allocation as opposed to the equal rate allocation on EE in MU-MC case with $N = 25$ and $K = 5$ in Fig. 3.3. Fig. 3.3 shows that the EE increases with the number of users and the SNR-rate proportional approach enhances the EE in the order of 10.2% (when N=25 and K=5) as compared to the equal rate allocation approach. This increase in EE is due to the fact that SNR-based rate proportional approach allocates higher rates (with lower power) to

subcarriers with higher SNRs.

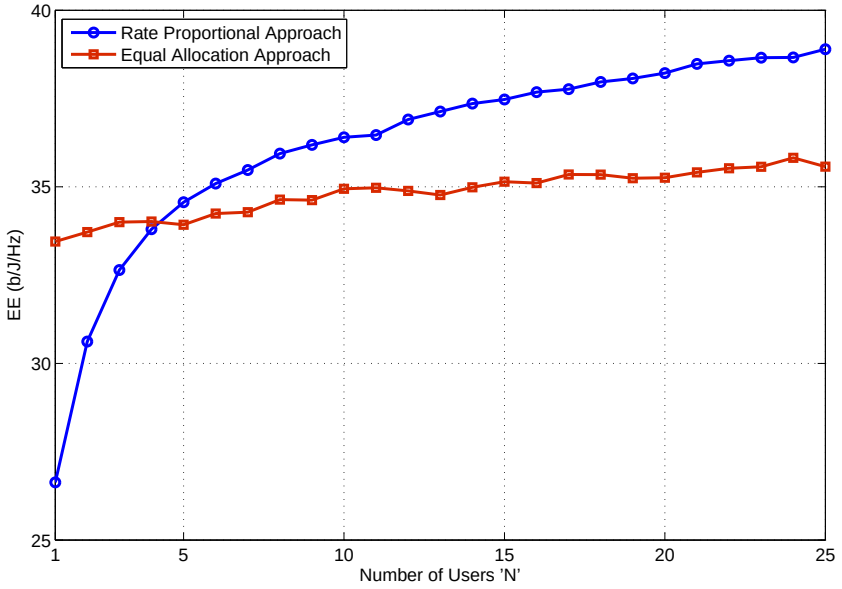

FIGURE 3.3: Achievable EE (measured in b/J/Hz) with $K = 5$ and $N = 25$ for proposed SNR rate proportional and equal rate allocation approaches.

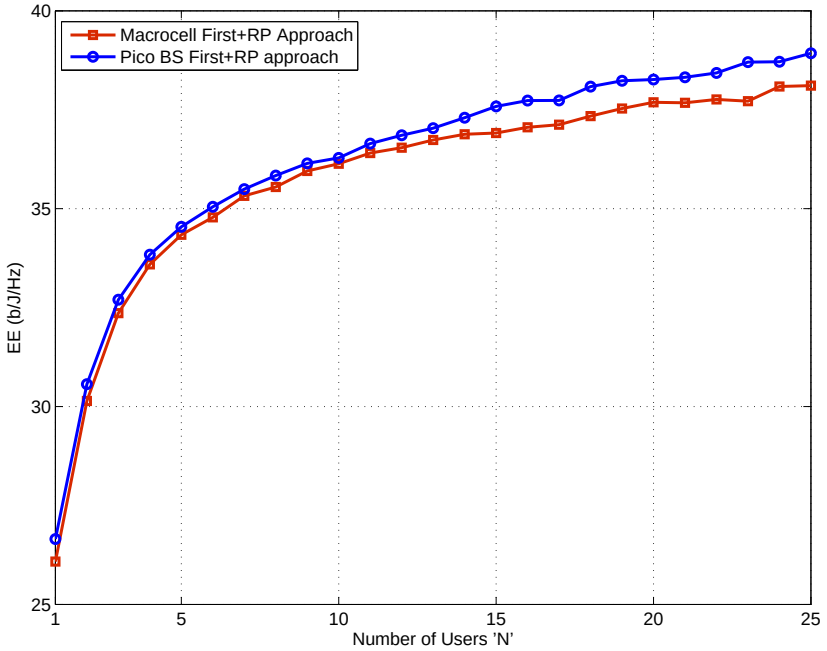

FIGURE 3.4: Performance of EE (measured in b/J/Hz) for pico BS first and Macrocell first user association scheme for varying number of users N with $K = 5$ and $P_C = 100$ mW.

We further investigate the impact of Macrocell-first and pico-BS-first user associations on EE while considering SNR-based rate proportional approach.Fig. 3.4 reveals that the EE of pico-BS-first user association is in order of 2.6% when compared to the EE of Macrocell-first for the case where $N_M >> N_P$. As the EE increases with the number of users, the pico-BS-first association will achieve higher EE at the cell boundary users. Since the large coverage area of Macrocell-first user association causes higher path loss for users far away from BS, higher transmit powers, which results in lower EE, is required to maintain the QoS of such users. In short, the pico-BS-first association could be a useful technique to offload the cell edge users from macrocell to pico BS, and as a result, increases the EE of the system.

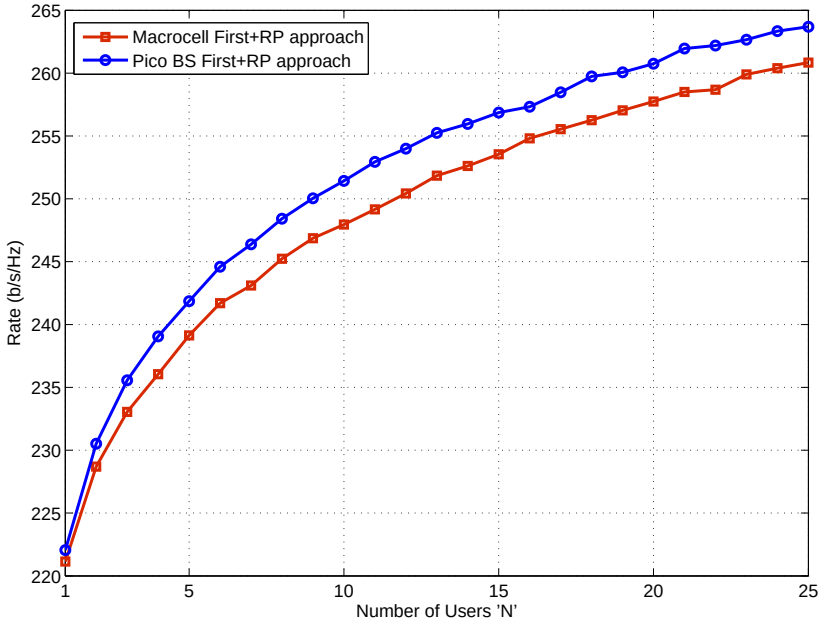

FIGURE 3.5: Performance of throughput b/s/Hz for pico BS first and Macrocell first user association schemes with $K = 5$, $P_C = 100$ mW and $N = 25$.

We also study the throughput for SNR-based rate proportional and equal rate allocation approaches for different user associations with $N = 25, K = 5$ and $P_C = 100$ mW as shown in Fig. 3.5. Fig. 3.5 depicts that pico-BS-first marginally performs better in terms of

throughput by utilizing the lower path-loss property as compared to the Macrocell-first. Similarly, an increase in P_C causes reduction in the overall EE of the system.

3.5 Optimising User Association and Power Allocation in Device-to-Device enabled Heterogeneous Networks

3.5.1 Related Work

A multi-tier architecture for 5G networks consisting of macrocell overlaid with small cells (e.g. pico BS) with provision of relays and device-to-device (D2D) networks is needed to satisfy the quality-of-service (QoS) requirements in a spectrum and energy-efficient manner. A D2D pair consists of a D2D transmitter and a D2D receiver lying in close proximity of each other. The concept of D2D communications in cellular networks is to allow the D2D pair in close proximity of each other to directly communicate instead of using a cellular infrastructure.

On the other hand, one of the solutions to jointly improve the system throughput and to reduce the energy consumption is using heterogeneous networks (HetNets) consisting of low-power small cells (e.g., microcells, picocells, and femtocells) overlaid within the macrocell geographical area, deployed by network operator who share the same spectrum with the macrocells [41]. Each promising solution alone is unlikely to meet the QoS and throughput requirements for 5G [2]. One of the promising solution is a three-tier hierarchical HetNets in which the two above mentioned technologies can coexist in parallel to improve the network performance. In tier 1, the macrocell is used to ensure outdoor coverage whereas in tier 2, small cells are used to serve the users with low mobility in indoor and outdoor coverage. In tier 3, the users in both macrocell and small cell coverage areas can engage to communicate directly using D2D communication.

The radio resource management (RRM) mechanism in D2D communication consist of mode selection, resource allocation and power control [43]. The spectrum sharing among D2D and cellular users can be classified as either overlay or underlay. In overlay spectrum sharing scheme, the orthogonal resources are dedicated to both cellular and D2D users in order to avoid mutual interference, whereas the D2D users are allowed to reuse

the resources occupied by the cellular users to improve the spectral efficiency in underlay spectrum sharing scheme [43]. One of the important RRM decisions in the D2D communication is mode selection mechanism in order to determine one of the possible three communication modes namely as cellular, dedicated (or orthogonal resource sharing) or reuse (or non-orthogonal resource sharing) mode.

In cellular mode, the two users can communicate with each other through cellular infrastructure whereas in dedicated mode the D2D pairs can communicate directly using the exclusively dedicated resources to avoid the mutual interference between D2D users and cellular users at the cost of reduced spectrum utilization. In reuse mode, the D2D pairs directly communicate with each other by reusing the partial or all of the resources currently occupied by the cellular user. One of the challenges in the reuse mode is to assign the reusing resources such that the co-channel interference between cellular and D2D links can be mitigated.

EE is, in fact, one of the key performance indicators for the next generation wireless communications systems. However, most of EE gains are achieved with sacrifices in SE. Most of the work in the literature mainly focuses on either maximizing the system throughput (e.g., [43] [44]) or EE (e.g., [45] [40]) for two-tier cellular networks (i.e., macrocell overlaid with D2D communication). In this direction, a pricing scheme for two-tier 5G networks using game theory and auction theory as mentioned is proposed in [46] which also outlines the significant gains achieved by both operators and users in two-tier cellular networks as compared to the macrocell only system. A joint mode selection, channel assignment and power control to maximise the system throughput for two-tier cellular networks is proposed in [47]. The problem is decomposed into two subproblems where the power control subproblem is solved by using standard optimization method, and the mode selection and subchannel assignment subproblem is solved using branch-and-bound (BB) method. A low complexity distributed resource allocation mechanism based on auction theory in multi-tier heterogeneous networks is proposed in [48]. The objective of the considered resource allocation scenario is to maximise the achievable throughput of the small cell and D2D users as long as the interference caused to the macrocell users are within a predefined threshold.

To the best of our knowledge, there is no work in the literature to jointly optimize the ASE-AEE tradeoff radio resource allocation in multi-tier HetNets overlaid with D2D communication (or Hierarchical HetNets) considering multi-user multi-carrier systems in distributed manner. In this work, we address the ASE-AEE tradeoff resource allocation technique in an uplink of hierarchical HetNets. By exploiting the fractional programming concept, the optimization problem can be transformed into its equivalent subtractive form which is tractable. Numerical results demonstrate the impact of the required AEE level and the transmit power constraints on the ASE-AEE tradeoff. It is worth to mention that the scope of this paper is not to investigate the benefits of D2D communication itself, but rather its opportunistic integration with HetNets to satisfy the requirements for 5G networks to achieve higher data rates with lower energy consumption.

3.5.2 System Setup

Each D2D pair $n \in \mathcal{N}_{\mathrm{D}}$ consists of a D2D transmitter and a D2D receiver. It is assumed that the neighbour discovery algorithms (e.g., [49] [50]) already exists to establish the D2D communication and the D2D proximity $r_{\max}$ is the maximum distance between the D2D pair due to the maximum transmit power $P_n^{\max}$ of a user and the receiver sensitivity [51]. It should be noted that the potential D2D user does not necessarily select the dedicated mode. The mode is selected based on a mode selection scheme presented later in the paper. It is also worthwhile to mention that due to the practicality reasons, it is assumed that $C > D$. Each D2D pair can communicate in two modes, i.e., cellular or dedicated. In cellular mode, the D2D transmitter communicate with a D2D receiver with the help of the macrocell or pico BS, whereas in dedicated mode, the D2D transmitter directly communicates with a D2D receiver.

Depending on this assumption, each D2D pair and cellular users will be allocated dedicated subcarriers for the case of $K > C + D$. In the case of $C < K < C + D$, some D2D pairs will use dedicated subcarriers whereas others will reuse the subcarriers allocated to the cellular users resulting in mutual interference. Similarly, in the case of $K \leq C$, all the D2D pairs need to reuse the subcarriers allocated to the cellular users. For example, Let D_{N} be the number of D2D pairs which cannot reuse the subcarriers allocated to the

cellular user. If $D_{\mathrm{N}} \leq K - C$, it means that all the D2D pairs can communicate as the number of available dedicated subcarriers are $K - C$. Similarly, if $D_{\mathrm{N}} > K - C$, it means that atleast $D_{\mathrm{N}} - K + C$ D2D pairs cannot communicate which is dependent on the level of interference caused by the D2D pair to the cellular user.

Furthermore based on the system model described in Section 3.3, AEE (η_{AEE}) of the three-tier HetNet can be defined as the sum of the amount of data transferred per unit energy consumed by the macrocell, the small-cell and D2D communication per unit bandwidth per unit coverage area (b/J/Hz/km^2) and can be expressed as

$$\eta_{\mathrm{AEE}} = \frac{\eta_{\mathrm{EE}}}{\theta} = \frac{\eta_{\mathrm{EE}}}{A \times B}, \tag{3.19}$$

where A represents the total coverage area and B is the total occupied bandwidth. SE (η_{SE}), on the other hand, is a measure that reflects the efficient utilization of the available spectrum in terms of throughput and it is commonly expressed in (b/s/Hz). η_{SE} is strictly increasing with transmission power P_{T} and is concave in P_{T}. η_{SE} is defined as:

$$\eta_{\mathrm{SE}} = \frac{R}{B}, \tag{3.20}$$

The ASE of the three-tier HetNet is defined as the sum of the achievable rates of the macrocell, the small-cell and D2D communication per unit bandwidth per unit coverage area (b/s/Hz/km^2) and can be formulated as

$$\eta_{\mathrm{ASE}} = \frac{R}{\theta}. \tag{3.21}$$

3.5.3 Problem Formulation of ASE-AEE Tradeoff

In order to analyse the ASE-AEE tradeoff, we formulate the optimisation problem to maximise ASE subject to a required AEE level and maximum transmission power constraints. The maximisation problem can be mathematically expressed as

$$\eta_{\{\mathrm{ASE,AEE}\}} = \max_{\sigma_{k,n}^{(m_n)}, p_{k,n}^{(m_n)}} \left(\frac{\sum_{m_n=0}^{1} \sum_{k=1}^{K} \sum_{n=1}^{N} \sigma_{k,n}^{(m_n)} r_{k,n}^{(m_n)}}{\theta} \right) \tag{3.22a}$$

s.t.

$$\frac{\sum_{m_n=0}^{1}\sum_{k=1}^{K}\sigma_{k,n}^{(m_n)}r_{k,n}^{(m_n)}}{\theta\left(\varepsilon_0\sum_{m_n=0}^{1}\sum_{k=1}^{K}p_{k,n}^{(m_n)}+P_{\mathrm{C}}\right)}\geq\eta_n^{\mathrm{req}},\forall n. \tag{3.22b}$$

$$\sum_{m_n=0}^{1}\sum_{k=1}^{K}\sigma_{k,n}^{(m_n)}p_{k,n}^{(m_n)}\leq P_n^{\max},\forall n. \tag{3.22c}$$

$$\sum_{m_n=0}^{1}\sum_{n=1}^{N}\sigma_{k,n}^{(m_n)}\leq 1,\forall k. \tag{3.22d}$$

$$p_{k,n}^{(m_n)}\geq 0,\sigma_{k,n}^{(m_n)}\in\{0,1\},\ \forall n,\forall k,\forall m. \tag{3.22e}$$

In (3.22a), $\eta_{\{\mathrm{ASE,AEE}\}}$ represents the ASE-AEE tradeoff objective function and $\sigma_{k,u}^{(m_n)}$ is a binary variable to indicate whether the subcarrier k is assigned to the user u with mode m_n or not, where $m_n\in\{0,1\}$. For the user $n\in\mathcal{N}_{\mathrm{C}}$, which is a cellular user with only the cellular mode of transmission, and hence $\sigma_{k,n}^{(1)}=0$. Further, η_n^{req} denotes the required AEE level. Specifically, the ratio of the total required achievable AEE over the total maximum achievable AEE is referred to as the AEE-loss-rate and can be expressed as follow:

$$\alpha_{\mathrm{AEE}}=\frac{\eta^{\mathrm{req}}}{\eta^{\max}}=\frac{\sum_{n=1}^{N}\eta_n^{\mathrm{req}}}{\sum_{n=1}^{N}\eta_n^{\max}}, \tag{3.23}$$

where $0\leq\alpha_{\mathrm{AEE}}\leq 1$. Similarly, we define the ASE that can be achieved corresponding to $\eta^{\max}$ by $\mathrm{ASE}_{\eta^{\max}}$. The ASE-gain-rate is the ratio of $\mathrm{ASE}_{\eta^{\mathrm{req}}}$ over $\mathrm{ASE}_{\eta^{\max}}$ and can be formulated as follow:

$$\alpha_{\mathrm{ASE}}=\frac{\mathrm{ASE}_{\eta^{\mathrm{req}}}}{\mathrm{ASE}_{\eta^{\max}}}. \tag{3.24}$$

It is worth to mention that for any required η_n^{req} level, there exists two optimal points for η_{ASE} for the case of $P_n^{\max}\geq P_{\eta^{\max}}$. As our optimization problem is to maximize the η_{ASE}, we will always choose the achievable $\mathrm{ASE}_{\eta^{\mathrm{req}}}$ which lies on the right side of the achievable $\eta_n^{\max}$.

3.5.3.1 Optimal Power Allocation

The maximisation problem (3.22*a*) is an integer combinatorial fractional programming problem and is generally NP-hard. For better tractability, we first relax the integer variables, $\sigma_{k,n}^{(m_n)} \in \{0,1\}$ into continuous variables, $\tilde{\sigma}_{k,n}^{(m_n)} \in [0,1]$. The $\eta_{\{\text{ASE,AEE}\}}$-maximisation problem, hence, can be expressed as

$$\eta_{\{\text{ASE,AEE}\}} = \max_{\tilde{\sigma}_{k,n}^{(m_n)}, p_{k,n}^{(m_n)}} \frac{\sum_{m_n=0}^{1}\sum_{k=1}^{K}\sum_{n=1}^{N}\tilde{\sigma}_{k,n}^{(m_n)} r_{k,u}^{(m_n)}}{\theta} \tag{3.25a}$$

s.t.

$$\frac{\sum_{m_n=0}^{1}\sum_{k=1}^{K}\tilde{\sigma}_{k,n}^{(m_n)} r_{k,n}^{(m_n)}}{\theta\left(\varepsilon_0\sum_{m_n=0}^{1}\sum_{k=1}^{K}p_{k,n}^{(m_n)} + P_{\text{C}}\right)} \geq \eta_n^{\text{req}}, \forall n. \tag{3.25b}$$

$$\sum_{m_n=0}^{1}\sum_{k=1}^{K}\sigma_{k,n}^{(m_n)} p_{k,n}^{(m_n)} \leq P_n^{\max}, \forall n. \tag{3.25c}$$

$$\sum_{m_n=0}^{1}\sum_{n=1}^{N}\tilde{\sigma}_{k,n}^{(m_n)} \leq 1, \forall k. \tag{3.25d}$$

$$p_{k,n}^{(m_n)} \geq 0, \tilde{\sigma}_{k,n}^{(m_n)} \in \{0,1\}, \ \forall n, \forall k, \forall m. \tag{3.25e}$$

The constraint (3.25b) in fractional form can be transformed into its equivalent subtractive form and can be rewritten as

$$\sum_{m_n=0}^{1}\sum_{k=1}^{K}\tilde{\sigma}_{k,n}^{(m_n)} r_{k,n}^{(m_n)} - \eta_n^{\text{req}}\theta\left(\varepsilon_0\sum_{m_n=0}^{1}\sum_{k=1}^{K}p_{k,n}^{(m_n)} + P_{\text{C}}\right) \geq 0 \tag{3.26}$$

We utilise the dual decomposition approach to solve the optimisation problem (3.25a). It is shown that the dual-composition approach has lower computational complexity and the duality gap for non-convex optimisation approaches to zero for sufficiently large number of subcarriers [52]. In order to apply dual decomposition method, we first need to find the Lagrangian function of (3.25a). Using standard optimisation methods proposed in [52],

the Lagrangian function of (3.25a) can be written as:

$$L\left(p_{k,n}^{(m_n)},\lambda_n\right)=\frac{1}{\theta}\sum_{m_n=0}^{1}\sum_{k=1}^{K}\sum_{n=1}^{N}\tilde{\sigma}_{k,n}^{(m_n)}r_{k,n}^{(m_n)}+\sum_{n=1}^{N}\lambda_n\Bigg(\sum_{m_n=0}^{1}\sum_{k=1}^{K}\tilde{\sigma}_{k,n}^{(m_n)}r_{k,n}^{(m_n)} -\eta_n^{\mathrm{req}}\theta\left(\varepsilon_0\sum_{m_n=0}^{1}\sum_{k=1}^{K}p_{k,n}^{(m_n)}+P_{\mathrm{C}}\right)\Bigg) \tag{3.27}$$

The equivalent dual problem can be decomposed into two subproblems, which is given by

$$\min_{\lambda_n\geq 0}\max_{p_{k,n}^{(m_n)}\geq 0} L\left(p_{k,n}^{(m_n)},\lambda_n\right) \tag{3.28}$$

The dual problem can be decomposed into two layers, namely, lower layer and master layer. In the lower layer, K subproblems are solved in parallel to compute the power and subcarrier allocation on each subcarrier $k\in K$ for the given values of λ_n. In the master layer, the Lagrangian multipliers are updated using subgradient method. By applying the Karush-Kuhn-Tucker (KKT) conditions, we get

$$\frac{\partial L\left(p_{k,n}^{(m_n)},\lambda_n\right)}{\partial p_{k,n}^{(m_n)}}=\begin{cases}>0, & p_{k,n}^{(m_n)}=P_n^{\max}\\ =0, & 0<p_{k,n}^{(m_n)}<P_n^{\max}\\ <0, & p_{k,n}^{(m_n)}=0\end{cases}$$

At the optimal power allocation ${p_{k,n}^{(m_n)}}^*$, we have

$$\left.\frac{\partial L\left(p_{k,n}^{(m_n)},\lambda_n\right)}{\partial p_{k,n}^{(m_n)}}\right|_{p_{k,n}^{(m_n)}={p_{k,n}^{(m_n)}}^*}=0,\Rightarrow \tag{3.29a}$$

$$\left(1+\gamma_{k,n}^{(m_n)}{p_{k,n}^{(m_n)}}^*\right)=\frac{B_k\gamma_{k,n}^{(m_n)}\left(1+\frac{1}{\theta\lambda_n}\right)}{\eta_n^{\mathrm{req}}\varepsilon_0\theta\ln(2)}, \tag{3.29b}$$

From (3.29b), the optimal power distribution scheme can be found as

$$p_{k,n}^{(m_n)*} = \begin{cases} \left[\frac{B_k\left(1+\frac{1}{\theta\lambda_n}\right)}{\eta_n^{\text{req}}\varepsilon_0\theta\ln(2)} - \frac{1}{\gamma_{k,n}^{(m_n)}} \right]^+, & \text{if } \tilde{\sigma}_{k,n}^{(m_n)} = 1. \\ 0, \quad \text{otherwise.} \end{cases} \tag{3.30}$$

where $[x]^+ = \max[0,x]$. Therefore, a feasible subcarrier assignment matrix for subcarrier $k \in K$ is given as:

$$\tilde{\sigma}_{k,n}^{(m_n)} = \begin{cases} 1, & \text{if } (m_n^*, n^*) = \arg\max_{m_n,n} r_{k,n}^{(m_n)}, \forall k \in K \\ 0, & \text{otherwise.} \end{cases} \tag{3.31}$$

where $\tilde{\sigma}_{k,n}^{(m_n)} = 1$ indicates that the subcarrier k is assigned to user n with the mode m_n. When using the optimal power from (3.30), the achieved rate of each user n on subcarrier k working in the mode m_n is computed as $r_{k,n}^{(m_n)} = B_k \log_2\left(1+\gamma_{k,n}^{(m_n)} p_{k,n}^{(m_n)}\right)$. In general, the user n on subcarrier k will choose the dedicated mode $m_n = 1$ if and only if the $r_{k,n}^{(m_n=1)} \geq r_{k,n}^{(m_n=0)}$ and otherwise it will choose cellular mode.

Therefore, optimal value for λ_n (referred to as λ_n^*) can be found such that the constraint (3.26) is satisfied with equality, yielding

$$\sum_{m_n=0}^{1}\sum_{k=1}^{K} B_k \log_2\left(1+\gamma_{k,n}^{(m_n)}\left[\frac{B_k\left(1+\frac{1}{\theta\lambda_n}\right)}{\eta_n^{\text{req}}\varepsilon_0\theta\ln(2)} - \frac{1}{\gamma_{k,n}^{(m_n)}}\right]^+\right)$$
$$-\eta_n^{\text{req}}\theta\left(\varepsilon_0\sum_{m_n=0}^{1}\sum_{k=1}^{K}\left[\frac{B_k\left(1+\frac{1}{\theta\lambda_n}\right)}{\eta_n^{\text{req}}\varepsilon_0\theta\ln(2)} - \frac{1}{\gamma_{k,n}^{(m_n)}}\right]^+ + P_{\text{C}}\right) = 0$$

For solving the minimisation problem, the Lagrangian multiplier can be updated by using the subgradient method [52]. The subgradient of λ_n are given by taking the derivative of $L\left(p_{k,n}^{(m_n)}, \lambda_n\right)$ with respect to λ_n, yielding

$$\frac{\partial L\left(p_{k,n}^{(m_n)}, \lambda_n\right)}{\partial \lambda_n} = \sum_{m_n=0}^{1}\sum_{k=1}^{K} \tilde{\sigma}_{k,n}^{(m_n)} r_{k,n}^{(m_n)} - \eta_n^{\text{req}}\theta$$

$$\left(\varepsilon_0 \sum_{m_n=0}^{1}\sum_{k=1}^{K} p_{k,n}^{(m_n)} + P_{\mathrm{C}}\right)$$

Then, λ_n are updated by using the subgradient method as

$$\lambda_n(i+1) = \left(\lambda_n(i) - \frac{s^i}{\sqrt{i}}\beta_n\right), \tag{3.32}$$

where $i \geq 0$ is the iteration index, s^i is the positive step size which is taken in the direction of the negative gradient for the dual variable at iteration i and β_n is given as follow:

$$\beta_n = \sum_{m_n=0}^{1}\sum_{k=1}^{K} \tilde{\sigma}_{k,n}^{(m_n)} r_{k,n}^{(m_n)} - \eta_n^{\mathrm{req}}\theta\left(\varepsilon_0 \sum_{m_n=0}^{1}\sum_{k=1}^{K} p_{k,n}^{(m_n)} + P_{\mathrm{C}}\right) \tag{3.33}$$

Based on $p_{k,n}^{(m_n)^*}$ (obtained from (3.30)) and $P_n^{\max}$, the solution for the maximization problem (3.25a) can be divided into two regions. When $p_{k,n}^{(m_n)^*} \geq P_n^{\max}$, the optimal solution of (3.25a) can then be expressed as $p_{k,n}^{(m_n)^*} = \min\left(p_{k,n}^{(m_n)^*}, P_n^{\max}\right)$. However, when $p_{k,n}^{(m_n)^*} \leq P_n^{\max}$, the optimal solution for (3.25a) is given by (3.30).

Algorithm 3.3 Joint Mode selection, Subcarrier and Power Allocation in D2D enabled HetNets

Input: $[\eta_n^{\mathbf{req}}, \varepsilon_0, \gamma_{k,n}^{(m)}]$
Step 1: Initialize
$i = 0$, $p_{k,n}^{(m_n)} = 0, \lambda_n^{(i)} = 0.01$, **for** $n = 1, \cdots, N$,
$k = 1, \cdots, K, m = 1, \cdots, M$.
Step 2:
For $k = 1 : K$
Calculate $p_{k,n}^{(m_n)}$ according to (3.30).
Obtain the mode selection and the subcarrier assignment according to (3.31).
end **For**
Step 3:
$i = i + 1$
Update $\lambda_n^{(i+1)}$ according to (3.32).
Step 4:
Repeat steps (2)-(3) until $\lambda_n^{(i+1)}$ are converged.
Output: $\left[p_{k,n}^{(m_n)}, \tilde{\sigma}_{k,n}^{(m_n)}, m_n\right]$

3.5.4 Simulation Results

We consider a three-tier Hierarchical HetNet environment with a single macrocell with $R_{\mathrm{M}} = 500$ m, as otherwise stated overlaid with uniformly distributed $N = 40$ pico BSs (where N is calculated as mentioned in [53]) of $R_{\mathrm{m}} = 50$ m. The pico BS's are deployed at the edge of a macrocell. The bandwidth of each subcarrier is 31.25 kHz. The maximum transmission power of users considered in the simulation is 200 mW and the value of circuit power of users is set fixed to $P_{\mathrm{C}} = 50$ mW. We assume that the users are uniformly distributed within the simulated scenario. The noise spectral density is assumed to be $N_0 = -174$dBm/Hz. In this work, the power amplifier efficiency is assumed as 38% i.e. $\varepsilon_0 = \frac{1}{0.38}$. The maximum transmission power for all users are same, hence, $P_n^{\max}$ will be referred to as $P^{\max}$. All the simulation results presented are averaged over 10,000 channel realizations.

Fig. 3.6 demonstrates the achievable AEE versus the macrocell radius R_{M} for various values of α_{AEE}. Due to the weaker SNR for the mobile user in the macrocell, the degradation of AEE is obvious due to the fact that more users transmit with their maximum transmission power with an increase in R_{M}. The hierarchical HetNet outperforms in terms of AEE as compared to the traditional HetNets and macrocell only system by 6.55% and 496% respectively, at $R_{\mathrm{M}} = 300$ m. This is due to the fact that the dedicated mode in hierarchical HetNet allows the cell edge users to communicate directly which enhances the overall system AEE as compared to the traditional HetNets.

Similalrly, the plot of achievable ASE versus the macrocell radius R_{M} for various values of α_{AEE} is shown in Fig. 3.7. Generally, as the AEE requirement level is reduced from $\eta_n^{\max}$ to $0.985\eta_n^{\max}$, each user will transmit with more power resulting in a higher achieved ASE and a lower achieved AEE. For example, in hierarchical HetNets by reducing the α_{AEE} from 100% to 98.5% (with only 1.5% loss in AEE) achieve an ASE gain for any value of R_{M}. Specifically, with $R_{\mathrm{M}} = 300m$, the ASE is improved from 374.3 b/s/Hz/km^2 to 395.8 b/s/Hz/km^2. It is also worthwhile to mention that ASE is non-decreasing with the respect of α_{AEE} whereas AEE is non-increasing with the respect of α_{AEE}. When $\alpha_{\mathrm{AEE}} = 100\%$ the tradeoff solution maximize the AEE whereas at the smaller values of

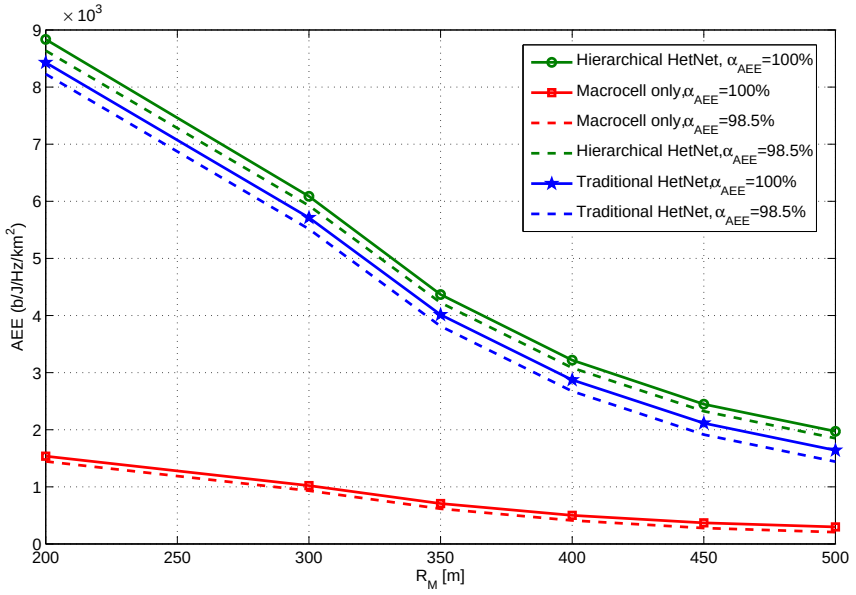

FIGURE 3.6: Comparison of AEE versus R_{M} with $N = 100$ and $K = 100$ for various α_{AEE} in three different configurations: (i) Macrocell only network, (ii) Traditional HetNet and (iii) Hierarchical HetNet with $N_d = 20$.

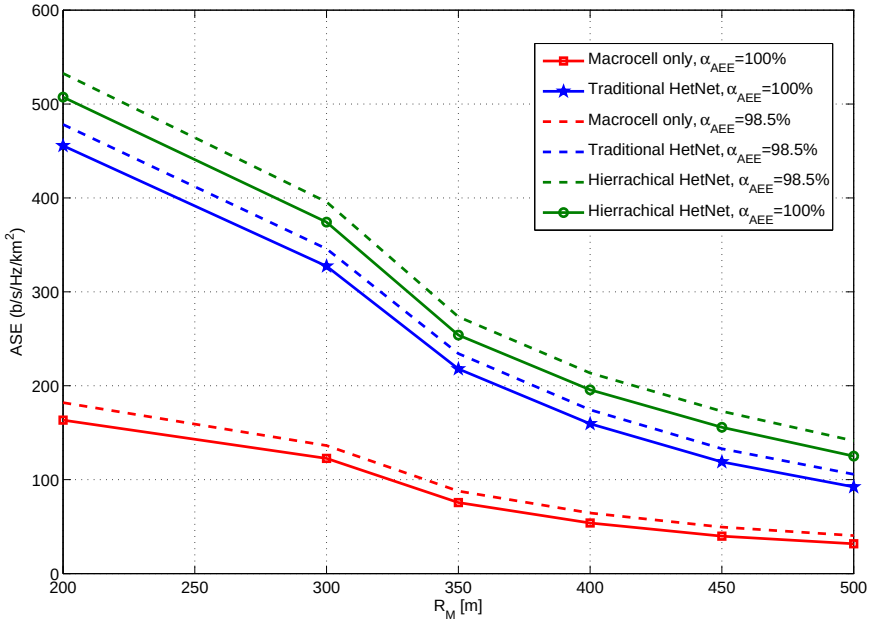

FIGURE 3.7: Comparison of ASE versus R_{M} with $N = 100$ and $K = 100$ for various α_{AEE} in three different configurations: (i) Macrocell only network, (ii) Traditional HetNet and (iii) Hierarchical HetNet with $N_d = 20$.

$\alpha_{\mathrm{AEE}} \approx 0\%$ the tradeoff solution maximize the ASE.

Fig. 3.8 demonstrates the total transmit power consumption of the macrocell only,

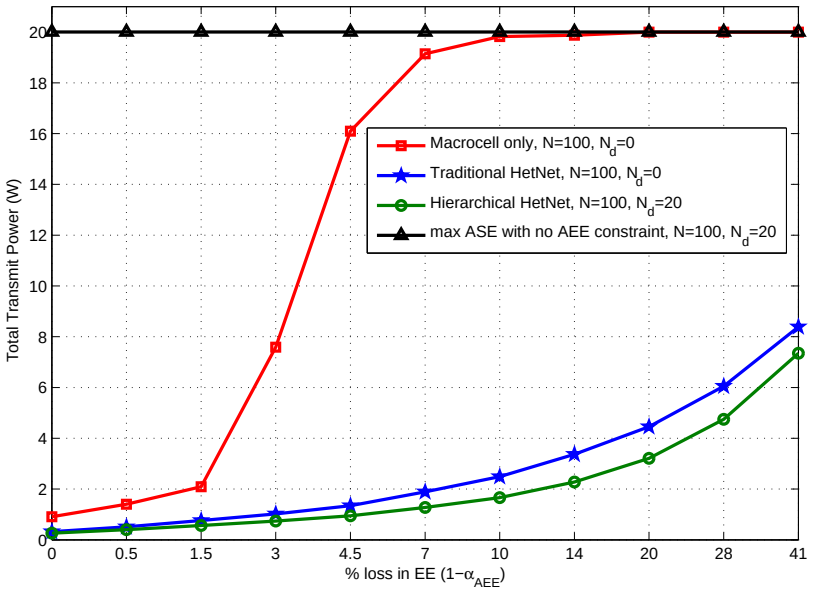

FIGURE 3.8: Total transmit power versus $(1-\alpha_{\text{AEE}})$ with $P^{\max} = 0.2$ W, $P_C = 0.05$ W, and $B_k^{(m)} = 31.25$ kHz.

traditional HetNets and Hierarchical Hetnets against the ratio of loss in AEE to the maximum achievable AEE; that is $1-\alpha_{\text{AEE}}$. With an increase in the value of $(1-\alpha_{\text{AEE}})$, the ASE gain increases, hence require the users to transmit with more power as long as $P^{\max} \geq P_{\eta^{\text{req}}}$. It is quite obvious that the Hierarchical HetNet users transmit with lower power due to close proximity between the D2D transmitter and receiver as compared to the pico BS and macrocell users. The Hierarchical HetNet users can reduce their transmit power with $R_{\text{M}} = 500$ m and $(1-\alpha_{\text{AEE}}) = 7\%$ upto 48.51% and 1404% as compared to the traditional HetNet and macrocell, respectively. Fig. 3.8 also depicts that the total transmit power is equal to the total available transmit power of 20 W irrespective of the value of $(1-\alpha_{\text{AEE}})$ in maximization ASE with no requirement AEE level as compared to the maximization ASE with the required AEE level where the total transmit power is dependent on the value of $(1-\alpha_{\text{AEE}})$. At the value of $(1-\alpha_{\text{AEE}}) = 10\%$, the total transmit power in the macrocell only system converges to the total available transmit power of 20 W.

Fig. 3.9 shows the AEE and ASE tradeoff for traditional HetNets and Hierarchical HetNets for the corresponding $P^{\max} = 0.2$ W and $P_{\text{C}} = 0.05$ W. As the required AEE level

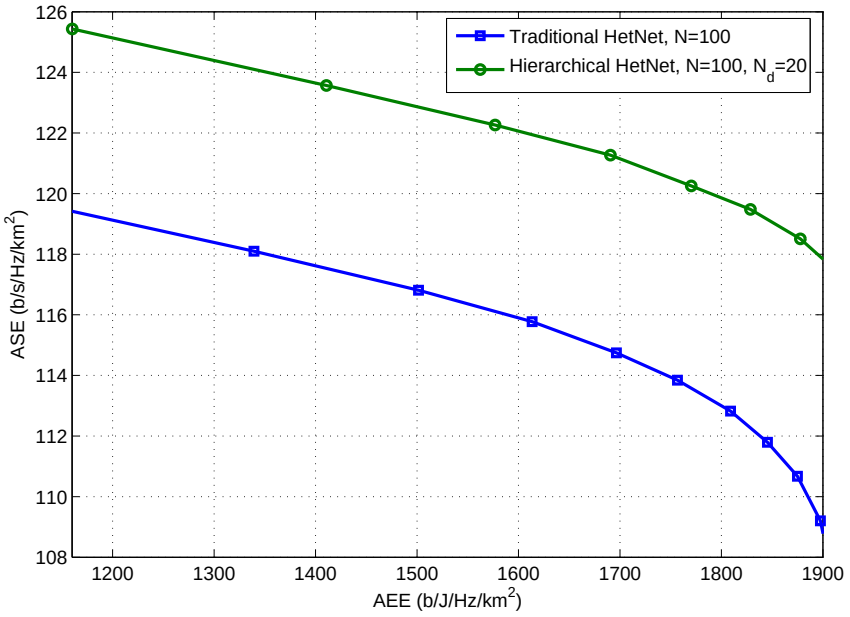

FIGURE 3.9: Achievable ASE versus required AEE level with $P^{\max} = 0.2$ W, $P_C = 0.05$ W, and $B_k^{(m)} = 31.25$ kHz.

is varied from 1160 b/J/HZ/km^2 to 1900 b/J/HZ/km^2, the corresponding ASE is obtained by Algorithm I. For the case of $P^{\max} \leq P^*_{\eta^{\max}}$, the maximum achievable ASE is limited by $P^{\max}$, resulting in lower AEE, as compared to the $\eta^{\max}$. As the required AEE level is increased, the corresponding achievable ASE is reduced. At the required AEE level of 1400 b/J/Hz/km^2, the corresponding ASE in the traditional and hierarchical HetNets are approximately 118 b/s/Hz/km^2 and 124 b/s/Hz/km^2, respectively. When the required AEE level is increased close to the $\eta^{\max}$, a significant loss in ASE occurs,causing the corresponding ASE of the traditional and hierarchical HetNets to 107 b/s/Hz/km^2 and 118 b/s/Hz/km^2 respectively. It should be mentioned that the achievable ASE of approximately 118 b/s/Hz/km^2, is obtained at the corresponding AEE level of 1900 b/J/Hz/km^2 and 1160 b/J/Hz/km^2 in the hierarchical and traditional HetNets respectively.

Fig.3.10 shows the plots for α_{AEE} in percentage versus the α_{ASE} in percentage for the traditional and Hierarchical HetNets. It also demonstrates that α_{ASE} monotonically increases with the decrease of α_{AEE}. Fig. 3.10 shows that a minor loss in AEE around its maximum (when α_{AEE} is close to 100%) results in a significant gain in ASE (i.e., rapid increase in α_{ASE}). When α_{AEE} is reduced beyond 95% , the gain in α_{ASE} versus reduction

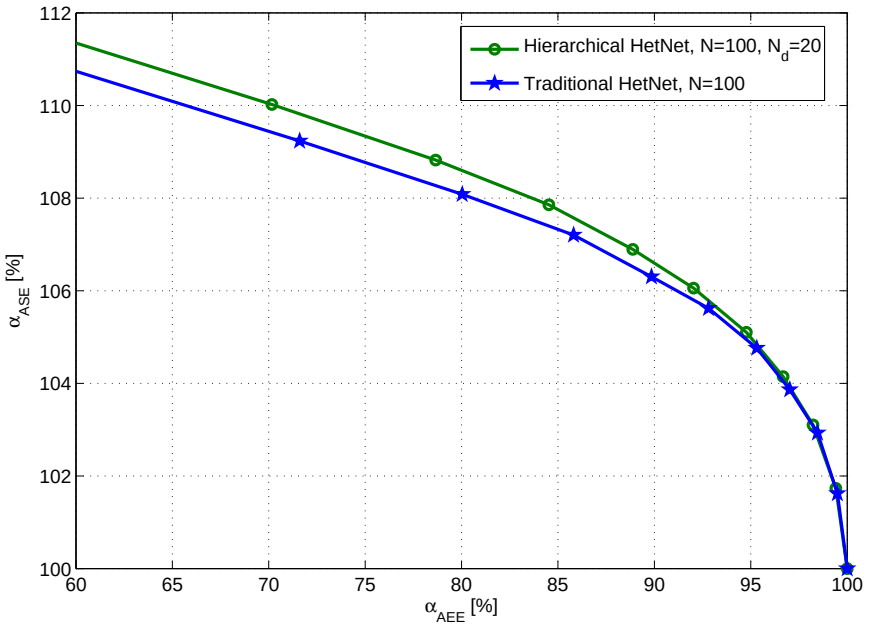

FIGURE 3.10: α_{AEE} in percentage versus α_{ASE} in percentage for Hierarchical and Traditional HetNets with $N_d = 20$

of α_{AEE} becomes slower. For example, at $\alpha_{\text{AEE}} = 80\%$, significant ASE gains of 108.1% and 108.7% are achieved in the traditional and hierarchical HetNets. Furthermore, higher ASE gain is observed in the hierarchical HetNet as compared to the traditional HetNet. These observations justify the simulations results obtained from Fig. 3.9.

3.6 Optimising User Association and Power Allocation in Heterogeneous Networks: A Fairness Perspective

3.6.1 Related Work

One of the emerging technologies towards enabling Fifth Generation (5G) is heterogeneous networks (HetNets) which include Green Small Cell Networks consisting of low-power base station (BS), (e.g., microcells, picocells, and femtocells), overlaid within the macrocell geographical area, deployed by either users or network operators who share the same spectrum with the macrocells [20] and [41]. The purpose of HetNets is to allow

user equipments (UEs) to access small cells even though the UEs are within the coverage of macrocell. The deployment of small cells has a great potential to improve the spatial reuse of radio resources and also to enhance the energy efficiency (EE) of the network [20] and [54]. Although, some works [55] and [56] have been done on fairness based energy efficient radio resource management in traditional OFDMA systems mainly maximising either EE or spectral efficiency (SE). In [57], authors proposed a MOP approach to jointly maximise EE and SE along with fairness for downlink transmission scheme of the traditional OFDMA systems.

Most of the work in the literature mainly focuses on maximising EE or SE with respect to the transmission power without considering the backhaul energy consumption [58]. The authors in [59] proposed a mechanism to compute backhaul energy efficiency (BEE) in a heterogeneous network deployment consisting of a macrocell with enabled device to device (D2D) communication to reduce the overall network power consumption in comparison to the small cell deployment. In [60], the authors analysed the energy efficiency optimisation with subject to SE constraint in the downlink of Green HetNets using Coordinated Multi-Point (CoMP) transmission scheme to reduce the total power consumption including the backhaul power consumption for two backhauling technologies, i.e., microwave and fiber. The contribution of the backhaul energy consumption to the total energy consumption is dependent on the network deployment scenario and technology and the topology of the backhaul itself [61].

According to the best of our knowledge, there is no previous work on joint throughput and BEE tradeoff with fairness in downlink transmission scheme of two-tier HetNets

considering multi-user multi-carrier systems. In this paper, we investigate the two conflicting objectives such as jointly maximising throughput and BEE subject to minimum QoS requirements, maximum input power constraint and rate fairness level ω as a multi-objective optimisation problem (MOP). The MOP is transformed into a single-objective optimisation problem (SOP) using weighted sum method obtaining a complete Pareto-optimal set or Pareto Frontier providing a quantitative insight into the throughput and BEE tradeoff with different rate fairness level ω.

3.6.2 System Setup and Problem Formulation

We consider a downlink scenario of two-tier HetNets consisting of a macrocell and $M-1$ pico BS's with the total number of users N and K non-overlapping subcarriers. We denote the index set of all subcarriers as $k = \{1, \cdots, K\}$, the set of all users as $n = \{1, \cdots, N\}$ and the set of networks as $m = \{1, \cdots, M\}$. Further, we consider an orthogonal subcarrier selection scheme which assigns each subcarrier exclusively to either pico BS (PB) or macrocell (Mc) at any time. We assume that N_{m} indicates the set of all subcarriers allocated to the network m and $|N_m|$ is the cardinality of the set N_m denoting the total number of subcarriers allocated to the network m.

To model fairness, we adopt ω-fair utility function

$$u_{\omega}(R_n) = \begin{cases} \ln(R_n), & \text{if } \omega = 1, \\ R_n^{1-\omega}/(1-\omega), & \text{if } \omega \neq 1,\ \omega \geq 0, \end{cases} \tag{3.34}$$

where the value of ω represents different rate fairness levels. For no fairness requirement, $\omega = 0$, and $u_{\omega}(R_n) = R_n$. By increasing ω, the rate fairness among users also increases.

For the special case of $\omega \to \infty$, an absolute rate fairness among users is achieved.

3.6.2.1 Power Consumption Model

Hence, the overall consumed power in downlink of two-tier HetNets can be modelled as below [59, 60]:

$$P = \varepsilon_0 \sum_{k=1}^{K} \sum_{n=1}^{N} \sum_{m=1}^{M} \sigma_{k,n}^{(m)} p_{k,n}^{(m)} + M \times P_{\mathrm{C}} + P_{BH}, \tag{3.35}$$

where P_{BH} is the backhaul power consumption. In two-tier HetNets, the backhaul power consumption consists of the backhaul power consumed at aggregation switch (or switches) $P_{BH}^{(mb)}$, to forward the traffic from all the macro BS's to the core network and the backhaul power consumed at sink switch (or switches) $P_{BH}^{(sc)}$, located at the macro BS to receive the traffic from the $M-1$ small cells then aggregate it with the macrocell BS traffic and forward it to the core network. Optical fiber is most commonly used for backhaul links between all macro BS's to the aggregation switch. The backhaul power consumption $P_{BH}^{(mb)}$ can be expressed as follow [62]:

$$P_{BH}^{(mb)} = \left\lceil \frac{I_{mb}}{\max_{dl}} \right\rceil \times P_{sw} + I_{mb} \times P_{dl} + L_{ul} \times P_{ul}, \tag{3.36}$$

where I_{mb} is the number of macro BS's which is equal to 1 according to our system model, $\max_{dl}$ is the maximum number of downlink interfaces at aggregation switch of macro BS and P_{dl} is the power consumption of a downlink interface at the macro BS aggregation switch. $L_{ul} = \left(\frac{T_{agg}}{C_{\max}}\right)$ and P_{ul} are the total number of uplink interfaces and power consumption of an uplink interface, respectively. T_{agg} and $C_{\max}$ are the total traffic

at the aggregation switches of the macrocell BS and the maximum transmission rate of an uplink interface, respectively. P_{sw} represents the power consumption of the aggregation switch at the macrocell BS and (3.36) can be rewritten as:

$$P_{BH}^{(mb)} = \left[\frac{1}{\max_{dl}}\right]\left(\beta.P_{sw}^{\max} + (1-\beta)\frac{C_{agg}}{C_{sw}^{\max}}P_{sw}^{\max}\right) + P_{dl} + \left(\frac{T_{agg}}{C_{\max}}\right)P_{ul}, \tag{3.37}$$

where $\beta \in [0,1]$, $P_{sw}^{\max}$ is the maximum power consumption of the switch, C_{agg} is the total traffic at the macrocell aggregation switch and $C_{sw}^{\max}$ denotes the maximum traffic switch can handle.

Similarly, either optical fiber or microwave can be used for backhaul links between all the small cells and the sink switch located at the macro BS. However, in this paper we assume that optical fiber is used and $P_{BH}^{(sc)}$ can be defined as [60]:

$$P_{BH-Fiber}^{(sc)} = \left[\frac{K-1}{\max_{dl}}\right]P_{sw} + \left(\frac{C_s}{C_{\max}}\right)P_{ul}, \tag{3.38}$$

where C_s denotes the total traffic of the small cells. Hence, $P_{BH}^{(sc)}$ can also be defined for the case where all the traffic from the small cells goes to the core network via internet without using aggregation node at macrocell as [59]:

$$P_{BH}^{(sc)} = \left[\frac{(M-1)C_s}{4Gbps}\right]\left[\frac{P_{\text{router}}}{40} + P_{\text{OLT}}\right] + (M-1)P_{\text{ONU}}, \tag{3.39}$$

where P_{router} represents the power consumption of the edge router, P_{OLT} denotes the power

consumption of the OLT and P_{ONU} represents power consumption of ONU. The total power consumption of two-tier HetNets can be written as:

$$P_{\text{total}} = \varepsilon_0 \sum_{m=1}^{M} P_m^{\max} + M \times P_{\text{C}} + P_{BH}^{\max}, \tag{3.40}$$

where $P_m^{\max}$ is the maximum transmission power of network m, P_{C}^m is the circuit power of network m and $P_{BH}^{\max}$ is the maximum power consumed by the backhaul to forward the collected traffic (i.e., when all networks are operating at their maximum transmission power) to the core network. Now, we can define the Backhaul Energy Efficiency (BEE) as follow:

$$\text{BEE} = \frac{\sum_{n=1}^{N} R_n}{\varepsilon_0 \sum_{k=1}^{K} \sum_{n=1}^{N} \sum_{m=1}^{M} \sigma_{k,n}^{(m)} p_{k,n}^{(m)} + M \times P_{\text{C}} + P_{BH}} \tag{3.41}$$

Similalrly, we can also define Energy Efficiency (EE) as a special case of (3.41) when no backhaul power consumption is assumed, i.e., $P_{BH} = 0$.

3.6.2.2 Problem Formulation

Our goal is to simultaneously optimise throughput and BEE with fairness and QoS guarantees while ensuring that the interference power does not exceed their specific thresholds. The joint optimisation problem to maximise the throughput and BEE is equivalent to maximising the sum rate and minimising the total power consumption. In this Section, we investigate the Throughput-BEE tradeoff in downlink transmission scheme of two-tier HetNets as a multi-objective optimization problem (MOP) by normalising the two

conflicting objective functions to ensure a consistent comparison as below:

$$\textbf{(P1)} \quad \max_{\mathbf{p},\sigma} \frac{\left(\sum_{n=1}^{N} u_\omega\left(R_n\right) - u_\omega^{\min}\right)}{\left(u_\omega^{\max} - u_\omega^{\min}\right)} \text{ and } \max_{\mathbf{p},\sigma} \frac{-P}{P_{\text{total}}}, \tag{3.42}$$

$$\begin{aligned}
\text{s.t. C1}: \quad & \sum_{k=1}^{K}\sum_{n=1}^{N} \sigma_{k,n}^{(m)} p_{k,n}^{(m)} \leq P_m^{\max}, \forall m, \\
\text{C2}: \quad & R_n \geq R_n^{\min}, \ \forall n. \\
\text{C3}: \quad & p_{k,n}^{(m)} \geq 0, \ \forall m, \forall n, \forall k, \\
\text{C4}: \quad & \sum_{n=1}^{N_m} \sigma_{k,n}^{(m)} \leq 1, \ \forall m, k, \\
\text{C5}: \quad & \sigma_{k,n}^{(m)} \in [0,1], \ \forall m, \forall n, \forall k,
\end{aligned}$$

where $u_\omega^{\max}$ are the maximum achievable utility value of (3.34) for a given value of ω under the constraints C1-C5. $u_\omega^{\min}$ is the minimum achievable utility value computed by setting $R_n = \delta$ in (3.34) for a given value of ω where $\delta > 0$ is a predefined sufficiently small value. $P_m^{\max}$ is the maximum transmission power of network m and $R_n^{\min}$ is the minimum rate requirement for each user n. C1 is the maximum transmission power of each network m which should not exceed $P_m^{\max}$. C2 is the minimum rate requirement for each user which is applicable only if user n is admitted, i.e., $\sigma_{k,n}^{(m)} = 1$. C3 ensures that the power $p_{k,n}^{(m)}$ should be positive. C4 and C5 indicate that $\sigma_{k,n}^{(m)}$ is a binary variable such that each subcarrier k can be exclusively assigned to one user within network m. For better tractability, we relax the constraint C6 by allowing time sharing.

The MOP defined in (3.42) can be transformed into a single objective optimization problem (SOP) by applying the *weighted sum method* [63] as follow:

$$\textbf{(P2)} \quad \max_{\mathbf{p},\sigma} \; \alpha \frac{\sum_{n=1}^{N} u_\omega(R_n) - u_\omega^{\min}}{u_\omega^{\max} - u_\omega^{\min}} - (1-\alpha)\frac{P}{P_{\text{total}}}, \tag{3.43}$$

$$\text{s.t.} \qquad \text{C1} - \text{C5},$$

where $\alpha \in [0,1]$ is the Throughput-BEE tradeoff biasing factor.

3.6.3 Proposed Distributed Solution

In this Section, we propose a distributed solution to the problem **(P2)** for different values of w which can collectively form the Pareto optimal set. In other words, by tuning α, we investigate the Throughput-BEE tradeoff for a given value of ω.

Firstly for the case of $\omega > 0$, we define a vector $\mathbf{x} = [x_1, x_2, ..., x_n]^T$ and rewrite **(P2)** as

$$\textbf{(P3)} \quad \max_{\mathbf{x},\mathbf{p},\sigma} \; \alpha \frac{\sum_{m=1}^{M} u_\omega(x_n) - u_\omega^{\min}}{u_\omega^{\max} - u_\omega^{\min}} - (1-\alpha)\frac{P}{P_{\text{total}}}, \tag{3.44}$$

$$\text{s.t.} \;\; \text{C1} - \text{C5}\,,$$

$$\text{C6}: \; x_n \le R_n, \; \forall m.$$

where $\mathbf{p} = \{p^{(1)}, p^{(2)}, \cdots, p^{(M)}\}$ and $\sigma = \{\sigma^{(1)}, \sigma^{(2)}, \cdots, \sigma^{(M)}\}$. It is worthwhile to mention that $p^{(1)}, p^{(2)}$ and $p^{(M)}$ are $K \times N$ power allocation indication matrix. The size of $\sigma^{(1)}, \sigma^{(2)}$ and $\sigma^{(M)}$ are also same as $p^{(1)}, p^{(2)}$ and $p^{(M)}$. $u_\omega(\cdot)$, is a strictly increasing function, hence, for an optimal solution, x_n must be equal to R_n.

We then utilize Hierarchical Decomposition method [64] to find an optimal solution

to **(P3)**. To characterize the duality gap between the primal and dual solutions, the *time-sharing* condition is first defined in [65] and it is proved that if it holds, the duality gap is zero even if the original optimization problem is not convex. In practical multicarrier systems with a large number of subcarriers, channel conditions in adjacent subcarriers are often similar. In such case, the time-sharing condition is approximately satisfied, and accordingly the duality gap is nearly zero [65]. We define the partial Lagrangian function of primal problem in **(P3)** formed by dualising the constraint C6:

$$\begin{aligned} L(\mathbf{p},\sigma,\mathbf{x},\lambda) &= \alpha\frac{\sum_{n=1}^{N} u_\omega(x_n)-u_\omega^{\min}}{u_\omega^{\max}-u_\omega^{\min}} - (1-\alpha)\frac{P}{P_{\text{total}}} + \sum_{n=1}^{N}\lambda_n(R_n-x_n) \\ &= \left(\alpha\frac{\sum_{n=1}^{N} u_\omega(x_n)-u_\omega^{\min}}{u_\omega^{\max}-u_\omega^{\min}} - \sum_{n=1}^{N}\lambda_n x_n\right) + \left(\sum_{n=1}^{N}\lambda_n R_n - (1-\alpha)\frac{P}{P_{\text{total}}}\right), \end{aligned} \tag{3.45}$$

where $\lambda = [\lambda_1, \lambda_2, ..., \lambda_N]^T$ is the dual vector for constraint C6 corresponding to each user. Then the dual function is

$$g(\lambda) = \begin{cases} \max\limits_{\mathbf{x},\mathbf{p},\sigma} \; L(\mathbf{p},\sigma,\mathbf{x},\lambda), \\ \text{s.t.} \;\; \text{C1} - \text{C5}\,. \end{cases} \tag{3.46}$$

Obviously, the dual function in (3.46) can be separated into two maximisation subproblems as shown in (3.47) and (3.48) respectively.

$$g_1(\lambda) = \max_{\mathbf{x}} \; f(\mathbf{x}) = \alpha\frac{\sum_{n=1}^{N} u_\omega(x_n) - u_\omega^{\min}}{u_\omega^{\max} - u_\omega^{\min}} - \sum_{n=1}^{N}\lambda_n x_n, \tag{3.47}$$

$$g_2(\lambda) = \begin{cases} \max\limits_{\mathbf{p},\sigma} \; \sum\limits_{n=1}^{N}\lambda_n R_n - (1-\alpha)\frac{P}{P_{\text{total}}}, \\ \text{s.t.} \;\; \text{C1} - \text{C5}\,. \end{cases} \tag{3.48}$$

3.6.3.1 Solution to subproblem $g_1(\lambda)$:

In (3.47), as $u_\omega(x_n)$ is a concave function of x_n and hence, $f(\mathbf{x})$ is also a concave function of x_n. Therefore, the optimality of (3.47) can be solved by taking the derivative of $f(\mathbf{x})$ with respect to x_n and setting it equal to zero as given by

$$x_n^* = \left[\sqrt[\omega]{\frac{\alpha}{\lambda_n \left(u_\omega^{\max} - u_\omega^{\min}\right)}} \right]^+, \forall n, \tag{3.49}$$

where $(y)^+ \triangleq \max(0, y)$ and x_n^* is the value of x_n which maximises (3.47).

The corresponding dual problem is

$$\min_{\lambda \geq 0} \; g_1(\lambda). \tag{3.50}$$

The dual problem (3.50) can be solved using subgradient method [65]. The dual vector λ can be updated as follow:

$$\lambda_n(i+1) = \left[\lambda_n(i) - s_0 \left(R_n - x_n\right)\right]^+, \forall n, \tag{3.51}$$

where s_0 is the positive step size.

3.6.3.2 Solution to subproblem $g_2(\lambda)$:

The subproblem (3.48) can be solved using Lagrangian dual decomposition method [64]. By relaxing the constraints C1-C2, the Lagrangian function becomes

$$T(\mathbf{p}, \sigma, \mu, \eta) = \sum_{n=1}^{N} \lambda_n R_n - (1-\alpha)\frac{P}{P_{\text{total}}} + \sum_{m=1}^{M} \mu_m \left(P_m^{\max} - \sum_{k=1}^{K} \sum_{n=1}^{N} \sigma_{k,n}^{(m)} p_{k,n}^{(m)} \right)$$

$$+\sum_{n=1}^{N}\eta_n\Big(R_n-R_n^{\min}\Big)$$

$$T\left(\mathbf{p},\sigma,\mu,\eta\right)=\sum_{k=1}^{K}\left[\sum_{m=1}^{M}\sum_{n=1}^{N}\left(\left(\lambda_n+\eta_n\right)r_{k,n}^{(m)}-\left(\frac{\left(1-\alpha\right)\varepsilon_0}{P_{\text{total}}}\right)\times p_{k,n}^{(m)}\right)\sigma_{k,n}^{(m)}\right]+\sum_{m=1}^{M}\mu_m P_m^{\max}$$
$$-\frac{\left(1-\alpha\right)\left(P_{\text{C}}+P_{\text{BH}}\right)}{P_{\text{total}}}-\sum_{n=1}^{N}\eta_n R_n^{\min},\tag{3.52}$$

where $\mu=[\mu_1,\mu_2,...,\mu_M]^T$ and $\eta=[\eta_1,\eta_2,...,\eta_N]^T$ are the dual vectors corresponding to the constraints C1 and C2. We further observe that the dual function

$$h\left(\mu,\eta\right)=\begin{cases}\max\limits_{\mathbf{p},\sigma}\;\; T\left(\mathbf{p},\sigma,\mu,\eta\right),\\ \text{s.t. C3, C4 and C5}\end{cases}\tag{3.53}$$

can be decoupled into K subproblems, which can be independently solved for each subcarrier k. The subproblem corresponding to subcarrier k at given (μ,η) is

$$T_k\left(\mu,\eta\right)=\max_{\mathbf{p}(:,\mathbf{k}),\sigma(:,k)}\left[\sum_{m=1}^{M}\sum_{n=1}^{N}\left(\left(\lambda_n+\eta_n\right)r_{k,n}^{(m)}-\left(\frac{\left(1-\alpha\right)\varepsilon_0}{P_{\text{total}}}+\mu_m\right)p_{k,n}^{(m)}\right)\sigma_{k,n}^{(m)}\right],$$

$$\text{subject to C3}-\text{C5}\,,\tag{3.54}$$

where $\mathbf{p}(:,\mathbf{k})$ and $\sigma(:,k)$ are the matrix of $p_{k,n}^{(m)}$ and $\sigma_{k,n}^{(m)}$ at subcarrier k respectively. Due to the constraints C4 and C5, the subcarrier allocation indicator $\sigma(:,k)$ is an all-zero matrix except for one binary non-zero entry. Hence, for a certain subcarrier k, we can

calculate $C_{k,n}^{(m)}$ for each user n associated with network m as

$$C_{k,n}^{(m)} = \begin{cases} \max\limits_{\mathbf{p}(:,\mathbf{k})} \left((\lambda_n + \eta_n) r_{k,n}^{(m)} - X p_{k,n}^{(m)} \right), \\ \text{s.t. } p_{k,n}^{(m)} \geq 0, \ \ \forall m, \forall k. \end{cases} \tag{3.55}$$

where $X = \left(\frac{(1-\alpha)\varepsilon_0}{P_{\text{total}}} + \mu_m \right)$. Therefore, we calculate the optimal value of (3.55) at given λ, μ and η to determine the subcarrier assignment indicator for subcarrier k as

$$\sigma_{k,n}^{(m)} = \begin{cases} 1, \ \text{if } (n^*, m^*) = \arg\max\limits_{n,m} C_{k,n}^{(m)}, \forall k. \\ 0, \ \text{otherwise.} \end{cases} \tag{3.56}$$

Then, by using the KKT conditions for a fixed set of Lagrange multipliers, an optimal power allocation to user n associated with network m on subcarrier k is obtained as

$$p_{k,n}^{(m)} = \left[\frac{(\lambda_n + \eta_n) B_k}{\left(\frac{(1-\alpha)\varepsilon_0}{P_{\text{total}}} + \mu_m \right) \ln 2} - \frac{1}{\gamma_{k,n}^{(m)}} \right]^+. \tag{3.57}$$

Once all K subproblems in (3.54) are solved, $h(\mu, \eta)$ is derived by using (3.52) and (3.54) at given (μ, η). The subproblem in (3.48) can be solved via the dual problem as given below

$$\min_{\mu \geq 0, \eta \geq 0} h(\mu, \eta). \tag{3.58}$$

In order to solve the dual problem (3.58), the subgradient method can be used to update the dual vectors μ and η in each iteration. The subgradient of $h(\mu, \eta)$ at the $i+1^{th}$

iteration are given by

$$\mu_m(i+1) = \left[\mu_m(i) - s_1\left(P_m^{\max} - \sum_{n=1}^{N}\sum_{k=1}^{K} p_{k,n}^{(m)}\right)\right]^+, \forall m, \tag{3.59}$$

$$\eta_n(i+1) = \left[\eta_n(i) - s_2\left(R_n - R_n^{\min}\right)\right]^+, \forall n, \tag{3.60}$$

where $s_j, j \in \{1,2\}$ are the positive step sizes.

Finally for the case of $\omega = 0$, i.e., $u_\omega(R_n) = R_n$, **(P2)** can be solved directly using dual decomposition method (similar to the solution to subproblem $g_2(\lambda)$). The optimal power allocation to user n associated with network m on subcarrier k is given by

$$p_{k,n}^{(m)} = \left[\frac{\left(\frac{\alpha}{u_0^{\max} - u_0^{\min}} + \eta_n\right) B_k}{\left(\frac{(1-\alpha)\varepsilon_0}{P_{\text{total}}} + \mu_m\right)\ln 2} - \frac{1}{\gamma_{k,n}^{(m)}}\right]^+, \tag{3.61}$$

Similarly, for a certain subcarrier k, we can calculate $D_{k,n}^{(m)}$ for each user n associated with network m as

$$D_{k,n}^{(m)} = \begin{cases} \max\limits_{\mathbf{p}(:,\mathbf{k})} \left(\left(\frac{\alpha}{u_0^{\max} - u_0^{\min}} + \eta_m\right) r_{k,n}^{(m)} - X p_{k,n}^{(m)}\right) \\ \text{s.t. } p_{k,n}^{(m)} \geq 0, \ \forall m, \forall n. \end{cases} \tag{3.62}$$

The subcarrier assignment indicator for subcarrier k as

$$\sigma_{k,n}^{(m)} = \begin{cases} 1, \text{if } (n^*, m^*) = \arg\max\limits_{n,m} D_{k,n}^{(m)}, \\ 0, \ \text{otherwise.} \end{cases} \tag{3.63}$$

3.6.4 Simulation Results

In the simulations, we consider a two-tier HetNets consisting of a macrocell overlaid with $M-1$ small cells with N users being randomly distributed with K subcarriers. More details about the simulation parameters can be found in [59] [60] and are mentioned in Table 3.I.

TABLE 3.I: Simulation Parameters.

Parameter	Value	Parameter	Value
K	256	M	5
N	8	B [MHz]	3
P_{C} [W]	0.4	ε_0	38%
$P_{\mathrm{macro}}^{\max}$[W]	40	$P_{\mathrm{small}}^{\max}$[W]	0.2
N_0[dBM/Hz]	-174	R_{macro}[m]	500
R_{small}[m]	100	Log-Normal Shadowing	$N(0,\sigma)$
std dev σ [dB]	8	$R_n^{\min}$ [Kbps]	500
$\max_{dl}$	24	$P_{sw}^{\max}$ [W]	300
P_{dl} [W]	1	P_{ul} [W]	2
$C_{\max}$ [Gbps]	10	β	0.9
$C_{sw}^{\max}$ [Gbps]	24	P_{router} [kW]	4
P_{ONU} [W]	4.69	P_{OLT} [W]	100

Fig. 3.11 investigates the impact of weighting coefficient α on the achievable EE and throughput for various values of ω. At $\alpha = 0$, the proposed MOP is transformed into minimising the total consumption power whereas at $\alpha = 1$ it is transformed into maximising throughput. As it can be seen from Fig. 3.11, achievable EE and throughput can be varied by adjusting the value of ω. For example, at $\alpha = 0$ and $\omega = 0$, an achievable throughput and EE are 1.358 b/s/Hz and 2.037 Mb/J, respectively whereas at $\alpha = 0$ and $\omega = 1$, an achievable Throughput and EE are 1.311 b/s/Hz and 1.967 Mb/J, respectively. We further observe that an achievable EE gradually increases with α to an optimal EE, and then afterwards starts decreasing with an increase in α. Similarly, an achievable SE always

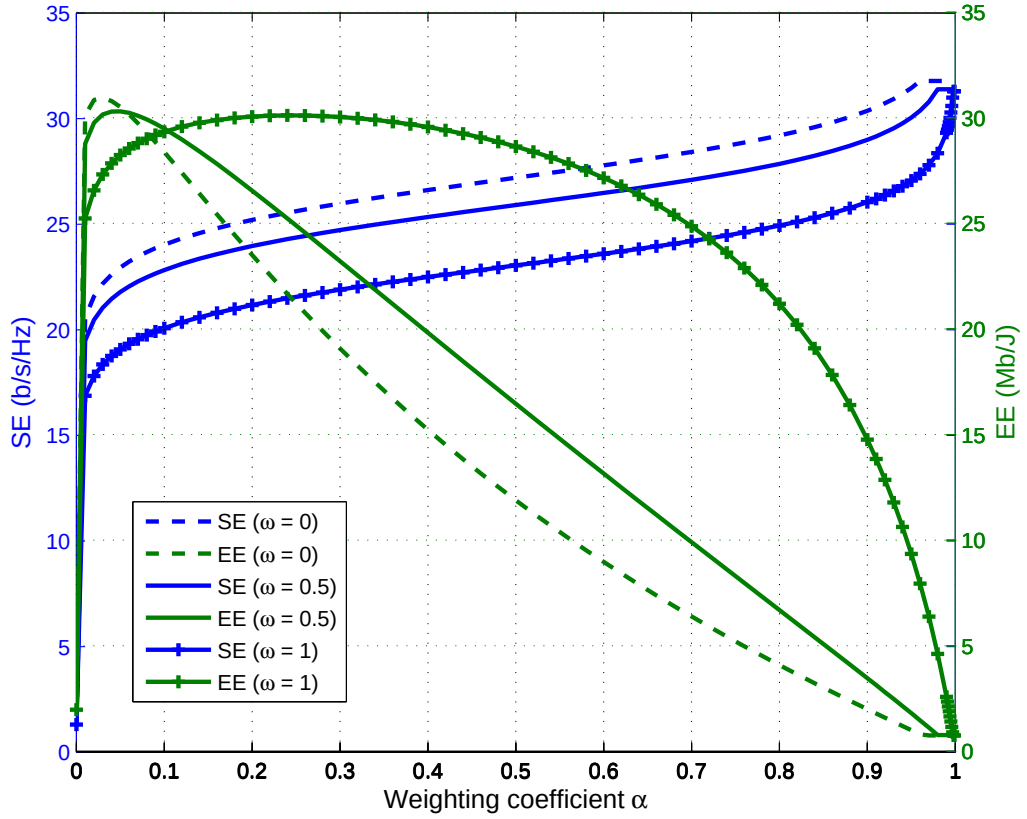

FIGURE 3.11: EE and SE versus α for different values of ω.

increases with an increase in α and on the other hand, an achievable SE always decreases with an increase in ω. One of the main observation is that an optimal EE decreases with an increase in ω, due to the fact that the higher level of fairness is achieved at the cost of degradation in achievable EE. It is also worthwhile to mention that an optimal EE at smaller value of ω results in higher achievable Throughput. Nevertheless, the proposed MOP approach achieves the entire Pareto Frontier or complete Pareto optimal set of the proposed problem with different rate fairness levels ω and weighting coefficient α.

Fig. 3.12 shows the impact of the weighting coefficient α on the normalised BEE over the total coverage area for various values of rate fairness level ω. In Fig. 3.12, the BEE

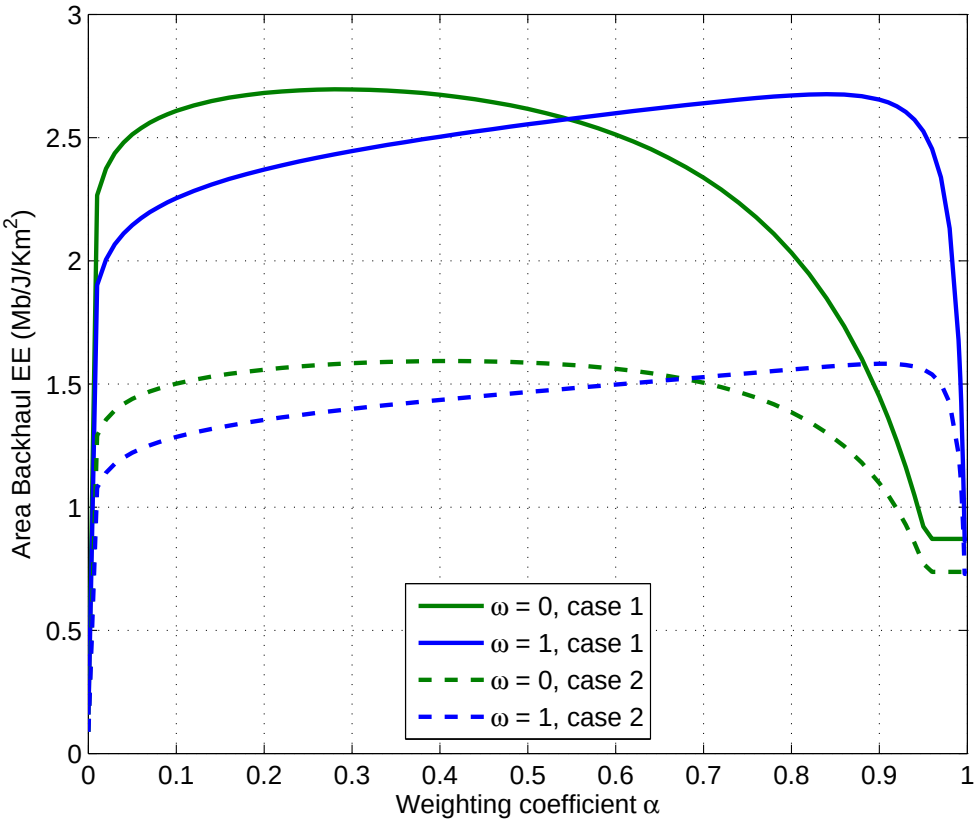

FIGURE 3.12: Area BEE versus α for various values of ω.

comparison in two-tier HetNets is shown for the two different cases of backhauling technologies. In case 1, an optical fiber is used as a technology to backhaul traffic from a macrocell to the aggregation switch (can be one or more) and all the traffic from $M-1$ small cells are backhauled via Internet without going through the aggregation switch at the macrocell. In case 2, an optical fiber is used as a technology to backhaul traffic from a macrocell to the aggregation switch (one or more) and all the traffic from $K-1$ small cells is collected at the sink node of the macrocell and backhauled from macrocell to the core network using an optical fiber link. One of the intuition from the figure is that BEE first increases with weighting coefficient α until an optimal value of α and afterwards it starts decreasing with weighting coefficient α. At the lower values of ω, an optimal BEE

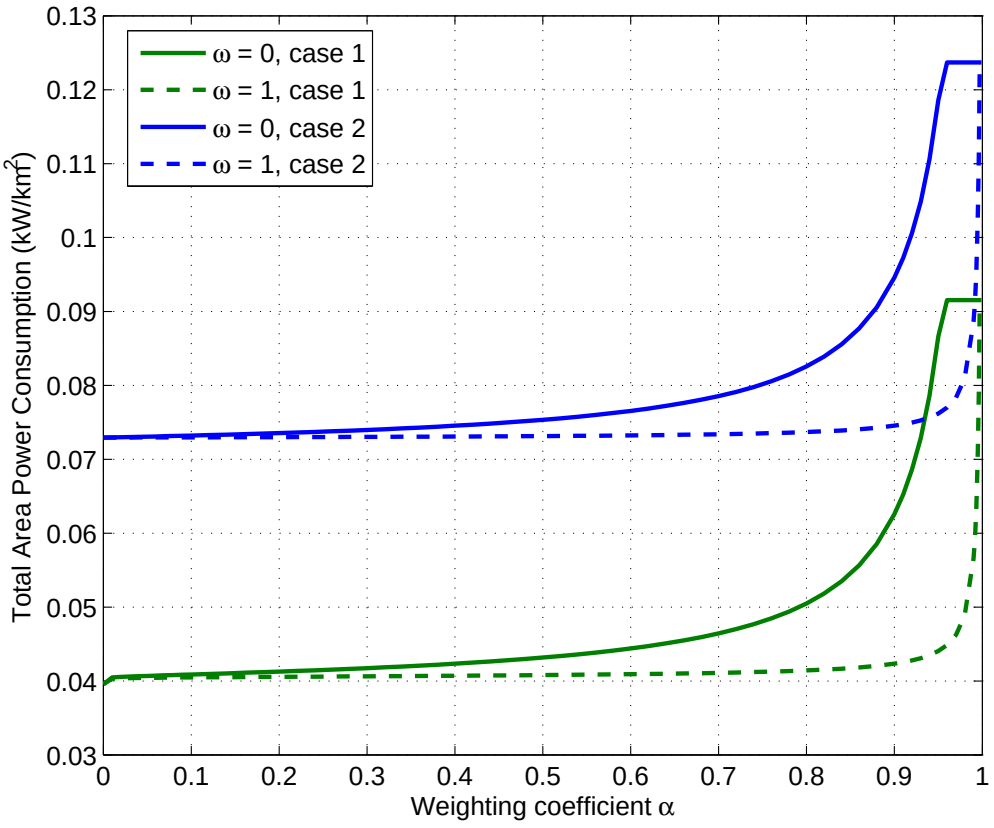

FIGURE 3.13: Total Area Power Consumption versus α for various values of ω.

is achieved at lower values of α whereas an optimal BEE is achieved at higher values of α for the case of the higher values of ω.

Fig. 3.13 shows the impact of two backhauling technologies on the total area power consumption of two-tier HetNets versus weighting coefficient α for various values of rate fairness level ω. The total area power consumption increases with an increase in α whereas it decreases with an increase in ω. It is quite obvious from the figure that at a given value of ω, the total area power consumption in case 1 is always less than case 2 at the expense of degradation in area BEE as shown in Fig 3.12. At the values of $\omega = 0$ and $\alpha = 1$, the total area power consumption in two-tier HetNets without backhaul power consumption is 0.05 kW/km^2 as compared to 0.092 kW/km^2 and 0.125 kW/km^2 for case

1 and case 2, respectively. This affirms the observation that the impact of backhaul power consumption in two-tier HetNets is larger than to the case where no backhaul power consumption is assumed irrespective of the used backhauling technology. By dynamically choosing a higher value of ω, the total area power consumption can be reduced for all values of α irrespective of the used backhauling technology.

3.7 Summary

This chapter provides a detailed description of the proposed maximising EE optimisation schemes in multi-tier HetNets. Firstly, the EE maximisation problem of an uplink of a two-tier OFDMA-based HetNets with maximum transmit power and minimum-rate constraints using adaptive channel and power allocation is addressed in Section 3.4. The EE-optimization problems for MU-MC scenarios are formulated and solved using KKT conditions. It is further analysed how the maximum transmit power and minimum-rate requirement constraint affects the EE. Simulation results indicate that the pico-BS-first user association combined with SNR-based rate proportional mechanism can enhance the EE considerably.

Secondly, a joint optimization problem is formulated for mode selection, subcarrier assignment and power allocation in a three-tier hierarchical HetNet consisting of an underlaid D2D communication in coverage of both macrocell and pico BS's as mentioned in Section 3.5. The optimization problem is such that each user tries to maximize its own ASE subject to a required AEE level and a maximum transmit power constraint. The proposed objective function takes into account the tradeoff between ASE and AEE, and

an iterative algorithm is proposed to solve the problem. The simulation results show that when the required AEE level is set to 93% of $\eta^{\max}$, the proposed scheme can reduce the tradeoff optimal transmit power upto 48.51% and 1404%, when compared to the traditional HetNets and macrocell only, respectively.

Finally, the concept of MOP is utilised to jointly optimise the throughput and BEE tradeoff in two-tier HetNets with QoS and fairness guarantee constraints is outlined in Section 3.6. The complete Pareto optimal set is obtained by employing the weighted sum method to transform our proposed MOP into an SOP which can be solved using Lagrangian Dual Decomposition (LDD) method. The impact of rate fairness level ω and weighting coefficient α on achievable throughput and EE is investigated with or without backhaul power consumption. The network operators can have more flexibility to satisfy the user's QoS requirements along with reducing their total area power consumption by dynamically tuning the weighting coefficient α and rate fairness level ω.

Chapter 4

Joint Optimisation of Energy and Spectral Efficiency Tradeoff in 5G Heterogeneous Networks Under QoS Constraints[1]

In Chapters 2 and 3, we have emphasised the importance of EE and SE in the design of the future generation networks. The focus of Chapter 2 was to maximise the system throughput of the two-tier HetNets using the evolutionary game theory whereas in Chapter 3 the energy efficient radio resource management has been outlined for D2D enabled multi-tier HetNets. In comparison to the previous works, we extend our system model to incorporate the joint energy and spectral efficient radio resource management in multi-tier HetNets subject to the minimum QoS requirement, maximum transmission power and interference threshold constraints. The multi-objective optimisation methods have gained a lot of interest recently to optimise the multiple objectives using scalar methods. In this context, we formulate a multi-objective optimisation problem (MOP) to jointly optimise

[1]The work presented in this chapter have been published in Special Issue on Ultra Dense Cellular Networks of IEEE ACCESS Journal and a shorter version was accepted in IEEE International Conference on Communications (ICC), held at London, UK in June 2015.

the two conflicting objectives such as EE and SE in multi-tier HetNets to address the joint energy and spectral efficient radio resource allocation issues.

A joint energy efficiency (EE) and spectrum efficiency (SE) trade-off analysis is proposed as a MOP in the uplink of multi-user multi-carrier two-tier Orthogonal Frequency Division Multiplexing Access (OFDMA) Heterogeneous Networks subject to users' maximum transmission power and minimum-rate constraints. The proposed MOP is modelled such that the network providers can dynamically tune the trade-off parameters to switch between different communication scenarios with diverse design requirements. In order to find its Pareto optimal solution, the MOP is transformed, by using a weighted sum method, into a single-objective optimisation problem (SOP), which itself can further be transformed from a fractional form, by exploiting fractional programming, into a subtractive form. Since the formulated SOP is hard to solve due to the combinatorial channel allocation indicators, the SOP is reformulated into a better tractable problem by relaxing the combinatorial indicators using the idea of time sharing. It is then proved that this reformulated SOP is strictly quasi-concave with respect to the transmission power and subcarrier allocation indicator. An iterative two-layer distributed framework is then proposed to achieve an upper bound Pareto optimal solution of the original proposed MOP. Numerical simulations demonstrate the effectiveness of our proposed two-layer framework achieving an upper bound Pareto-optimal solution, which is very close to an optimal solution, with fast convergence, lower and acceptable polynomial complexity and balanced EE-SE tradeoff.

4.1 Related Work

The heterogeneous networks (HetNets) include low-power overlaid base stations 'BSs'(or small cells, e.g., microcells, picocells, and femtocells) within the macrocell geographical area, deployed by either users or network operators who share the same spectrum with the macrocells [4, 41, 66]. The purpose of HetNets is to allow the user equipments (UEs) to access small cells, even though the UEs are within the coverage of macrocell [5]. HetNets aim at achieving high data rates with low powers while satisfying the users' quality-of-service constraints (in terms of minimum-rate requirements) by offloading the users with low signal-to-interference-plus-noise-ratios (SINR) from macrocells to the pico BSs. The deployment of small cells has a great potential to improve the spatial reuse of radio resources and also to enhance the transmit power efficiency [6], and in turn, the energy efficiency (EE) of the network. EE is, in fact, one of the key performance indicators for the next generation wireless communications systems [67]. The motivation behind considering EE as the performance metric arises due to the current energy cost payable by operators for running their access networks as a significant factor of their operational expenditures (OPEX) [68]. It is however, known that most of EE gains are achieved with sacrifices in spectrum efficiency (SE) [20].

In this trend, the energy-efficient resource allocation technique is proposed in the uplink transmission scheme of traditional Orthogonal Frequency Division Multiple Access (OFDMA) systems [35]. This result is later generalized to maximize the uplink EE in

frequency selective channels in [36]. Similarly, a low complexity energy-efficient resource allocation in an uplink transmission scheme considering frequency-selective channels for multi-user networks, with and without fairness considerations, is studied in [69]. A energy-efficient resource allocation scheme for OFDMA systems under a fairness guarantee factor among users is proposed in [70], wherein, an optimisation problem is formulated as an integer fractional programming problem which is further simplified into an integer linear programming (ILP) form using an iterative fractional method. Further advances on green networking, which focus on the means to reduce the energy consumption in traditional wireless networks, can be accessed in [71] and [72]. Few of the recent works in the literature studying the characteristics of EE and SE analysis in traditional OFDMA systems is investigated for single user case in [73, 74], and for multi user case in [75–77]. The impact of the number of deployed femtocells in a macrocell area, the average number of users, and the number of open channels in a femtocell using the Markov chain model on the EE and SE of two-tier femtocell networks is investigated in [78].

Most of the existing works in the literature for resource allocation in HetNets have focused on maximising either EE (in terms of Utopia EE for each individual user in [79, 80], and in terms of the overall system EE in [80–82]) or SE [83]. In this trend, the EE-maximisation problem in an uplink of HetNets is analytically solved for a single user case under the minimum target rate and maximum transmission power constraints in [84]. Further, a distributed joint bandwidth and power allocation scheme to optimise EE for a set of users within the heterogeneous wireless networks is proposed in [85]. A joint BS association and power control scheme which is intent to satisfy the user's targeted SINR

for the uplink of a large-scale HetNet is proposed in [86]. In [87], a distributed non-cooperative game was proposed to improve the system EE in the downlink transmission scheme of HetNets. The BSs autonomously choose their optimal transmission strategies while balancing the load among themselves and satisfying the users' quality-of-service (QoS) requirements [87]. A distributed novel cooperative game to establish cooperation among macrocell and femtocell to quantify the user's utility in terms of throughput and delay was formulated in [88]. Afterwards, a coalition formation algorithm was proposed to solve the formulated cooperative game so that it achieves a stable partition with the help of a recursive core [88].

None of the previous works in the literature have considered maximising overall system EE and SE of HetNets simultaneously, while imposing a threshold on the cross-tier interference to protect the macrocell user. Considering that simply maximising either EE or SE does not utilise the resources efficiently, there is an increasing attention in fifth generation (5G) networks to jointly optimise the two conflicting objectives, i.e., EE and SE. It should be noted that the user lying within the coverage area of the heterogeneous environment can efficiently utilise its transmission power for its allocated bandwidth in order to either improve its achievable EE or SE. One of the key performance indicators in the 5G networks is to reduce the EE-SE tradeoff region which can be enabled by HetNets.

According to the best of our knowledge, there is no work in the literature focusing on jointly optimising EE and SE in an uplink of multi-user two-tier HetNets considering the cross-tier interference limitations and providing users' QoS in terms of minimum rate requirements and maximum transmission power constraints. In this chapter, an MOP

framework for joint power allocation and subcarrier assignment for EE-SE tradeoff under maximum transmission power constraints is formulated when satisfying a rate QoS requirement in two-tier HetNets. The proposed multi-objective framework jointly performs power allocation and subcarrier assignment while optimising the two conflicting objectives, namely, EE and SE. The formulated MOP is transformed into a single-objective optimisation problem (SOP) using a weighted sum method [ref]. Proving that the formulated SOP is strictly quasi-concave with respect to the transmit power, a unique optimal solution is derived. By exploiting the fractional programming concepts, the SOP problem can be transformed into an equivalent subtractive form which is tractable in nature. Then, an iterative two-layer solution combining Dinkelbach type method and Lagrangian dual decomposition approach is proposed to solve the formulated SOP.

4.2 Chapter Organisation

The remainder of the chapter is organised as follows. In Section 4.3 describes the system model and define the concept of EE and SE. In Section 4.4, the problem of jointly optimising EE and SE is formulated in an uplink of two-tier HetNets as an MOP. In Section 4.5, a two-layer solution is proposed to obtain the optimal allocation strategy to solve the formulated MOP. Numerical results are presented to demonstrate the effectiveness of the proposed approach in Section 4.6. Section 4.7 concludes the chapter.

4.3 System Model

In this work, an uplink two-tier HetNets is considered consisting of M networks (i.e., one macrocell (m_0), overlaid with $M-1$ pico BSs $(m_1, \cdots, m_{M-1})$), with a total number

of users N and a total number of subacrriers K. It is assumed that the $M-1$ pico BSs are deployed around the edge of the reference macrocell m_0. Let define the index set of all subcarriers as $\mathscr{K} = \{1,\cdots,K\}$, the set of all users as $\mathscr{N} = \{1,\cdots,N\}$ and the set of all networks as $\mathscr{M} = \{m_0, m_1, \cdots, m_{M-1}\}$. The total number of available networks in two-tier HetNets can be calculated as follows [89]:

$$M = 1 + \beta \left(\frac{(R_{m_0} + R_i)^2 - (R_{m_0} - R_i)^2}{R_i^2} \right), \tag{4.1}$$

where R_{m_0} and R_i represent the radius of macrocell and pico BS, respectively. When $\beta = 0$, it is the case of macrocell only, and therefore, $M = 1$, whereas in the case of HetNets, $0 < \beta \leq 1$ which indicates the number of pico BSs per macrocell.

Each network $m \in \mathscr{M}$ has its own bandwidth B_m equally divided among its subcarriers[2] $\mathscr{K}_m$, where $\mathscr{K}_m = \{1,\cdots,K_m\}$ represent the set of subcarriers in network m. The pico BS is connected to the macrocell via a high capacity wired backhaul. It is further assumed that the channel state information (CSI) corresponding to each subcarrier is perfectly known to the UE transmitters.

To maintain the QoS requirements, each user has a minimum-rate requirement constraint. It is assumed that the required minimum-rate level of all users are identical and is equal to $R_{\min}$. Assume $\sigma_{k,n}^{(\mathrm{m}_0)}$ and $\sigma_{k,n}^{(\mathrm{m}_i)}$ denoting the subcarrier allocation indices for macrocell m_0 and pico BS m_i, respectively. Particularly, when subcarrier $k \in \mathscr{K}_{\mathrm{m}_i}$ is allocated to user n, then $\sigma_{k,n}^{(\mathrm{m}_i)} = 1$, and otherwise, $\sigma_{k,n}^{(\mathrm{m}_i)} = 0$. Similarly, if the subcarrier

[2]It is worth to mention that the partition of subcarriers into the sets $\mathscr{K}_{m_0}$ and $\mathscr{K}_{m_i}, i = 1,2,\cdots,M-1$ is not predefined in the present formulation. The optimisation problem in (4.13a)-(4.13f) include an optimisation over $\mathscr{K}_{m_0}$ and $\mathscr{K}_{m_i}, i = 1,2,\cdots,M-1$ as well.

$k \in \mathscr{K}_{\mathrm{m}_0}$ is allocated to user n, $\sigma_{k,n}^{(\mathrm{m}_0)} = 1$, and otherwise, $\sigma_{k,n}^{(\mathrm{m}_0)} = 0$. The instantaneous data rate achieved on each subcarrier k by user n for macrocell m_0 and pico BS m_i can be written as follows:

$$\mathrm{r}_{k,n}^{(\mathrm{m}_0)} = \sigma_{k,n}^{(\mathrm{m}_0)} B_k \log_2\left(1 + \gamma_{k,n}^{(\mathrm{m}_0)} \times p_{k,n}^{(\mathrm{m}_0)}\right) \tag{4.2a}$$

$$\mathrm{r}_{k,n}^{(\mathrm{m}_i)} = \sigma_{k,n}^{(\mathrm{m}_i)} B_k \log_2\left(1 + \gamma_{k,n}^{(\mathrm{m}_i)} \times p_{k,n}^{(\mathrm{m}_i)}\right), \forall i \in \{1, 2, \cdots, M-1\} \tag{4.2b}$$

where B_k is the subcarrier bandwidth spacing assumed to be fixed in different networks. Here, $p_{k,n}^{(\mathrm{m}_i)}$ and $p_{k,n}^{(\mathrm{m}_0)}$ indicate the power allocated to the subcarrier k for user n in the pico BS m_i and macrocell m_0, respectively. Similarly, the rate of user n using subcarrier k choosing macrocell or pico BS m_i is represented by $r_{k,n}^{(\mathrm{m}_0)}$ and $r_{k,n}^{(\mathrm{m}_i)}$, respectively. $\gamma_{k,n}^{(\mathrm{m}_0)}$ and $\gamma_{k,n}^{(\mathrm{m}_i)}$ represent the signal-to-noise-ratio (SNR) of user n on subcarrier k in the macrocell m_0 and pico BS m_i, respectively, and are defined as follows:

$$\gamma_{k,n}^{(\mathrm{m}_0)} = \frac{|h_{k,n}^{(\mathrm{m}_0)}|^2}{\left(B_k N_0 + \sum\limits_{\substack{m \in \mathscr{M} \\ m \neq m_0}} \sum\limits_{n \in \mathscr{N}_m} \sigma_{k,n}^{(\mathrm{m})} p_{k,n}^{(m)} g_{k,n}^{mm_0}\right) \mathrm{PL}_n^{(\mathrm{m}_0)}}, \tag{4.3a}$$

$$\gamma_{k,n}^{(\mathrm{m}_i)} = \frac{|h_{k,n}^{(\mathrm{m}_i)}|^2}{\left(B_k N_0 + \sum\limits_{n \in \mathscr{N}_{m_0}} \sigma_{k,n}^{(\mathrm{m}_0)} p_{k,n}^{(m_0)} g_{k,n}^{m_0 m_i}\right) \mathrm{PL}_n^{(\mathrm{m}_i)}}, \forall i \in \{1, 2, \cdots, M-1\} \tag{4.3b}$$

where $h_{k,n}^{(\mathrm{m}_0)}$ and $h_{k,n}^{(\mathrm{m}_i)}$ represent the channel amplitude gains for user n on subcarrier k from macrocell m_0 and pico BS m_i, respectively. $\mathscr{N}_m$ and $\mathscr{N}_{m_0}$ represent the set of users associated with network m and macrocell m_0, respectively. The distance-based path loss in macrocell m_0 and pico BS m_i are denoted by $\mathrm{PL}_n^{(\mathrm{m}_0)}$ and $\mathrm{PL}_n^{(\mathrm{m}_i)}$, respectively. Note that

in (4.3a) and (4.3b), the co-tier interference from other pico BSs or macrocells is assumed to be a part of thermal noise N_0 due to the severe penetration loss and low transmission power of pico BSs as mentioned in [83] and [90].

The focus of this work is to investigate the trend of EE-SE tradeoff in the two-tier HetNets consisting of a macrocell m_0 overlaid with a number of pico BSs m_i, $\forall i \in \{1,2,\cdots,M-1\}$, the co-tier interference caused from the neighbouring macrocells or pico BSs can be easily considered and will appear as a constant term in (4.3a) and (4.3b).

In order to protect the macrocell users QoS, we implement the cross-tier interference protection by imposing the maximum cross-tier interference threshold suffered by macro BS. Let I_k^{th} denote the maximum threshold interference level on subcarrier k for the macro BS, we have,

$$\sum_{\substack{m\in\mathscr{M}\\ m\neq m_0}} \sum_{n\in\mathscr{N}_m} \tilde{\sigma}_{k,n}^{(\mathrm{m})} p_{k,n_m^*}^{(m)} g_{k,n_m^*}^{(m)} \leq I_k^{\text{th}}, \forall k, \tag{4.4}$$

where $n_m^* = \arg\max_n g_{k,n}^{(m)}, \forall n \in \mathscr{N}_m$ using the concept of the reference user [91]. The aggregate rate for the n^{th} user in macrocell m_0 and pico BS m_i are shown as follows:

$$\mathrm{r}_n^{(\mathrm{m}_0)} = \sum_{k\in\mathscr{K}_{\mathrm{m}_0}} r_{k,n}^{(\mathrm{m}_0)}, \forall n \in \mathscr{N} \tag{4.5a}$$

$$\mathrm{r}_n^{(\mathrm{m}_i)} = \sum_{k\in\mathscr{K}_{\mathrm{m}_i}} r_{k,n}^{(\mathrm{m}_i)}, \forall n \in \mathscr{N}, \forall i \in \{1,2,\cdots,M-1\} \tag{4.5b}$$

The overall rate of HetNets, R is composed of two components; The first component is the sum rate of the users choosing macrocell and the second one is the sum rate of the

users choosing pico BS, formulated as

$$\mathrm{R} = \sum_{n \in \mathscr{N}_{\mathrm{m}_0}} r_n^{(\mathrm{m}_0)} + \sum_{i=1}^{M-1} \left(\sum_{n \in \mathscr{N}_{\mathrm{m}_i}} r_n^{(\mathrm{m}_i)} \right), \tag{4.6}$$

where $\mathscr{N}_{\mathrm{m}_0}$ and $\mathscr{N}_{\mathrm{m}_i}$ denote the set of users associated with macrocell m_0 and pico BS m_i, respectively.

In order to avoid frequent vertical handoffs in HetNets, user association rules are defined for wireless transmissions [41]. In traditional homogeneous cellular networks, the user association is based on the received signal strength. Unique association of users with the macrocell or pico BS is assumed [41]. Therefore, a feasible subcarrier assignment index matrix C_m is given by:

$$\mathrm{C}_m \in \mathscr{C}_m = \left\{ \left(\sigma_{k,n}^{(m)} \right)_{k=1,n=1}^{K,N_m} \middle| \sum_{n \in \mathscr{N}} \sigma_{k,n}^{(m)} \leq 1, \forall k \in \mathscr{K}_m; \sigma_{k,n}^{(m)} \in \{0,1\}, \ \forall n \in \mathscr{N}_m, \forall k \in \mathscr{K}_m \right\}, \tag{4.7}$$

For simplicity, it is assumed that a set of available networks in two-tier HetNets are known. In practice, the transmission power available at user n is limited to a maximum threshold, i.e., $P_n^{\max}$, which can be formulated as:

$$\mathrm{P}_n \leq P_n^{\max}, \forall n \in \{1,2,\cdots,N\} \tag{4.8a}$$

$$\mathrm{P}_n = \sum_{k \in \mathscr{K}_m} p_{k,n}^{(m)}, \forall m \in \{m_0, m_1, m_2, \cdots, m_{M-1}\} \tag{4.8b}$$

In an uplink transmission scenario, multiple users transmit data towards a BS so each

communication link between user and BS introduces an individual circuit power [9]. Since the circuit power is related to the UE handsets, the circuit power in macrocell and pico BSs are denoted by $P_{\mathrm{C}}^{(\mathrm{m}_0)}$ and $P_{\mathrm{C}}^{(\mathrm{m}_i)}$, respectively such that $P_{\mathrm{C}}^{(\mathrm{m}_0)} = P_{\mathrm{C}}^{(\mathrm{m}_i)} = P_{\mathrm{C}}$. Hence, the overall power consumption in an uplink of HetNets is modelled as:

$$P = \varepsilon_0 P_{\mathrm{T}} + N \times P_{\mathrm{C}}, \tag{4.9a}$$

$$P_{\mathrm{T}} = \sum_{m\in\mathscr{M}} \sum_{k\in\mathscr{K}_m} \sum_{n\in\mathscr{N}} \sigma_{k,n}^{(m)} p_{k,n}^{(m)}, \tag{4.9b}$$

where ε_0 is the inverse of power amplifier efficiency.

The EE (η_{EE}) is defined as the amount of data transferred per unit energy consumed by the system (usually measured in (b/J) and is given by:

$$\eta_{\mathrm{EE}} = \frac{R}{P} = \frac{\sum_{m\in\mathscr{M}} \sum_{k\in\mathscr{K}_m} \sum_{n\in\mathscr{N}} r_{k,n}^{(m)}}{\varepsilon_0 \left(\sum_{m\in\mathscr{M}} \sum_{k\in\mathscr{K}_m} \sum_{n\in\mathscr{N}} \sigma_{k,n}^{(m)} p_{k,n}^{(m)} \right) + N \times P_{\mathrm{C}}} \quad \left[\text{bits/Joule}\right], \tag{4.10}$$

In (4.10), $r_{k,n}^{(m)}$ is concave with respect to the transmission power P_{T} because P_{T} is a non decreasing linear function of $p_{k,n}^{(m)}$. Since, the η_{EE} is strictly quasi-concave with respect to transmission power P_{T}, there exists one and only one optimal solution that maximises η_{EE}, denoted by $P_{\eta_{\mathrm{EE}}}^{*}$. η_{EE} strictly increases with $P_{\mathrm{T}} \in [0, P_{\eta_{\mathrm{EE}}}^{*}]$ while it strictly decreases with $P_{\mathrm{T}} \in [P_{\eta_{\mathrm{EE}}}^{*}, \infty)$. SE ($\eta_{\mathrm{SE}}$), on the other hand, is a measure that reflects the efficient utilization of the available spectrum in terms of throughput and is commonly defined as the amount of throughput that the BS can transmit over a given bandwidth, expressed in b/s/Hz. η_{SE} is a strictly increasing function of transmission power P_{T}, and is concave with

P_{T}. The SE (η_{SE}) is defined as:

$$\eta_{\mathrm{SE}} = \frac{\sum\limits_{m\in\mathscr{M}}\sum\limits_{k\in\mathscr{K}_m}\sum\limits_{n\in\mathscr{N}} r_{k,n}^{(m)}}{B} = \frac{\sum\limits_{m\in\mathscr{M}}\sum\limits_{k\in\mathscr{K}_m}\sum\limits_{n\in\mathscr{N}} r_{k,n}^{(m)}}{\sum\limits_{k\in\mathscr{K}} B_k} \qquad \left[\text{bits/s/Hz}\right], \tag{4.11}$$

First of all, in order to give readers an intuitive insight into our problem to jointly optimise EE and SE, Fig. 4.1 shows achievable EE and SE as a function of transmission power P_{T} with $N = 10$, $K = 10$, $B_k = 30$ kHz, $P_{\mathrm{C}} = 0.1$ W and $P_{\max} = 0.5$ W based on (4.10) and (4.11), respectively. From Fig. 4.1, it is quite obvious that in most of the cases, it is not usually possible to optimise both EE and SE simultaneously. In details, EE and SE both increase with transmission power P_{T} until the energy-efficient transmission power $P_{\mathrm{T}} = P^*_{\eta_{\mathrm{EE}}}$. However, when $P_{\mathrm{T}} > P^*_{\eta_{\mathrm{EE}}}$ and afterwards, EE decreases with an increase in SE as shown in Fig. 4.1. The corresponding optimal transmit power (highlighted by red circles in Fig. 4.1) to maximise EE and SE individually without any QoS requirements are obtained by solving (4.10) and (4.11) using standard convex optimisation methods. To visualise the effect of QoS requirements on the optimisation of EE and SE, Fig. 4.1 depicts the corresponding optimal transmit power which maximises EE and SE individually with the QoS requirement set at $15, 16, 18$ and 20 b/s/Hz as indicated by series of blue circles. It is quite obvious that a particular QoS requirement constraint can effect the existence of power region which allows all the constraints to be met simultaneously. Secondly, due to the Shannon Hartley theorem, increasing the transmit bandwidth reduces the transmit power for a same target rate requirement. For achieving a fixed minimum

rate, as the bandwidth increases, EE increases whereas SE decreases. Finally, the maximisation of EE produces a different optimal point if the user can access subcarriers with better channel gains resulting in improving its utility. This motivates us to dynamically tune the EE and SE trade-off curve dependent on the available resources, in terms of bandwidth and the transmission power for next generation networks to achieve two-fold benefits in the form of satisfactory SE and saving as much transmission power as possible. It is also worthwhile to mention that in most of the power regions, the power allocation strategies to increase these metrics are conflicting approaches. This motivates the work in the following Section which is to jointly optimise EE and SE using a multi-objective optimisation problem.

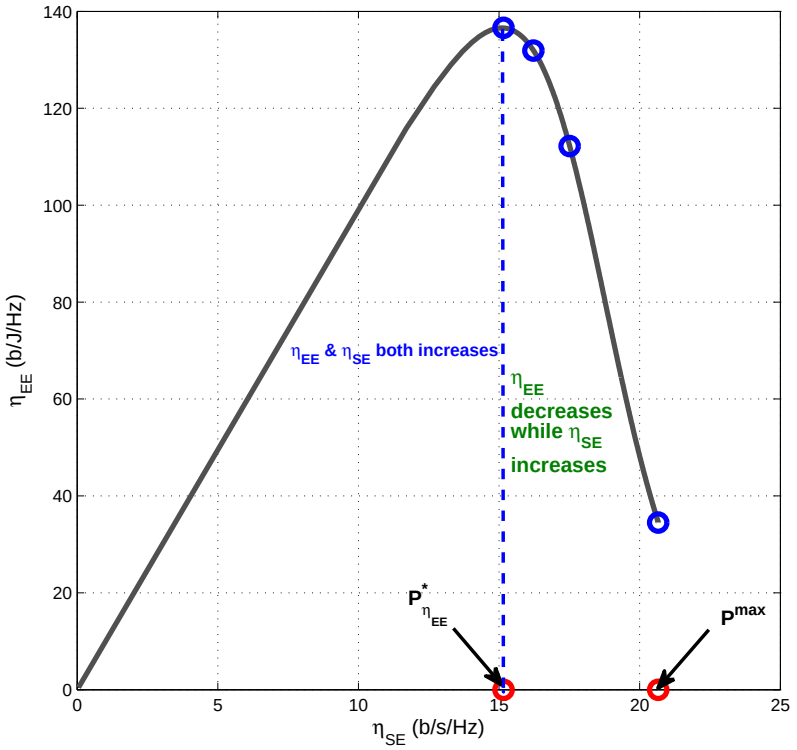

FIGURE 4.1: η_{EE}-η_{SE} tradeoff curve as a function of transmission power P_{T}.

4.4 Problem Formulation of EE-SE Tradeoff

Our goal is to optimise EE and SE simultaneously. We start by formulating the joint EE and SE trade-off with the minimum throughput and maximum transmission power constraints in an uplink transmission scheme of Two-Tier HetNets as a multi-objective optimisation approach. The MOP can be formulated as follows:

$$\max_{\sigma_{k,n}^{(m)},p_{k,n}^{(m)}} \eta_{\mathrm{EE}} \quad \text{and} \quad \max_{\sigma_{k,n}^{(m)},p_{k,n}^{(m)}} \eta_{\mathrm{SE}} \tag{4.12}$$

To solve this MOP, the concept of Pareto optimality [92] is utilised. The EE-SE tradeoff is usually illustrated as a two dimensional curve consisting of set of all feasible $(\eta_{\mathrm{SE}}, \eta_{\mathrm{EE}})$ pairs.

Definition 1: A point $p_0 \in \mathscr{P}_{\mathrm{S}}$, where $\mathscr{P}_{\mathrm{S}} = \{P_{\mathrm{T}} \big| P_{\min} \leq P_{\mathrm{T}} \leq P_n^{\max}\}$ is Pareto efficient if and only if there does not exist any other point $p_1 \in \mathscr{P}_{\mathrm{S}}$ such that $\eta_{\mathrm{EE}}(p_1) \geq \eta_{\mathrm{EE}}(p_0)$, $\eta_{\mathrm{SE}}(p_1) \geq \eta_{\mathrm{SE}}(p_0)$ and at least one η_{EE} or η_{SE} has been strictly improved. In simple terms, a point is Pareto efficient if there is no other point that can improve both η_{EE} and η_{SE} simultaneously. The set of all Pareto efficient points is called the Pareto Frontier or the complete Pareto optimal set. The Pareto Frontier illustrates an optimal tradeoff between η_{SE} and η_{EE} such that it provides the maximum value of $\eta_{\mathrm{SE}}(\eta_{\mathrm{EE}})$ for a given $\eta_{\mathrm{EE}}(\eta_{\mathrm{SE}})$. In particular, the weighted sum method can provide the complete Pareto optimal set of the considered problem by solving the MOP and provide the necessary condition for Pareto optimality.

In MOP, the process of ordering the objectives can be done either as priori or posteriori

of executing the optimisation algorithm. We combine the maximisation of EE and SE by choosing appropriate weights decided a priori. Since the bandwidth is larger than the transmission power so a simple summation of EE and SE will tend to focus on the optimisation of EE. In order to maintain the balance between EE and SE, the optimisation problem is transformed using the normalised factors θ_{EE} and θ_{SE} such that EE and SE are in the similar scale. Using the weighted sum method [63], the MOP in (4.12) can be converted into SOP defined as:

$$\max_{\sigma_{k,n}^{(m)}, p_{k,n}^{(m)}} \quad \omega\theta_{\text{EE}}\eta_{\text{EE}} + (1-\omega)\theta_{\text{SE}}\eta_{\text{SE}} \tag{4.13a}$$

s.t.

$$\sum_{m\in\mathscr{M}} \sum_{k\in\mathscr{K}_m} r_{k,n}^{(m)} \geq R_n^{\min}, \forall n. \tag{4.13b}$$

$$\sum_{m\in\mathscr{M}} \sum_{k\in\mathscr{K}_m} \sigma_{k,n}^{(\text{m})} p_{k,n}^{(m)} \leq P_n^{\max}, \forall n. \tag{4.13c}$$

$$\sum_{\substack{m\in\mathscr{M} \\ m\neq m_0}} \sum_{n\in\mathscr{N}_m} \tilde{\sigma}_{k,n}^{(\text{m})} p_{k,n}^{(m)} g_{k,n}^{mm_0} \leq I_k^{\text{th}}, \forall k. \tag{4.13d}$$

$$\sum_{n\in\mathscr{N}_m} \sigma_{k,n}^{(m)} \leq 1, \forall k, \forall m. \tag{4.13e}$$

$$p_{k,n}^{(m)} \geq 0, \sigma_{k,n}^{(m)} \in \{0,1\}, \ \forall n, \forall k, \forall m. \tag{4.13f}$$

Here, (4.13a) represents the EE-SE tradeoff optimisation problem and ω is the tradeoff

parameter such that $0 \leq \omega \leq 1$ which provides flexibility to achieve the EE-SE trade-off. The QoS constraint (4.13b) guarantees the minimum user rate requirement. Constraint (4.13c) limits the maximum transmission of each user to be less than $P_n^{\max}$. The constraint in (4.13d) sets the maximum tolerable cross-tier interference on each subcarrier k of the macrocell m_0. The constraint (4.13e) and (4.13f) ensure that each subcarrier can be only assigned to at most one user in each network m at a time. The constraint (4.13f) also confirms the feasibility of non-negative transmission power on each subcarrier. It should be noted that when $p_{k,n}^{(m)^*} \geq P_n^{\max}$, the proposed solution for (4.13a) contains a unique global optimal solution, i.e., $P_n^{\max}$. Therefore, the case of $p_{k,n}^{(m)^*} < P_n^{\max}$ is analysed for the rest of this chapter. Hence, (4.13a) can be written as

$$\overline{\eta} = \max_{\sigma_{k,n}^{(m)}, p_{k,n}^{(m)}} \quad \theta_{\mathrm{EE}}\eta_{\mathrm{EE}} + \left(\frac{1-\omega}{\omega}\right)\theta_{\mathrm{SE}}\eta_{\mathrm{SE}} \qquad \left[\text{bits/s}\right] \tag{4.14}$$

In (4.14), $\left(\frac{1-\omega}{\omega}\right)$ can be replaced with α which can hold any real value from zero to ∞. After some mathematical manipulations, (4.14) can be simplified to

$$\eta = \frac{\overline{\eta}}{\theta_{\mathrm{EE}}} = \max_{\sigma_{k,n}^{(m)}, p_{k,n}^{(m)}} \quad \eta_{\mathrm{EE}} + \alpha\left(\frac{\theta_{\mathrm{SE}}\eta_{\mathrm{SE}}}{\theta_{\mathrm{EE}}}\right) \qquad \left[\text{bits/Joule}\right], \tag{4.15a}$$

s.t.

$$(4.13\text{b}) - (4.13\text{e}). \tag{4.15b}$$

$$\alpha \geq 0, p_{k,n}^{(m)} \geq 0, \tilde{\sigma}_{k,n}^{(m)} \in \{0,1\}, \ \forall n, \forall k, \forall m. \tag{4.15c}$$

where $\alpha \in \left[0, \infty\right)$ is the weighted coefficient. When $\alpha = 0$, the problem in (4.15a) is

transformed into an EE maximisation problem whereas it is transformed into an SE maximisation problem when $\alpha \to \infty$. In other words, the importance of SE gradually increases as α increases from 0 to ∞.

Remark 1: The optimisation problem in (4.15a) has two important properties stated as follow:

Property 1: The optimal transmit power to achieve η^* is non-decreasing with the weighted coefficient α. When $\alpha = 0$, the optimal transmit power is $P^*_{\eta_{\text{EE}}}$; whereas when $0 < \alpha < \infty$, the optimal transmit power strictly increases with α until it approaches the maximum transmit power. In other words, an increase of α gives more importance to η_{SE} resulting in lesser importance to η_{EE}. Due to this, the optimal transmit power shift from $P^*_{\eta_{\text{EE}}}$ towards the maximum transmit power.

Property 2: η_{SE} is non-decreasing with the weighted coefficient α, while η_{EE} is non-increasing with the weighted coefficient α. Lets us assume that α_1 and α_2 are the weighted coefficients such that $\alpha_2 > \alpha_1$. From property 1, the optimal transmit power $P^*_{\eta}\Big|_{\alpha_2} > P^*_{\eta}\Big|_{\alpha_1}$. As η_{SE} increases monotonically with transmit power whereas η_{EE} decreases monotonically with transmit power beyond $P^*_{\eta_{\text{EE}}}$. Hence, the Property 2 can be easily verified.

The maximisation problem (4.15*a*) is an integer combinatorial fractional programming problem and is generally NP-hard. For better tractability, the integer variables, $\sigma^{(m)}_{k,n} \in \{0,1\}$ is first relaxed into continuous variables, $\tilde{\sigma}^{(m)}_{k,n} \in [0,1]$. Then, the modified problem

for (4.15a) can be written as

$$\eta = \max_{\tilde{\sigma}_{k,n}^{(m)}, p_{k,n}^{(m)}} \quad \eta_{\mathrm{EE}} \left(1 + \alpha \left(\frac{\theta_{\mathrm{SE}} \times \eta_{\mathrm{SE}}}{\theta_{\mathrm{EE}} \times \eta_{\mathrm{EE}}} \right) \right), \tag{4.16a}$$

s.t.

$$(4.13b) - (4.13e). \tag{4.16b}$$

$$\alpha \geq 0, p_{k,n}^{(m)} \geq 0, \tilde{\sigma}_{k,n}^{(m)} \in [0,1], \ \forall n, \forall k, \forall m. \tag{4.16c}$$

Lemma 1: η is jointly quasi-concave with respect to $p_{k,n}^{(m)}$ and $\tilde{\sigma}_{k,n}^{(m)}$.

Proof:- Please refer to the **Appendix A**.

η is quasi-concave with respect to the optimisation variables and a unique optimal solution can be obtained using convex optimisation techniques such as bisection method and Lagrangian dual decomposition method [52]. As mentioned in [93] and [94], any sum-of-ratios (or fractional form) optimisation problem can be transformed into an equivalent optimisation problem in sum-of-ratios subtractive form. It has been proven in [93, Theorem 1] that problems (4.16a) and (4.17) are equivalent to each other, i.e., the solution of (4.17) corresponds to the optimal transmission power. As a result, the focus will be on the equivalent subtractive objective function in the rest of the chapter. Hence, the non-linear fractional optimisation problem in (4.16a) can be transformed into the parameterized function as

$$G(\eta)=\left(\underbrace{\sum_{m\in\mathscr{M}}\sum_{k\in\mathscr{K}_m}\sum_{n\in\mathscr{N}} r_{k,n}^{(m)}\left(1+\alpha\left(\frac{\theta_{\mathrm{SE}}P}{\theta_{\mathrm{EE}}B}\right)\right)}_{\text{First term}}-\eta\underbrace{\left(N\times P_{\mathrm{C}}+\varepsilon_0\sum_{m\in\mathscr{M}}\sum_{k\in\mathscr{K}_m}\sum_{n\in\mathscr{N}}\tilde{\sigma}_{k,n}^{(m)}p_{k,n}^{(m)}\right)}_{\text{Second term}}\right). \tag{4.17}$$

Remark 2: The concavity of transformed objective function in (4.17) with respect to the optimisation variables $\tilde{\sigma}_{k,n}^{(m)}$ and $p_{k,n}^{(m)}$ can be proved in two steps. Firstly, the concavity of first term in (4.17) is proved with respect to the optimisation variables $\tilde{\sigma}_{k,n}^{(m)}$ and $p_{k,n}^{(m)}$. For notational simplicity, we define a vector $z_{k,n}^{(m)}=\left[\tilde{\sigma}_{k,n}^{(m)}\quad p_{k,n}^{(m)}\right]$ and a function $f_{k,n}^{(m)}\left(z_{k,n}^{(m)}\right)=r_{k,n}^{(m)}\left(1+\alpha\left(\frac{\theta_{\mathrm{SE}}P}{\theta_{\mathrm{EE}}B}\right)\right)$ which takes $z_{k,n}^{(m)}$ as an input. The Hessian matrix $H\left(f_{k,n}^{(m)}\left(z_{k,n}^{(m)}\right)\right)$ of $f_{k,n}^{(m)}\left(z_{k,n}^{(m)}\right)$ is a negative semi-definite matrix and its corresponding both eigenvalues are also negative. Therefore, $f_{k,n}^{(m)}\left(z_{k,n}^{(m)}\right)$ is jointly concave with respect to the optimisation variables $\tilde{\sigma}_{k,n}^{(m)}$ and $p_{k,n}^{(m)}$.

Subsequently, $\sum_{m\in\mathscr{M}}\sum_{k\in\mathscr{K}_m}\sum_{n\in\mathscr{N}} r_{k,n}^{(m)}\left(1+\alpha\left(\frac{\theta_{\mathrm{SE}}P}{\theta_{\mathrm{EE}}B}\right)\right)$ is also concave since it is the linear combination of $f_{k,n}^{(m)}\left(z_{k,n}^{(m)}\right)$ which preserves the concavity. Finally, $\left(N\times P_{\mathrm{C}}+\varepsilon_0\sum_{m\in\mathscr{M}}\sum_{k\in\mathscr{K}_m}\sum_{n\in\mathscr{N}}\tilde{\sigma}_{k,n}^{(m)}p_{k,n}^{(m)}\right)$ is an affine function with respect to the optimisation variables $\tilde{\sigma}_{k,n}^{(m)}$ and $p_{k,n}^{(m)}$. Therefore, it is proved that $G(\eta)$ is jointly concave with respect to the optimisation variables $\tilde{\sigma}_{k,n}^{(m)}$ and $p_{k,n}^{(m)}$. As a result, strong duality holds and solving the dual problem is equivalent to solving the primal problem of (4.17). It has been shown that the duality gap approaches to zero for sufficiently large number of subcarriers and it is quite small for practical number of subcarriers as mentioned in [95] [96]. In [96], it is shown that only 8 subcarriers are sufficient in some cases to achieve zero duality gap .

It is worth to mention that $G(\eta)$ monotonically decreases with an increase in η, i.e.,

$G(\eta^{'}) > G(\eta)$ if $\eta^{'} > \eta$. The optimal solution $\eta = \eta^{*}$ of (4.17) can be determined by finding the root to the $G(\eta)$, i.e., the transformed fractional form in substractive form of (4.16a), using various root finding methods [52].

Lemma 2: $\mathscr{G}(\eta) \triangleq \max_{\tilde{\sigma}_{k,n}^{(m)}, p_{k,n}^{(m)}} G(\eta)$ under the constraints (4.16b) – (4.16c), satisfies

$$\mathscr{G}(\eta) = 0 \quad \text{iff} \quad \eta = \eta^{*}.$$

From Lemma 2, $\mathscr{G}(\eta)$ is strictly monotonically decreasing with respect to η. The lemma also implies that when $\eta \to -\infty, \mathscr{G}(\eta) > 0$ and when $\eta \to \infty, \mathscr{G}(\eta) < 0$. (4.17) shows that $G(\eta) > 0$, when $\eta \leq 0$, because the first and second terms in (4.17) are definitely positive. Therefore, $G(\eta) = 0$ occurs at $\eta > 0$, and hence, (4.17) will be solved for $\eta > 0$. Details of its proof can be found in **Appendix B**.

4.5 EE and SE tradeoff Resource Allocation scheme

In HetNets, there exists two different channel deployment schemes, co-channel and orthogonal channel deployment schemes. In the former scheme, the macrocell and a set of pico BSs are permitted to use the same resource for data transmission at any time, which will cause co-tier and cross-tier interference. In orthogonal channel deployment scheme, the spectrum is divided into two orthogonal parts, one part for macrocell use and the second part for the set of pico BSs such that each resource is exclusively assigned to either macrocell m_0 or a set of pico BSs $m_i, \forall i \in \{1, 2, \cdots, M-1\}$, at any time causing no cross-tier interference between macrocell and the set of pico BSs. The co-tier interference will still occur among those pico BSs sharing the same resources. However in this work,

the co-channel deployment scheme is considered such that co-tier interference is assumed to be part of thermal noise N_0 as discussed earlier in Section 4.4.

In this Section, an iterative algorithm is proposed for solving (4.17) with an equivalent subtractive objective function such that the obtained solution satisfies the conditions stated in Lemma 2. The solution to the EE-SE tradeoff problem is formulated as a two-layer solution. An iterative Dinkelbach type method[3] (Algorithm 4.1) is proposed as an outer layer solution to find an optimal solution to (4.17) by determining a root to $G(\eta) = 0$. Note that for any value of η, generated by Algorithm 4.1 in each iteration, $G(\eta) \geq 0$ is always valid; negative utility value will not occur. In particular, $\sum_{m\in\mathscr{M}} \sum_{k\in\mathscr{K}_m} \sum_{n\in\mathscr{N}} r_{k,n}^{(m)} \left(1+\alpha\left(\frac{\theta_{\text{SE}}P}{\theta_{\text{EE}}B}\right)\right)$ represents the system utility due to the data transmission while $\eta\left(N\times P_{\text{C}}+\varepsilon_0 \sum_{m\in\mathscr{M}} \sum_{k\in\mathscr{K}_m} \sum_{n\in\mathscr{N}} \tilde{\sigma}_{k,n}^{(m)} p_{k,n}^{(m)}\right)$ represents the associated cost due to the energy consumption. The optimal value of η indicates a scaling factor for balancing the system utility and cost. At an iteration $i-1$, the value of η is initialised and the $G(\eta)$ is solved for a given value of η, i.e., η_{i-1}, and the optimal power p_{i-1}^* is computed using the dual decomposition approach, i.e., inner layer solution, explained in the next Section. The optimal power computed in iteration $i-1$ can be used to update the value of η for iteration i. This process is repeated until it converges to an optimal value η^*. The proof of convergence for the proposed method is guaranteed and its pseudo code is shown in Algorithm 4.1. In particular, η increases in each iteration i such that $\eta_{i+1} > \eta_i$. For a large number of iterations $iter$, η converges to an optimal value η^* such that it satisfies the optimality condition in **Lemma 2**, i.e., $G(\eta) = 0$. The proof of the convergence can

[3]It is an application of Newton method to find the root of an objective function.

be achieved using a similar approach as mentioned in [93, Appendix A][94] and is not provided here due to the space limitations.

4.5.1 Dual Decomposition Formulation

In this Subsection, we solve the tradeoff optimisation problem by solving its dual to the primal problem for a given value of η. By using the dual decomposition approach [93][95], an iterative procedure can be obtained to solve $G(\eta)=0$ in each iteration of the proposed Algorithm 4.1. It is shown that the dual decomposition approach has lower computational complexity as compared to the exhaustive search or the branch-and-bound schemes [97]. In order to apply dual decomposition method, the Lagrangian function of (4.17) using standard convex optimisation methods as mentioned in [52] can be written as follow:

$$\begin{aligned} L(p,\underline{\lambda},\underline{\mu},\underline{\nu}) = & \sum_{m\in\mathscr{M}}\sum_{k\in\mathscr{K}_m}\sum_{n\in\mathscr{N}} r_{k,n}^{(m)}\left(1+\alpha\frac{\tau_{\mathrm{EE}}}{\tau_{\mathrm{SE}}}\right) - \eta\left(\varepsilon_0\sum_{m\in\mathscr{M}}\sum_{k\in\mathscr{K}_m}\sum_{n\in\mathscr{N}}\tilde{\sigma}_{k,n}^{(m)}p_{k,n}^{(m)} + N\times P_{\mathrm{C}}\right) \\ & + \sum_{n\in\mathscr{N}}\lambda_n\left(\sum_{m\in\mathscr{M}}\sum_{k\in\mathscr{K}_m} r_{k,n}^{(m)} - R_n^{\min}\right) + \sum_{n\in\mathscr{N}}\mu_n\left(P_n^{\max} - \sum_{m\in\mathscr{M}}\sum_{k\in\mathscr{K}_m}\tilde{\sigma}_{k,n}^{(m)}p_{k,n}^{(m)}\right) \\ & + \sum_{k\in\mathscr{K}_m}\nu_k\left(I_k^{\mathrm{th}} - \sum_{m\in\mathscr{M}}\sum_{n\in\mathscr{N}_m}\tilde{\sigma}_{k,n}^{(\mathrm{m})}p_{k,n}^{(m)}g_{k,n}^{mm_0}\right) \end{aligned} \tag{4.18}$$

where $\tau_{\mathrm{EE}}=\dfrac{P}{\theta_{\mathrm{EE}}}$ and $\tau_{\mathrm{SE}}=\dfrac{B}{\theta_{\mathrm{SE}}}$. $\underline{\lambda}=(\lambda_1,\lambda_2,\cdots,\lambda_N)$ is the Lagrange multiplier vector associated with the minimum data rate constraint (4.13b). $\underline{\mu}=(\mu_1,\mu_2,\cdots,\mu_N)$ is the Lagrange multiplier vector associated with the total transmit power constraint (4.13c).

$\underline{\nu} = (\nu_1, \nu_2, \cdots, \nu_K)$ is the Lagrange multiplier vector corresponding to the cross-tier interference constraint (4.13d) and $\nu_k = 0$ for $k \in K_{m_0}$. The constraints in (4.13e) and (4.16c) are later considered by dual decomposition method such that each subcarrier can be exclusively assigned to a single user within a network m and the non-negative optimal powers are computed. The dual problem corresponding to the primal problem of (4.17) can be given by [64]:

$$\min_{\underline{\lambda},\underline{\mu},\underline{\nu}\geq 0} \max_{\sigma,p} L(p,\underline{\lambda},\underline{\mu},\underline{\nu}) \tag{4.19}$$

The Lagrange dual function corresponding to problem (4.17) is

$$g(\underline{\lambda},\underline{\mu},\underline{\nu}) = \max_{\sigma,p} L(p,\underline{\lambda},\underline{\mu},\underline{\nu}) \tag{4.20}$$

Similarly, $g(\underline{\lambda},\underline{\mu},\underline{\nu})$ is the dual function and can be shown as

$$g(\underline{\lambda},\underline{\mu},\underline{\nu}) = \sum_{k\in\mathscr{K}_m} g_k(\underline{\lambda},\underline{\mu},\underline{\nu}) - \eta\varepsilon_0 \mathrm{N}P_{\mathrm{C}} - \sum_{n\in\mathscr{N}} \lambda_n R_n^{\min} + \sum_{n\in\mathscr{N}} \mu_n P_n^{\max} + \sum_{k\in\mathscr{K}} \nu_k I_k^{\mathrm{th}}, \tag{4.21}$$

where $g_k(\underline{\lambda},\underline{\mu},\underline{\nu})$ is defined by

$$g_k(\underline{\lambda},\underline{\mu},\underline{\nu}) = \max_{\tilde{\sigma}_k,p_k} \left(\sum_{m\in\mathscr{M}}\sum_{n\in\mathscr{N}} r_{k,n}^{(m)} \left(1+\alpha\frac{\tau_{\mathrm{EE}}}{\tau_{\mathrm{SE}}}\right) - \eta\varepsilon_0 \sum_{m\in\mathscr{M}}\sum_{n\in\mathscr{N}} \tilde{\sigma}_{k,n}^{(m)} p_{k,n}^{(m)} + \sum_{m\in\mathscr{M}}\sum_{n\in\mathscr{N}} \lambda_n r_{k,n}^{(m)} \right.$$
$$\left. - \sum_{m\in\mathscr{M}}\sum_{n\in\mathscr{N}} \mu_n \tilde{\sigma}_{k,n}^{(m)} p_{k,n}^{(m)} - \sum_{m\in\mathscr{M}}\sum_{n\in\mathscr{N}_m} \nu_k \tilde{\sigma}_{k,n}^{(\mathrm{m})} p_{k,n}^{(m)} g_{k,n}^{mm_0} \right) \tag{4.22}$$

The corresponding dual problem to the primal problem of (4.17) is hence given by

$$\begin{aligned} &\min_{\underline{\lambda},\underline{\mu},\underline{\nu}} g(\underline{\lambda},\underline{\mu},\underline{\nu}) \\ \text{s.t.} \quad &\underline{\lambda} \geq 0, \underline{\mu} \geq 0, \underline{\nu} \geq 0 \end{aligned} \tag{4.23}$$

4.5.2 Dual Decomposition Solution

To solve the dual problem in (4.19), we have decomposed it into a hierarchy of two problems. The slave problem is an inner maximisation in (4.20) consisting of K subproblems solved in parallel to compute the power and subcarrier allocation on each subcarrier $k \in \mathscr{K}$ for the given values of λ, μ, ν and η; whereas an outer minimisation in (4.23) is the master problem in which the Lagrangian multipliers are updated using a subgradient method. After a few mathematical manipulations, (4.22) can be written as

$$\begin{aligned} g_k(\underline{\lambda},\underline{\mu},\underline{\nu}) = \max_{\tilde{\sigma}_k, p_k} \Bigg(&\sum_{m\in\mathscr{M}} \sum_{n\in\mathscr{N}} \tilde{\sigma}_{k,n}^{(m)} B_k \log_2\left(1+\gamma_{k,n}^{(m)} p_{k,n}^{(m)}\right) \left[\left(1+\alpha\frac{\tau_{\text{EE}}}{\tau_{\text{SE}}}\right)+\lambda_n\right] \\ &- \sum_{m\in\mathscr{M}} \sum_{n\in\mathscr{N}} \left(\mu_n + \eta\varepsilon_0 + \nu_k g_{k,n}^{mm_0}\right) \tilde{\sigma}_{k,n}^{(m)} p_{k,n}^{(m)} \Bigg) \end{aligned} \tag{4.24}$$

Now, by taking the first-order derivatives of (4.24) with respect to $\tilde{\sigma}_{k,n}^{(m)}$, we get

$$\frac{\partial g_k(\underline{\lambda},\underline{\mu},\underline{\nu})}{\partial \tilde{\sigma}_{k,n}^{(m)}} = B_k \log_2\left(1+\gamma_{k,n}^{(m)} p_{k,n}^{(m)}\right) \left[\left(1+\alpha\frac{\tau_{\text{EE}}}{\tau_{\text{SE}}}\right)+\lambda_n\right] - \left(\mu_n + \eta\varepsilon_0 + \nu_k g_{k,n}^{mm_0}\right) p_{k,n}^{(m)} \tag{4.25}$$

The subcarrier assignment index $\tilde{\sigma}_{k,n}^{(m)}$ at given λ, μ, ν and η can be determined as:

$$\tilde{\sigma}_{k,n}^{(m)} = \begin{cases} 1, & \text{if } (k,m^*,n^*) = \arg\max_{m,n} B_k \log_2\left(1+\gamma_{k,n}^{(m)} p_{k,n}^{(m)}\right)\left[\left(1+\alpha\frac{\tau_{\text{EE}}}{\tau_{\text{SE}}}\right)+\lambda_n\right] \\ -\left(\mu_n+\eta\varepsilon_0+\nu_k g_{k,n}^{mm_0}\right) p_{k,n}^{(m)} \\ 0, & \text{otherwise.} \end{cases} \tag{4.26}$$

Note that (4.26) also gives us an insight into the user association and the set of subcarriers assigned to the network m, i.e., $\mathscr{K}_m$, which consists of all the subcarriers $k \in \mathscr{K}$ with $\tilde{\sigma}_{k,n}^{(m)} = 1$. For a fixed set of Lagrange multipliers and a given parameter η, the power for user n on subcarrier k can be computed by taking the first-order derivative of (4.24) with respect to $p_{k,n}^{(m)}$, yielding

$$\frac{\partial g_k(\underline{\lambda},\underline{\mu},\underline{\nu})}{\partial p_{k,n}^{(m)}} = \frac{\tilde{\sigma}_{k,n}^{(m)} B_k\left[\left(1+\alpha\frac{\tau_{\text{EE}}}{\tau_{\text{SE}}}\right)+\lambda_n\right]\times\gamma_{k,n}^{(m)}}{\ln(2)\left(1+\gamma_{k,n}^{(m)} p_{k,n}^{(m)}\right)} - \left(\mu_n+\eta\varepsilon_0+\nu_k g_{k,n}^{mm_0}\right) \tag{4.27}$$

Applying the KKT conditions results in

$$\left.\frac{\partial g_k(\underline{\lambda},\underline{\mu},\underline{\nu})}{\partial p_{k,n}^{(m)}}\right|_{p_{k,n}^{(m)}=p_{k,n}^{(m)*}} = 0 \Longrightarrow$$

Hence,

$$p_{k,n}^{(m)} = \begin{cases} \left(\dfrac{B_k\left((1+\alpha\frac{\tau_{\text{EE}}}{\tau_{\text{SE}}})+\lambda_n\right)}{\ln 2\left(\mu_n+\eta\varepsilon_0+\nu_k g_{k,n}^{mm_0}\right)} - \dfrac{1}{\gamma_{k,n}^{(m)}}\right)^+, & \text{if } \tilde{\sigma}_{k,n}^{(m)} = 1. \\ 0, & \text{otherwise.} \end{cases} \tag{4.28}$$

The optimal solution of (4.17) can then be expressed as

$$p_{k,n}^{(m)^*} = \max\left(\min\left(p_{k,n}^{(m)}, P_n^{\max}\right), P_n^{\min}\right), \tag{4.29}$$

where $P_n^{\min} = \left(2^{\left(\sigma_{k,n}^{(\mathrm{m})} R_n^{\min}/B_k\right)} - 1\right)/\gamma_{k,n}^{(\mathrm{m})}$. Thus, the optimal power allocation for each user n on subcarrier k has a semi-closed form expression in terms of dual variables λ, μ and ν. It is also observed that the optimal power allocation given by (4.28) is a modified water filling solution, where the channel gain is given by $\gamma_{k,n}^{(m)}$ and the water levels are determined both by the Lagrangian multipliers λ, μ, ν and weighting coefficient α as well by the EE-SE tradeoff metric η. The dual variables $\{\underline{\lambda}, \underline{\mu}, \underline{\nu}\}$ must satisfy the KKT conditions in order to be optimal and $\tilde{\sigma}_{k,n}^{(m)} = 1$ indicates that the subcarrier k is assigned to user n associated with network m.

It should be noted that the weighted coefficient $\alpha = 0$ maximises the EE whereas at $\alpha = \alpha_{\mathrm{SE}}$ the SE is maximised. For a given subcarrier assignment, the SE is maximised when each user transmits at their maximum transmission power. It is assumed that each user distribute its maximum transmission power equally among its subcarriers such that $p_{k,n}^{(m)} = \frac{P_n^{\max}}{|K_n|}$, where K_n is the set of subcarriers allocated to user n. In order to compute the weighted coefficient $\alpha_{\mathrm{SE}}^{(n)}$ which can achieve the maximum SE for user n, (4.28) can be rewritten as:

$$\frac{P_n^{\max}}{|K_n|} = \left(\frac{B_k\left((1+\alpha_{\mathrm{SE}}^{(n)}\frac{\tau_{\mathrm{EE}}}{\tau_{\mathrm{SE}}})+\lambda_n\right)}{\ln 2\left(\mu_n+\eta\varepsilon_0+\nu_k g_{k,n}^{mm_0}\right)} - \frac{1}{\gamma_n^{min}}\right), \tag{4.30}$$

where γ_n^{min} is the minimum channel-to-noise-ratio (SNR) among all the subcarriers allocated to the user n. From (4.30), $\alpha_{\text{SE}}^{(n)}$ can be easily derived as:

$$\alpha_{\text{SE}}^{(n)} = \frac{\tau_{\text{SE}}}{\tau_{\text{EE}}} \left[\left(\frac{P_n^{\max}}{|K_n|} + \frac{1}{\gamma_n^{min}} \right) \frac{\ln 2 \left(\mu_n + \eta \varepsilon_0 + \nu_k g_{k,n}^{mm_0} \right)}{B_k} - \lambda_n - 1 \right]. \tag{4.31}$$

Finally, α_{SE} can be computed as

$$\alpha_{\text{SE}} = \max\{\alpha_{\text{SE}}^{(1)}, \alpha_{\text{SE}}^{(2)}, \cdots, \alpha_{\text{SE}}^{(N)}\}. \tag{4.32}$$

4.5.3 Updating the Dual Variables

In order to minimise the dual function $g(\underline{\lambda}, \underline{\mu}, \underline{\nu})$, since the dual function is differentiable the subgradient method can be used to update the dual variables λ, μ and ν. The subgradient of λ, μ and ν are respectively given by taking the derivative of $L(p, \underline{\lambda}, \underline{\mu}, \underline{\nu})$ with respect to λ, μ and ν, yielding

$$\triangle\lambda = \sum_{m \in \mathscr{M}} \sum_{k \in \mathscr{K}_m} r_{k,n}^{(m)} - R_n^{\min}, \tag{4.33a}$$

$$\triangle\mu = P_n^{\max} - \sum_{m \in \mathscr{M}} \sum_{k \in \mathscr{K}_m} p_{k,n}^{(m)}. \tag{4.33b}$$

$$\triangle\nu = I_{th}^{(k)} - \sum_{\substack{m \in \mathscr{M} \\ m \neq m_0}} \sum_{n \in \mathscr{N}_m} \tilde{\sigma}_{k,n}^{(\text{m})} p_{k,n}^{(m)} g_{k,n}^{mm_0}. \tag{4.33c}$$

Then, the Lagrange multipliers (λ, μ) can be updated according to

$$\lambda_n(i+1) = \left[\lambda_n(i) - \frac{s^1}{\sqrt{i}}\left(\sum_{m\in\mathscr{M}}\sum_{k\in\mathscr{K}_m} r_{k,n}^{(m)} - R_n^{\min}\right)\right]^+, \forall n \tag{4.34a}$$

$$\mu_n(i+1) = \left[\mu_n(i) - \frac{s^2}{\sqrt{i}}\left(P_n^{\max} - \sum_{m\in\mathscr{M}}\sum_{k\in\mathscr{K}_m} p_{k,n}^{(m)}\right)\right]^+, \forall n \tag{4.34b}$$

$$\nu_k(i+1) = \left[\nu_k(i) - \frac{s^3}{\sqrt{i}}\left(I_{th}^{(k)} - \sum_{\substack{m\in\mathscr{M}\\ m\neq m_0}}\sum_{n\in\mathscr{N}_m} \tilde{\sigma}_{k,n}^{(\mathrm{m})} p_{k,n}^{(m)} g_{k,n}^{mm_0}\right)\right]^+, \forall k \tag{4.34c}$$

Here, i is the iteration number and $s^l = \frac{0.1}{\sqrt{i}}, l \in \{1,2,3\}$ are the positive step sizes assumed in this work. The process of computing the optimal power allocation and Lagrangian multipliers are updated accordingly until the convergence is achieved, indicating that the dual optimal point is achieved. The subgradient update is guaranteed to converge to optimal values of λ, μ and ν, as long as s^l is chosen to be sufficiently small [52]. A common practice is to choose square summable step sizes in contrast to absolute step sizes [95] [64].

4.5.4 Complexity Analysis

The computational complexity of the proposed approach depends on the complexity of both inner and outer layer solutions. It is observed that the computational complexity of Algorithm 4.1 to solve all K independent subproblems in (4.21), to solve $g(\underline{\lambda}, \underline{\mu}, \underline{\nu})$ is $O(KN)$. In addition, with the accuracy requirement, i.e., $|U(\eta(i)) - U(\eta(i-1))| < \triangle$, set in Algorithm 4.2, the total computational complexity of our proposed approach is

approximately $O\left(C_\eta KN\log_2(\frac{1}{\triangle})\right)$, where C_η is the number of iterations required for updating η until Algorithm 4.1 converges. It is demonstrated in the simulation results that less than 5 iterations are needed for Algorithm 4.1 to converge. The proposed approach has polynomial complexity regarding the problem scale K and N, which is attractive in the practical OFDMA implementation. Therefore, it can be concluded that the computational complexity of the proposed approach is low and acceptable.

Algorithm 4.1 Iterative EE and SE Tradeoff Algorithm in Two-Tier HetNets

Initialize

iter = max number of iterations, $\triangle$=*maximum acceptable tolerance*,

Set i=1 and $\eta(1)=\eta_{\text{initial}}$,

While $(|G(\eta)|<\triangle)\,||\,(i<\text{iter})$ **do**

Solve (4.17) for a given value of $\eta\,(i)$ using Algorithm 4.2.

Update $\eta\,(i+1)=\dfrac{\left(\sum\limits_{m\in\mathscr{M}}\sum\limits_{k\in\mathscr{K}_m}\sum\limits_{n\in\mathscr{N}} r_{k,n}^{(m)}\left(1+\alpha\frac{\tau_{\text{EE}}}{\tau_{\text{SE}}}\right)\right)}{\left(\text{N}\times P_{\text{C}}+\varepsilon_0\sum\limits_{m\in\mathscr{M}}\sum\limits_{k\in\mathscr{K}_m}\sum\limits_{n\in\mathscr{N}}\tilde{\sigma}_{k,n}^{(m)}p_{k,n}^{(m)}\right)}$

Update $i=i+1$

end While

Output: $[\eta]$

4.6 Simulation Results

We consider a two-tier HetNets environment with a single macrocell with 500 m radius overlaid with $M-1$ pico BSs with a radius of 50 m. The bandwidth of each subcarrier is 30 kHz. The maximum transmission power for all users are the same, hence, $P_n^{\max}$ will be referred to as $P^{\max}$. Similarly, the minimum rate requirement $R_n^{\min}$ can be referred to as $R^{\min}$. The minimum-rate requirement for each user is considered to be 4 b/s/Hz unless stated otherwise. The maximum transmission power of users considered in the simulation vary from 200 mW to 500 mW, whereas the value of circuit power of users is set fixed

Algorithm 4.2 Joint User Association, Subcarrier and Power Allocation in Two-Tier HetNets: Near Optimal Approach

Input: $[\eta, \alpha, \varepsilon_0, \gamma_{k,n}^{(m)}]$
Step 1: Initialize
$i = 0$, $p_{k,n}^{(m)} = 0, \lambda_n^{(i)} = 0.001, \mu_n^{(i)} = 0.01, \nu_k^{(i)} = 0.001$, **for** $n = 1, \cdots, N, k = 1, \cdots, K$ $m = 1, \cdots, M$.
Step 2:
For $n = 1 : N$
For $k = 1 : K$
Calculate $p_{k,n}^{(m)}$ according to (4.28).
end **For**
Obtain the user association and subcarrier assignment according to (4.26).
end **For**
Step 3:
i=i+1
Update $\lambda_n^{(i+1)}$, $\mu_n^{(i+1)}$ and $\nu_k^{(i+1)}$ according to (4.34).
Step 4:
Repeat steps (2)-(3) until $\lambda_n^{(i+1)}$, $\mu_n^{(i+1)}$ and $\nu_k^{(i+1)}$ are converged.
Output: $\left[p_{k,n}^{(m)}, \tilde{\sigma}_{k,n}^{(m)}\right]$

to $P_{\mathrm{C}} = 100$ mW and the threshold interference level is assumed as $I_n^{\mathrm{th}} = 1.1943 \times 10^{-14}$ W, unless stated otherwise. We assume that the users are uniformly deployed within the simulated scenario. The path-loss model for macrocell and pico BS m_i are given as $\mathrm{PL}_n^{(\mathrm{m}_0)}(\mathrm{dB}) = 128.1 + 37.6\log_{10}(d_n)$ and $\mathrm{PL}_n^{(\mathrm{m}_i)}(\mathrm{dB}) = 140.7 + 36.7\log_{10}(d_n)$ [41], where d_n is the distance of user n from the serving BS in km, and therefore, $\mathrm{PL}_n^{(\mathrm{m}_0)} = 10^{(\mathrm{PL}_n^{(\mathrm{m}_0)}(\mathrm{dB})/10)}$ and $\mathrm{PL}_n^{(\mathrm{m}_i)} = 10^{(PL_n^{(\mathrm{m}_i)}(\mathrm{dB})/10)}$. The noise spectral density is assumed to be $N_0 = -174$ dBm/Hz. In this work, the power amplifier efficiency is assumed as 38%, i.e., $\varepsilon_0 = \frac{1}{0.38}$. Note that if the user is unable to meet the minimum rate requirement $R^{\min}$, or the maximum transmission power constraint $P^{\max}$, we set the EE and SE for that channel realisation to zero. All the simulation results presented in this Section are averaged over 10^6 independent network realizations.

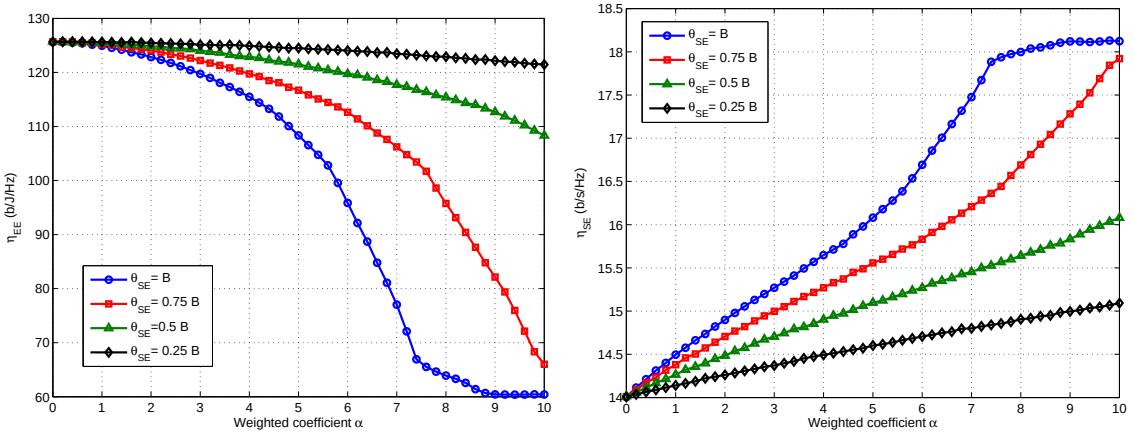

(a) (b)

FIGURE 4.2: EE and SE versus α for various θ_{EE} with $\theta_{\text{SE}} = B$, $N = 10$, $K = 10$, $P^{\max} = 0.2$ W and $P_{\text{C}} = 0.1$ W.

The initial selections of θ_{EE} and θ_{SE} are critical to the overall performance of the EE-SE tradeoff in HetNets. Fig. 4.2 illustrates the impact of different notions of normalization factor θ_{EE} on the achievable EE and achievable SE in Figs. **??**2a and **??**2b, respectively. First, we fix the value of θ_{SE}, the proposed notions of θ_{EE} is depicted with both minimum transmission power $P^{\min}$ $\left(\theta_{\text{EE}}^{(\min)} = \varepsilon_0 P^{\min} + P_{\text{C}}\right)$, maximum transmission power $P^{\max}$ $\left(\theta_{\text{EE}}^{(\max)} = \varepsilon_0 P^{\max} + P_{\text{C}}\right)$, and with the energy-efficient transmission power $P^*_{\eta_{\text{EE}}}$ $\left(\theta_{\text{EE}}^{(\text{EE})} = \varepsilon_0 P^*_{\eta_{\text{EE}}} + P_{\text{C}}\right)$, as the benchmark case. For the $\theta_{\text{EE}}^{(\min)}$ case, $P^{\min}$ is the minimum transmission power required to achieve the minimum rate requirement $R^{\min}$ which lies in the set of $[0, P^{\max}]$. For the benchmark case, $P^*_{\eta_{\text{EE}}}$ is the energy-efficient transmission power at which the maximum EE is achieved and it lies in the set of $[P^{\min}, P^{\max}]$. The optimal transmit power P^*_{η} monotonically increases with α regardless of θ_{EE}. P^*_{η} achieves the maximum transmission power $P^{\max}$ at $\alpha \approx 3$ and $\alpha \approx 3.2$ for the proposed $\theta_{\text{EE}}^{(\min)}$ and benchmark cases, respectively. On the other hand, P^*_{η} achieves the maximum

transmission power $P^{\max}$ at $\alpha \approx 9$ for the proposed $\theta_{\mathrm{EE}}^{(\max)}$ case. For the weighted coefficient $0 \leq \alpha \leq 0.6$, the achieved EE for all three cases are marginally close to each other whereas as the value of α increases beyond 0.6 the achieved EE by the proposed $\theta_{\mathrm{EE}}^{(\max)}$ is far higher as compared to the proposed $\theta_{\mathrm{EE}}^{(\min)}$ and benchmark cases. The figure shows that in $\theta_{\mathrm{EE}}^{(\max)}$ case, the achieved EE decreases more gradually with α, when compared to the $\theta_{\mathrm{EE}}^{(\min)}$ and benchmark cases. After several implementations of our proposed normalization factor, we choose the setting of $\theta_{\mathrm{EE}} = \theta_{\mathrm{EE}}^{(\max)} = \varepsilon_0 P^{\max} + P_{\mathrm{C}}$ as the optimal θ_{EE}. One of the major observation is that optimal θ_{EE} provides the complete range of η_{EE} and η_{SE} values as compared to the two baseline cases and gives more flexibility to set preferences for either EE or SE.

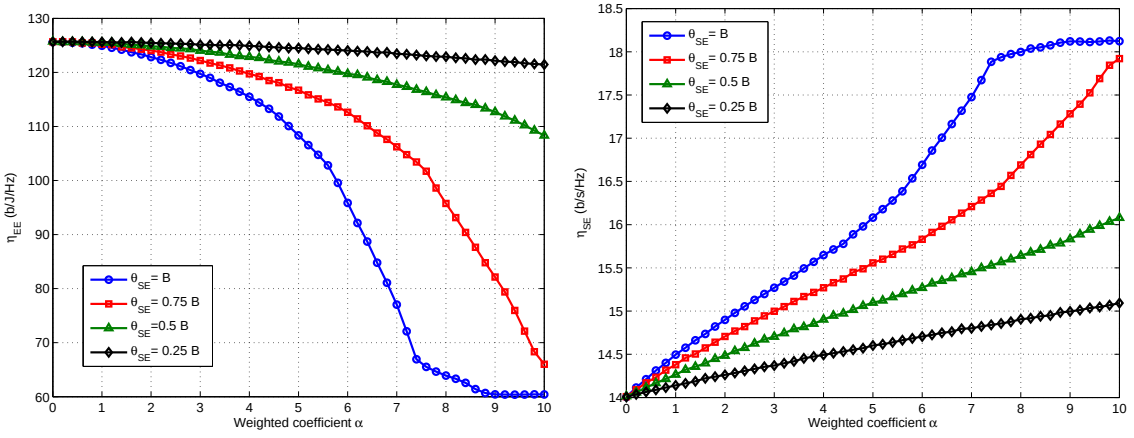

(a) (b)

FIGURE 4.3: EE and SE versus α for various θ_{SE} with $\theta_{\mathrm{EE}} = (\varepsilon_0 P^{\max} + P_{\mathrm{C}})$, $N = 10$, $K = 10$, $P^{\max} = 0.2$ W and $P_{\mathrm{C}} = 0.1$ W.

Fig. 4.3 illustrates the impact of θ_{SE} on the achievable EE and achievable SE. First, we fix the value of $\theta_{\mathrm{EE}} = \theta_{\mathrm{EE}}^{(\max)}$. The proposed notions of θ_{SE} are defined as $\theta_{\mathrm{SE}}^{(\mathrm{tot})}$, $\theta_{\mathrm{SE}}^{(1)}$, $\theta_{\mathrm{SE}}^{(2)}$ and $\theta_{\mathrm{SE}}^{(3)}$ for B, $0.75B$, $0.5B$ and $0.25B$ respectively. τ_{SE} decreases with θ_{SE}, which in turn, reduces $\alpha \frac{\tau_{\mathrm{EE}}}{\tau_{\mathrm{SE}}}$ as defined in (4.18). Hence, for smaller values of θ_{SE}, the achieved

optimal tradeoff power level P_{η}^{*} is approximately close to the $P_{\eta_{\mathrm{EE}}}^{*}$ at $\alpha = 0$. For the higher values of θ_{SE}, the achieved optimal tradeoff power level P_{η}^{*} monotonically increases with α towards the maximum transmission power $P^{\max}$. We note that P_{η}^{*} converges to $P^{\max}$ at different values of α depending on the set value of θ_{SE}. The figure reveals that for the weighted coefficient $0 \leq \alpha \leq 2$, the optimal transmission power and achieved EE for all four cases are approximately close to each other whereas as α increases beyond 2, the achieved EE by the proposed $\theta_{\mathrm{SE}}^{(\mathrm{tot})}$ is far lower than the remaining three proposed notions of θ_{SE}. As θ_{SE} is a normalization factor for the achieved SE in the optimisation problem so the optimal θ_{SE} is chosen such that it achieves highest SE. After several implementations of our proposed normalization factor, we choose the setting of $\theta_{\mathrm{SE}} = \theta_{\mathrm{SE}}^{(\mathrm{tot})} = \sum_{k \in \mathscr{K}} B_k$ as the optimal θ_{SE}. The optimal θ_{SE} can achieve a higher SE as compared to the other cases, however, at the cost of reduction in EE. For clarity purpose, from this point onwards θ_{EE} and θ_{SE} are assumed to be $\theta_{\mathrm{EE}} = \varepsilon_0 P^{\max} + P_{\mathrm{C}}$ and $\theta_{\mathrm{SE}} = \sum_{k \in \mathscr{K}} B_k$.

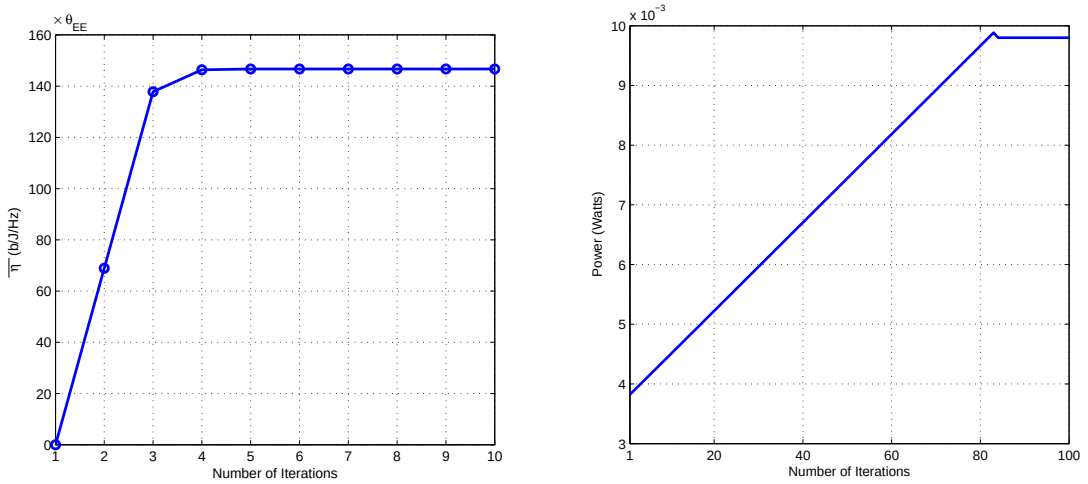

(a) Algorithm 4.1 (b) Algorithm 4.2

FIGURE 4.4: Convergence of Proposed Algorithms 4.1 & 4.2 with $\alpha = 1$, $\theta_{\mathrm{SE}} = B$, $\theta_{\mathrm{EE}} = (\varepsilon_0 P^{\max} + P_{\mathrm{C}})$, $N = 10$, $K = 10$, $P^{\max} = 0.2$ W and $P_{\mathrm{C}} = 0.1$ W.

Fig. 4.4 depicts the average achieved $\overline{\eta}$ and the average transmission power versus the number of iterations to study the convergence speed of the proposed Algorithms 4.1 and 4.2, respectively. The achieved $\overline{\eta}$ is corresponding to the objective function defined in (4.15a). Fig. 4.4(a) depicts the achieved $\overline{\eta}$ of the proposed Algorithm 4.1 versus the number of iterations with the maximum uplink transmission power of $P^{\max} = 0.2W$, with the normalisation factors $\theta_{\text{EE}} = 0.63$W, and $\theta_{\text{SE}} = 3 \times 10^4$ Hz. The algorithm converges to an optimal value within 4-5 iterations. Fig. 4.4(b), on the other hand, includes the plots for the average transmission power of Algorithm 4.2 versus the number of iterations. The algorithm converges to an optimal value within around 80 iterations. The polynomial complexity of the proposed Algorithm 4.1 and 4.2 depends on the problem scale of the number of users N and subcarriers K, which is desirable for practical implementation and has a fast convergence speed. This result demonstrates the fact that the proposed Algorithm 4.1 and 4.2 gaurantee convergeance by using the subgradient method in uplink HetNets.

By fixing θ_{SE} to B, the maximum achievable $\overline{\eta}$ versus $P^{\max}$ for different values of α are plotted in Fig. 4.5 which reveals that $\overline{\eta}$ increases with α; whereas $\overline{\eta}$ first increases with $P^{\max}$, and after a particular value of $P^{\max}$, it starts decreasing. This is due to the fact that τ_{EE} is defined as $\frac{P}{\theta_{\text{EE}}}$, where θ_{EE} depends on $P^{\max}$ as defined in (4.18). For smaller values of $P^{\max}$, the achievable $\overline{\eta}$ increases with $P^{\max}$. Furthermore, for higher values of $P^{\max}$, the achievable $\overline{\eta}$ decreases with $P^{\max}$. This is an important observation which can allow the flexibility to save more power by choosing the sensible $P^{\max}$ which results in improving the achieved EE and SE.

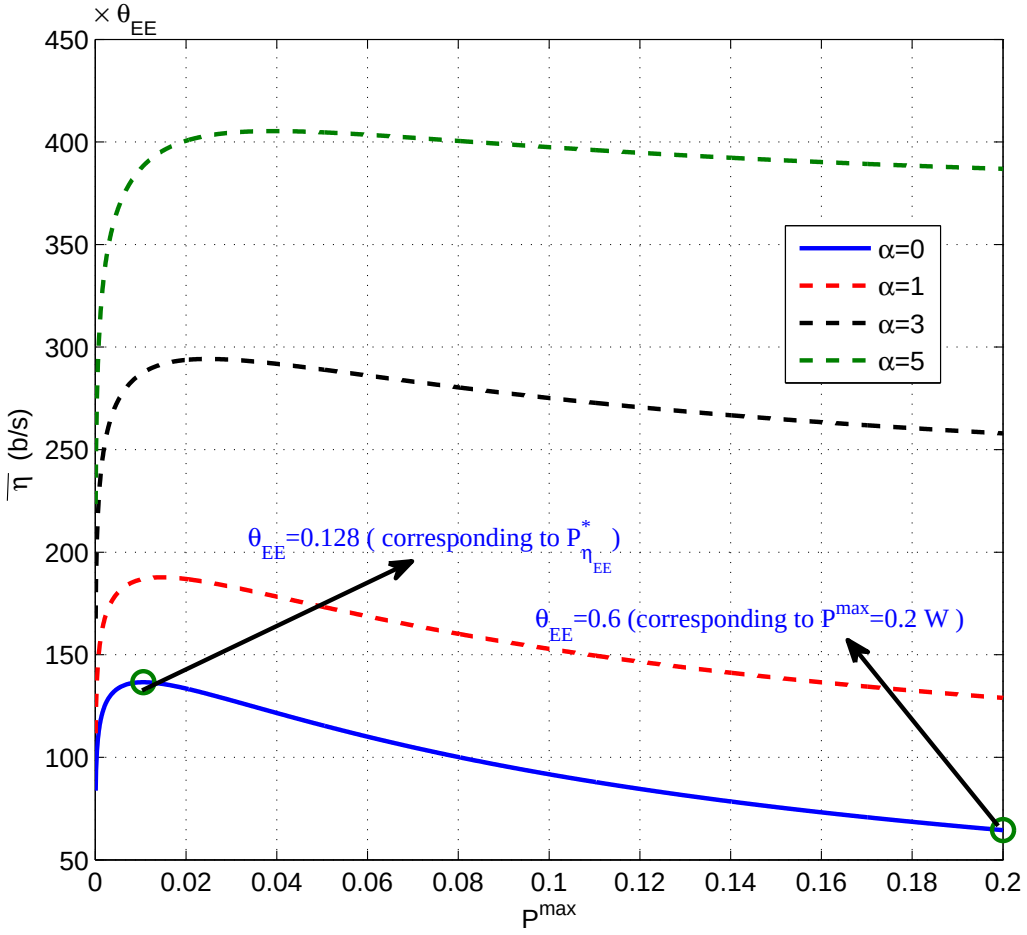

FIGURE 4.5: $\overline{\eta}$ versus $P^{\max}$ for various values of α.

Fig. 4.6 shows the EE-SE tradeoff of a macrocell overlaid with 4 pico BSs when $P^{\max} = 0.2$ W, for the threshold intereference level $I_n^{\text{th}} = 1.1943 \times 10^{-14}$ W, 3.7768×10^{-15} W, 7.7357×10^{-15} W, 1.1943×10^{-16} W, 3.7768×10^{-16} W and 7.7357×10^{-16} W. The simulation results show that the maximum achievable EE and SE decreases monotonically with I_n^{th}. The figure further reveals that the lower values of I_n^{th} results in higher achievable EE and SE in comparison to the lower achieavble EE and SE at the higher values of I_n^{th}. We note that the maximum achievable EE is reduced from 126 b/J/Hz to 94 b/J/Hz when the I_n^{th} is reduced from 1.1943×10^{-14} W to 7.7357×10^{-16} W. Further, the figure shows

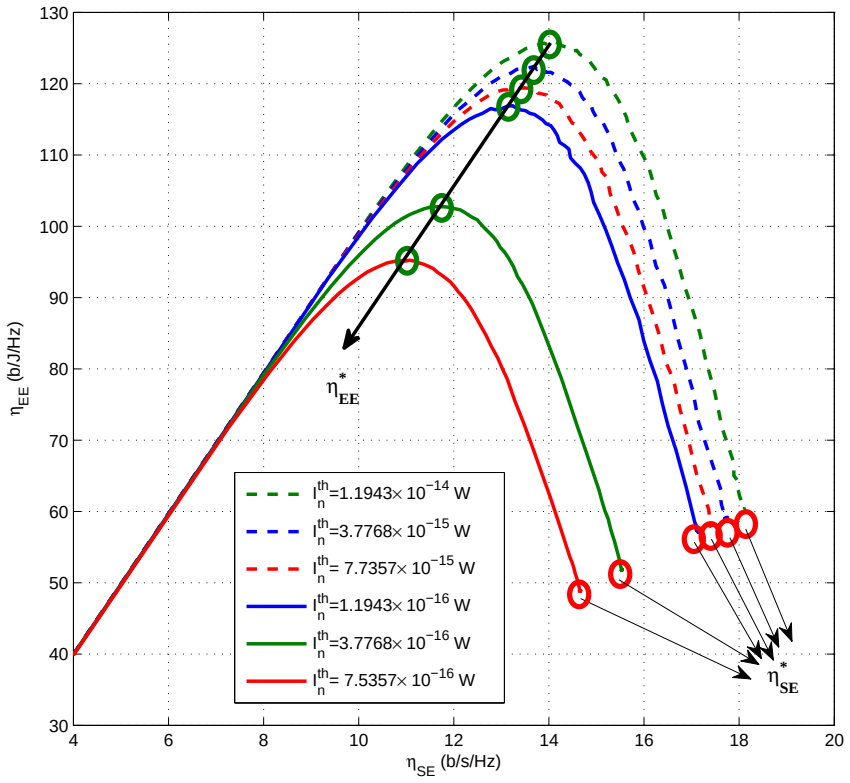

FIGURE 4.6: η_{EE} versus η_{SE} for various threshold interference levels I_n^{th}

that higher threshold interference level I_n^{th} achieves higher achievable EE and SE. For the remainder of the simulation results, we assume $I_n^{\text{th}} = 1.1943 \times 10^{-14}$ W.

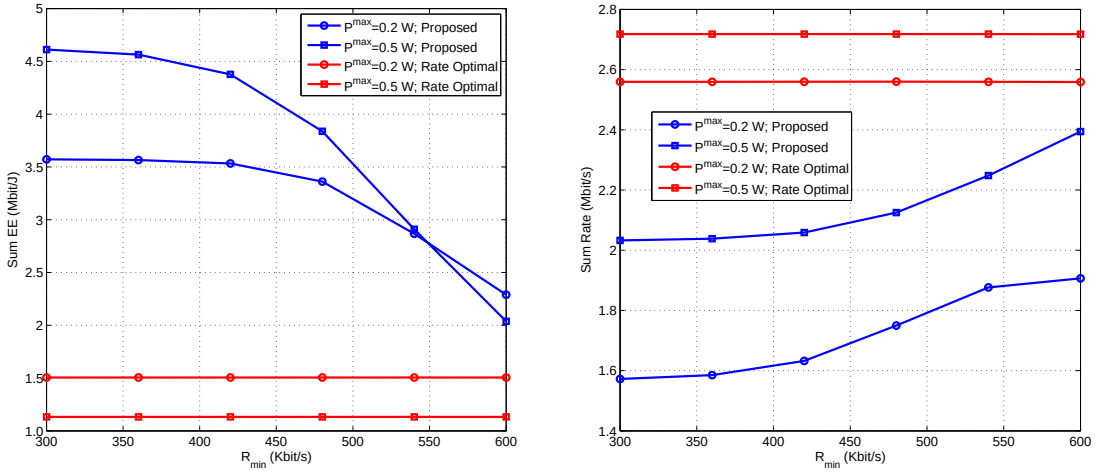

(a) Sum EE versus $R_{\min}$

(b) Sum rate versus $R_{\min}$

FIGURE 4.7: Sum EE and Sum Rate versus $R^{\min}$ for various values of $P^{\max}$, $N = 4$, $K = 4$, $P_{\text{C}} = 0.1$ W and $I_n^{th} = 1.1943 \times 10^{-14}$ W.

We present a baseline algorithm, namely, a rate-optimal algorithm which maximises the overall system rate. Figs. 4.7(a) and 4.7(b), which respectively shows the performance in terms of the sum EE and the sum rate versus $R^{\min}$. We assume four users are randomly located within the coverage area. The two figures show that the proposed algorithm achieves a higher sum EE than the rate-optimal algorithm. The rate-optimal algorithm can achieve a higher sum rate, however, at a cost of reduction in EE. Moreover, both EE and the sum rate increases with $P^{\max}$. It should be also noted that the sum EE decreases with $R^{\min}$, whereas the sum rate increases with it. We note that at $R^{\min} = 600$ Kbit/s, the achievable EE at $P^{\max} = 0.2$ W is higher than the achievable EE at $P^{\max} = 0.5$ W. This is due to the fact that the normalisation factor θ_{EE} depends on the maximum transmission power $P^{\max}$.

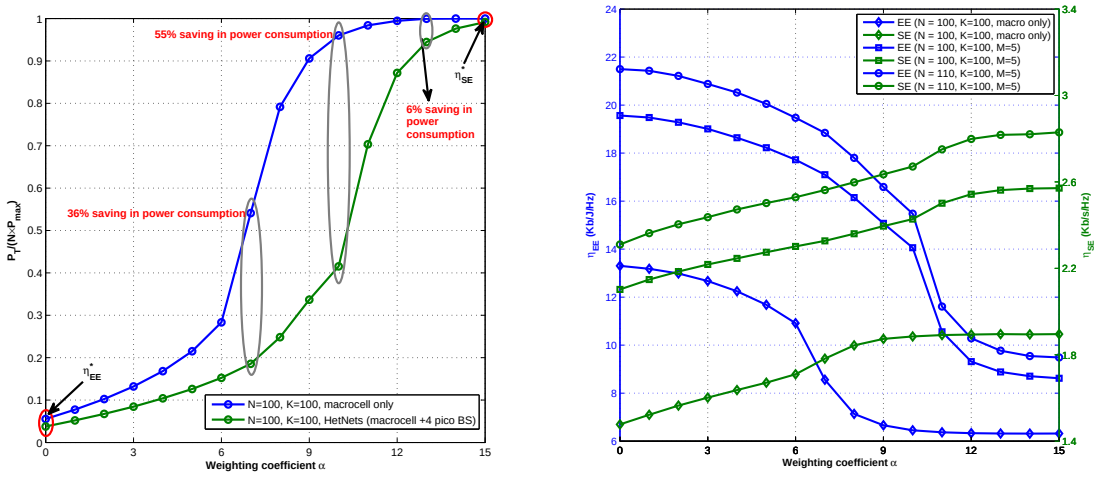

(a) $\left(\frac{P_T}{N \times P^{\max}}\right)$ vs. α for varying M

(b) η_{EE} and η_{SE} vs α for varying N and M

FIGURE 4.8: Relative Optimal transmit power, η_{EE} and η_{SE} versus weighted coefficient α with $N_{\text{macro}} = 0.2 * N$, $N_0 = -174$ dbm/Hz and $R_n^{\min} = 4$ b/s/Hz.

In order to measure the performance gains of two-tier HetNet configuration of $M = 5$ as compared to a macrocell only $M = 1$ with minimum rate requirement of 4 b/s/Hz,

Fig. 4.8(a) and 4.8(b) show the plots for optimal average transmit power normalised by $P^{\max}$ and achievable EE along with achievable SE versus weighted coefficient α for varying number of users N resulting in user densities of 200 and 220 active UE's per km^2 and $K = 100$. For the case of $M = 1$, all the users are served by macrocell $N_{\text{macro}} = N$ whereas for $M = 5$, the number of users per macrocell are $N_{\text{macro}} = 0.2 * N$ and number of users per pico BSs are $N_{\text{small}} = N/M$. It can be seen that the optimal transmit power P_η^* irrespective of $M = 1$ and $M = 5$ configurations monotonically increases with α. It is worth to mention that power saving $\left(P^{\max} - P_\eta^*\right)$ of $M = 5$ (denoted by green line) in comparison to $M = 1$ (denoted by blue line) first monotonically increases with α and afterwards it start decreasing as α approaches towards α_{EE}. Fig. 4.8(b) shows the corresponding achievable EE and SE in $M = 1$ and $M = 5$ at the optimal tradeoff transmit values ($P_\eta{}^*$ as previously shown in Fig. 4.8(a)) versus α for varying user densities and $K = 100$. Another observation is that achievable EE and SE also increases with an increase in number of user N. The figure reveals that for a given N, K and α, the two-tier HetNet configuration always outperforms in terms of both the power consumption and the achievable EE along with corresponding achievable SE as compared to the traditional macrocell only configuration: by averaging over all the values of α, the average achievable EE is 15.025 kb/J/Hz with average achievable SE of 2.358 kb/s/Hz and power consumption of 78.27 mW in $M = 5$ for $N = 100$ and $K = 100$ compared to the average achievable EE of 9.216 kb/J/Hz with average achievable SE of 1.7525 kb/s/Hz and power consumption of 1842.236 mW in $M = 1$ for $N = 100$ and $K = 100$.

Fig. 4.9 shows the impact of the varying number of users per pico BS denoted by

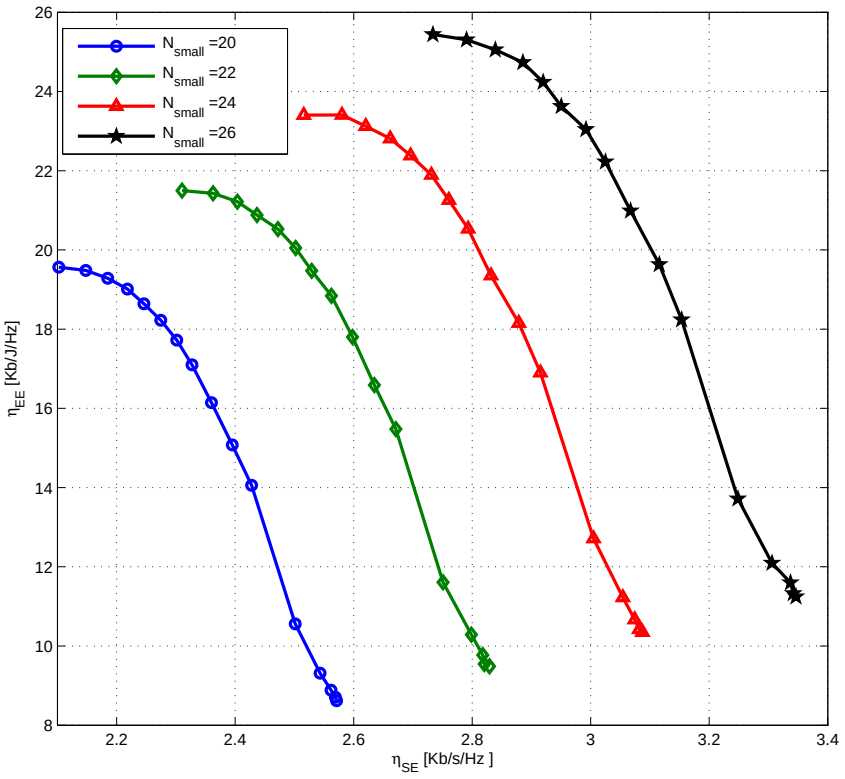

FIGURE 4.9: η_{EE} and η_{SE} of two-tier HetNet configuration for various values of N_{small} with $K = 100$, $M = 5$, $N_0 = -174$ dbm/Hz and $R_n^{\min} = 4$ b/s/Hz

N_{small} on the EE-SE tradeoff in two-tier HetNets with 4 pico BSs lying on the cell edge of a macrocell. The total number of users per pico BS denoted by N_{small} are set to vary at 20, 22, 24 and 26. It is observed that when N_{small} is increased from 20 to 26, the EE-SE tradeoff curve expands which improves the achievable EE from 19.56 Kb/J/Hz to 25.44 Kb/J/Hz at $\alpha = 0$ whereas the achievable SE improves from 2.102 Kb/s/Hz to 2.734 Kb/s/Hz due to multi-user diversity. For the given $N_{\text{small}} = 20$ and $\alpha = 3$, the figure reveals the significant improvements in achievable EE (50% gain) and SE (39% gain) along with reduction in power consumption (47.5%) in case of two-tier HetNets as compared to the macrocell only configuration.

Fig. 4.10 shows the achievable EE and SE versus β, as defined in (4.1), ranging from 0 (macrocell only) to 1 increasing the number of pico BSs deployed on the edge of a macrocell from 1 to 40 with user densities set at $200, 400$ and 600 active UE's per km^2 randomly deployed within the area of 500×500 m^2 and minimum rate requirement set as 4 b/s/Hz. It is evident from this figure that deploying pico BSs on the edge of a macrocell can achieve significant gains for all the performance metrics to satisfy the objectives and requirements of 5G systems. As it can be seen from the figure, the achievable EE and SE increase both with an increase in network densification and user density. The HetNet configuration with $\beta = 0.1$ which results in 4 pico BSs deployed on the cell edge of a macrocell with user density of 600 active UE's per km^2 achieves an area energy efficiency of 64.617 kb/J/Hz/km^2 as comapred to 51.745 kb/J/Hz/km^2 for macrocell only, i.e., $\beta = 0$. Similarly, an area spectrum efficiency at $\beta = 0.1$ increases from 2.702 kb/s/Hz/km^2 to 5.325 kb/s/Hz/km^2 as user denisty is increased from 200 to 400 active UE's per km^2. It is important to mention that introducing too many pico BSs can cause increase in the deployment and maintaineance costs, backhauling costs and system complexity which are not considered in this analysis. However, it is evident from Fig. 4.10(a) and 4.10(b) that the tradeoff exists between deployed number of pico BSs and the achieved values of performance metrics subject to the given user density. For example, it is suitable to choose an optimal β as 0.2, 0.5 and 0.8 for the given user densities of $200, 400$ and 600 active UE's per km^2 and afterwards, an increase in β result in a very minor improvement in performance metrics.

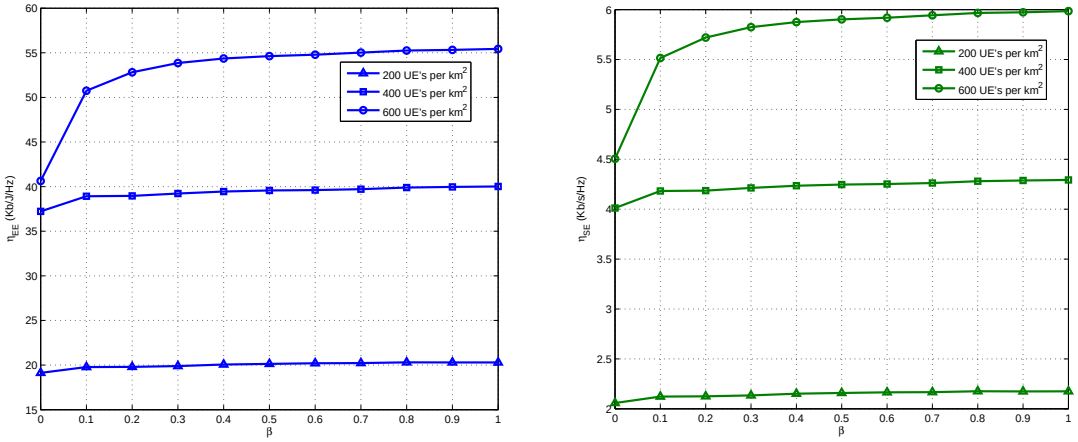

(a) η_{EE} versus β (b) η_{SE} versus β

FIGURE 4.10: η_{EE} and η_{SE} versus β for varying user densities, $P^{\max} = 0.2$ W, $P_{\text{C}} = 0.1$ W and $I_n^{th} = 1.1943 \times 10^{-14}$ W.

4.7 Summary

In this chapter, the problem of simultaneously maximising the overall system EE and SE in an uplink of a two-tier OFDMA-based HetNet using adaptive channel and power allocation was addressed by considering the maximum transmission power, cross-tier interference threshold and users' minimum-QoS constraints. The quasi-concavity of the proposed approach was proved, and due to this property, the Pareto optimal solution was derived using LDD approach based on joint user association, subcarrier and power allocation. An iterative two-layer framework was proposed in which the outer layer was solved by Dikelbach method as shown in Algorithm 4.1; whereas the inner layer was solved using LDD approach as shown in Algorithm 4.2. From simulation results, we can refer two main observations. Firstly, SE is maximised at different values of weighted coefficient α depending on the maximum transmission power. Secondly, our proposed tradeoff metric α can help us to save much power by lowering the maximum transmission power. The

tradeoff parameter η is an increasing function of transmission power for smaller values of $P^{\max}$, whereas it is a decreasing function of transmission power for higher values of $P^{\max}$.

Chapter 5

Conclusions and Future Work

5.1 Conclusions

This thesis was dedicated to the energy efficiency and spectral efficiency optimisation in multi-tier HetNets.

The joint network selection algorithm from both user and network perspectives are proposed in cooperative heterogeneous wireless systems as outlined in Chapter 2. Compared with the state-of-the-art network selection algorithms such as [10–12], the proposed evolutionary game-theoretic approach utilising the inverse cumulative ranking scheme significantly improves the overall QoS performance and system parameters. By incorporating the proposed RoI-based Dynamic Contextual strategy can significantly reduce the complexity of the evolutionary game, with or without network re-configuration by 23% and 58%, respectively.

Chapter 3 provides a detailed description of the proposed maximising EE optimisation schemes in multi-tier HetNets. Firstly, the EE maximisation problem of an uplink of a

two-tier OFDMA-based HetNets with maximum transmit power and minimum-rate constraints using adaptive channel and power allocation is addressed in section 3.4. As one of the pioneer works on joint user association and power allocation in two-tier HetNets, the proposed suboptimal algorithm has low complexity and provides the solution not far from an optimal solution. Secondly, a joint optimization problem is formulated for mode selection, subcarrier assignment and power allocation in a three-tier hierarchical HetNet consisting of an underlaid D2D communication in coverage of both macrocell and pico BS's as mentioned in section 3.5. The optimization problem is formulated such that each user tries to maximize its own ASE subject to a required AEE level and a maximum transmit power constraint. The simulation results show that when the required AEE level is set to 93% of $\eta^{\max}$, the proposed scheme can reduce the tradeoff optimal transmit power transmit power upto 48.51% and 1404%, when compared to the traditional HetNets and macrocell only, respectively. Finally, the concept of MOP is utilised to jointly optimise the throughput and BEE tradeoff in two-tier HetNets with QoS and fairness guarantee constraints is outlined in section 3.6. The complete Pareto optimal set is obtained by employing the weighted sum method to transform our proposed MOP into an SOP. The proposed algorithm provide flexibility to the network operators to dynamically tune the weighting coefficient α and rate fairness level ω in order to satisfy the user's QoS requirements along with reducing their total area power consumption.

In Chapter 4, the problem of simultaneously maximising the overall system EE and SE in an uplink of a two-tier HetNets by considering the maximum transmission power,

cross-tier interference threshold and users' minimum-QoS constraints. An iterative two-layer proposed algorithm in which the outer layer was solved by Dikelbach method; whereas the inner layer was solved using LDD approach. From simulation results, we can refer two main observations. Firstly, SE is maximised at different values of weighted coefficient α depending on the maximum transmission power. Secondly, our proposed tradeoff metric α can help us to save much power by lowering the maximum transmission power.

5.2 Future Work

The series of future directions arising from the direct outcome of the analysis carried out in this thesis have been identified as follow:

5.2.1 Energy and Spectral efficient design for multi-band HetNets

Carrier aggregation (CA) is considered as a key enabler for next generation networks such as 5G in order to meet the large transmission bandwidth requirement to achieve high peak data rate (500 Mbps in the uplink and 1 Gbps in the downlink). The energy efficiency for multi-tier HetNets for uplink and downlink transmission schemes have been investigated in chapter 3. It was assumed that all tiers of HetNets operate at same frequency band with orthogonal channel deployment. A trade-off between energy efficiency and spectral efficiency for two-tier HetNets with co-channel deployment has been described in chapter 4. It is envisaged that there will be an ultra dense deployment of low power small cells within the traditional macrocells in order to cope with the higher data rate requirements for 5G. Moreover, it would also be interesting to study the impact of

availability of different frequency bands under different dense deployment scenarios on the overall energy efficiency of the multi-tier HetNets. Therefore, the work presented in this thesis can be further extended to investigate different carrier aggregation approaches in a multi-band HetNet model.

In this trend, a two layer non-cooperative game theoretic approach can be formulated to examine the impact of the available bands in multi-tier HetNets to best exploit CA. In the first layer, the small cells deployed within the coverage area of the traditional macrocell can intelligently decide among the available frequency bands to operate in order to increase the spectral efficiency of their associated users. Once the small cells have chosen their operating frequency band, user-centric selection mechanism can be utilised to allow the macrocell users to select a strategy to maximize their payoff while keeping in view the overall network performance.

5.2.2 Analysis of Energy and Spectral Efficiency in HetNets with Traditional Macrocells and Small Cells exploiting mmWave band

One of the emerging technologies towards enabling fifth generation (5G) is multiple radio access technologies (multi-RAT) such that the traditional macrocells operate at sub 6 GHz frequency band whereas the small cells operate at mmWave frequency band within the same geographical area. In the past, mmWave technology was not considered to be feasible for wireless communication due to the larger penetration loss. In [98]– [99], authors have analysed mmWave for cellular networks by using highly directional antennas and beam-forming to provide coverage in the range of about 150-200 m.

In this trend, the deployment of mmWave small cells has great potential to improve the

spatial reuse of radio resources and also to enhance the energy and spectral efficiency of the network. This traffic surge and the projected traffic requirements combined with congestion in the available spectrum has made evident the need to shift to unused frequency bands. The use of the mmWave band, ranging from 10 GHz to 300 GHz, is an attractive solution to the spectrum congestion problem due to an enormous amount of available transmission bandwidth upto 2 GHz within the E and W frequency bands. Investigation of the use of mmWave technology in 5G cellular networks is already underway [100]–[101]. Although mmWave communication will require large numbers of antennas with more required power for complex signal processing along with the reduced caused interference, it still can be efficient by serving more users, with less transmission power per user resulting in higher spectral efficiency. Keeping this in mind, an efficient solutions should be investigated to formulate a trade-off between the number of BSs operating in mmWave frequency band and the respective BS load for different deployment scenarios such as urban and suburban areas.

Therefore, it can be concluded that combining multi-tier HetNets with mmWave communications is a promising research area which requires attention to fulfil its role in the design of 5G networks.

Appendix A

Appendix of Chapter 4

A.1 Proof of Lemma I

In this Appendix, we prove that η is quasi-concave in $\tilde{\sigma}_{k,n}^{(m)}$ and $p_{k,n}^{(m)}$.

$$\eta = \frac{R}{P}\left(1+\alpha\frac{\theta_{\mathrm{SE}}\times\eta_{\mathrm{SE}}}{\theta_{\mathrm{EE}}\times\eta_{\mathrm{EE}}}\right)$$

$$\begin{aligned}&= \frac{R}{P}\left(1+\alpha\frac{\theta_{\mathrm{SE}}\times P}{\theta_{\mathrm{EE}}\times B}\right)\\ &= \frac{R}{P}(1+\overline{\alpha}P)\end{aligned}$$

$$= \frac{R}{P}+\overline{\alpha}R = \eta_{\mathrm{EE}}+\overline{\alpha}R \tag{A.1}$$

$$\text{where} \quad \overline{\alpha} = \alpha \frac{\theta_{\text{SE}}}{\theta_{\text{EE}} B}$$

First, we prove that $r_{k,n}^{(m)}$ is concave with respect to $\tilde{\sigma}_{k,n}^{(m)}$ and $p_{k,n}^{(m)}$. By taking the first order derivative of $r_{k,n}^{(m)}$ with respect to $p_{k,n}^{(m)}$ we get

$$\frac{\partial r_{k,n}^{(m)}}{\partial p_{k,n}^{(m)}} = \max_{k \in \mathscr{K}_m, n \in \mathscr{N}} \frac{B_k \gamma_{k,n}^{(m)}}{\ln(2)\left(1 + \gamma_{k,n}^{(m)} p_{k,n}^{(m)}\right)} \tag{A.2}$$

From (A.2), it is clear that $\frac{B_k \gamma_{k,n}^{(m)}}{\ln(2)\left(1+\gamma_{k,n}^{(m)} p_{k,n}^{(m)}\right)}$ is strictly monotonically decreasing with $p_{k,n}^{(m)}$ and thus $\frac{\partial^2 r_{k,n}^{(m)}}{\partial {p_{k,n}^{(m)}}^2} < 0$. Since R is the linear combination or sum of $r_{k,n}^{(m)}$, and therefore, R is also concave in $p_{k,n}^{(m)}$. Using the same principle, we can also show that R is concave in $\tilde{\sigma}_{k,n}^{(m)}$.

Denote the superlevel sets of η_{EE} in order to prove the quasi-concavity as follow:

$$\tau_\alpha = \{\tilde{\sigma}_{k,n}^{(m)} \geq 0, p_{k,n}^{(m)} \geq P_n^{\min}, \forall k, m, n \mid \eta_{\text{EE}} \geq \alpha\}$$

η_{EE} is quasi-concave in $\tilde{\sigma}_{k,n}^{(m)}$ and $p_{k,n}^{(m)}$, if τ_y is convex for any real number y [52]. When $y < 0$, no points exist on the contour $\eta_{\text{EE}} = y$. When $y \geq 0$, τ_y is equivalent to $y \left(\text{N} \times P_{\text{C}} + \sum_{m \in M} \sum_{k \in \mathscr{K}_m} \sum_{n \in N} \tilde{\sigma}_{m,n}^{(k)} B_k \log_2 \left(1 + \frac{\gamma_{k,n}^{(m)} p_{k,n}^{(m)}}{\rho_{(m)}^2 \text{PL}_n^{(m)}}\right)\right)$ which is convex. Hence, η_{EE} is quasi-concave in $\tilde{\sigma}_{k,n}^{(m)}$ and $p_{k,n}^{(m)}$. Since R is strictly concave in $\tilde{\sigma}_{k,n}^{(m)}$ and $p_{k,n}^{(m)}$. Therefore, η is also quasi-concave in $\tilde{\sigma}_{k,n}^{(m)}$ and $p_{k,n}^{(m)}$. Since P_{T} is monotonically increasing linear function of $p_{k,n}^{(m)}$, then η is also quasi-concave in P_{T}.

A.2 Proof of Lemma II

Let us assume $\eta^* = \max_{\tilde{\sigma}_{k,n}^{(m)}, p_{k,n}^{(m)}} \eta$ is an optimal solution to the objective function (4.17). Similar to [93], $\mathscr{G}(\eta)$ can be equivalently written as:

$$\mathscr{G}(\eta) = \max_{\tilde{\sigma}_{k,n}^{(m)}, p_{k,n}^{(m)}} (\tilde{\eta} - \eta) \left(N \times P_{\mathrm{C}} + \varepsilon_0 \sum_{m \in \mathscr{M}} \sum_{k \in \mathscr{K}_m} \sum_{n \in \mathscr{N}} \tilde{\sigma}_{k,n}^{(m)} p_{k,n}^{(m)} \right)$$

If $\eta = \eta^*$, then $\tilde{\eta} - \eta = \tilde{\eta} - \eta^* \leq 0$ which means $\mathscr{G}(\eta^*) \leq 0$. However, we can always find some $\tilde{\sigma}_{k,n}^{(m)}$ and $p_{k,n}^{(m)}$ that can make $\tilde{\eta} = \eta^*$ which result in $\mathscr{G}(\eta^*) = 0$. Hence, $\mathscr{G}(\eta) > 0$ if $\eta < \eta^*$ and $\mathscr{G}(\eta) < 0$ if $\eta > \eta^*$. Hence, it is proven that $\mathscr{G}(\eta) = 0$ iff $\eta = \eta^*$.

Bibliography

[1] Cisco. Cisco visual networking index: Global mobile data traffic forecast update 2014-2019 white paper. Technical report, Feb. 2015.

[2] J.G. Andrews, S. Buzzi, Wan Choi, S.V. Hanly, A. Lozano, A.C.K. Soong, and J.C. Zhang. What will 5G be? *IEEE Journal on Selected Areas in Communications*, 32 (6):1065–1082, June 2014. ISSN 0733-8716. doi: 10.1109/JSAC.2014.2328098.

[3] E. Hossain and M. Hasan. 5G cellular: key enabling technologies and research challenges. *IEEE Instrumentation Measurement Magazine*, 18(3):11–21, June 2015. ISSN 1094-6969. doi: 10.1109/MIM.2015.7108393.

[4] D. Lopez-Perez, I. Guvenc, G. de la Roche, M. Kountouris, T. Q. Quek, and J. Zhang. Enhanced inter-cell interference coordination challenges in heterogeneous networks. *IEEE Wireless Comm.*, 18(3):22–30, June 2011.

[5] K. Kikuchi and H.Otsuka. Proposal of adaptive control CRE in heterogeneous networks. In *Proc. IEEE PIMRC 2012*, pages 910–914, Sydney, Australia, Sept. 2012.

[6] C. S. Chen, F. Baccelli, and L. Roullet. Joint optimization of radio resources in small and macro cell networks. In *Proc. IEEE VTC 2011 Spring*, pages 1–5, Budapest, Hungary, May 2011.

[7] M. Condoluci, M. Dohler, G. Araniti, A. Molinaro, and K. Zheng. Toward 5G densenets: architectural advances for effective machine-type communications over

femtocells. *IEEE Communications Magazine*, 53(1):134–141, January 2015. ISSN 0163-6804. doi: 10.1109/MCOM.2015.7010526.

[8] S. Khakurel, L. Musavian, and T. Le-Ngoc. Energy-efficient resource and power allocation for uplink multi-user OFDM systems. In *Proc. IEEE PIMRC 2012*, pages 357–361, Sydney, Australia, Sept. 2012.

[9] E. Hossain, M. Rasti, H. Tabassum, and A. Abdelnasser. Evolution toward 5G multi-tier cellular wireless networks: An interference management perspective. *IEEE Wireless Communications*, 21(3):118–127, June 2014. ISSN 1536-1284. doi: 10.1109/MWC.2014.6845056.

[10] D. Niyato and E. Hossain. Dynamics of network selection in heterogeneous wireless networks: An evolutionary game approach. *Vehicular Technology, IEEE Transactions on*, 58(4):2008–2017, May 2009. ISSN 0018-9545. doi: 10.1109/TVT.2008.2004588.

[11] D. Niyato and E. Hossain. Modeling user churning behavior in wireless networks using evolutionary game theory. In *Wireless Communications and Networking Conference, 2008. WCNC 2008. IEEE*, pages 2793–2797, March 2008. doi: 10.1109/WCNC.2008.489.

[12] Kun Zhu, Dusit Niyato, and Ping Wang. Network selection in heterogeneous wireless networks: evolution with incomplete information. In *Wireless Communications and Networking Conference (WCNC), 2010 IEEE*, pages 1–6. IEEE, 2010.

[13] J. Roslof T. Jokikyyny S. Pierrel, T. Erlin and H. Lehtinen. A prototype for policy driven control of heterogeneous network access. Technical report, Turku Polytechnic, School of Telecommunications and e-Business, Finland, 2004. Available online at http://www.cs.hut.fi/p̃mrg/publications/VHO/2004/Pierrel_Erlin_Roslof_APPDCHNA.pdf.

[14] O. Markaki, D. Charilas, and D. Nikitopoulos. Enhancing quality of experience in next generation networks through network selection mechanisms. In *Personal, Indoor and Mobile Radio Communications, 2007. PIMRC 2007. IEEE 18th International Symposium on*, pages 1–5, Sept 2007. doi: 10.1109/PIMRC.2007.4394198.

[15] Qingyang Song and A. Jamalipour. A network selection mechanism for next generation networks. In *Communications, 2005. ICC 2005. 2005 IEEE International Conference on*, volume 2, pages 1418–1422 Vol. 2, May 2005. doi: 10.1109/ICC.2005.1494578.

[16] Qingyang Song and A. Jamalipour. Quality of service provisioning in wireless lan/umts integrated systems using analytic hierarchy process and grey relational analysis. In *Global Telecommunications Conference Workshops, 2004. GlobeCom Workshops 2004. IEEE*, pages 220–224, Nov 2004. doi: 10.1109/GLOCOMW.2004.1417577.

[17] G. Mapp, F. Shaikh, M. Aiash, R.P. Vanni, M. Augusto, and E. Moreira. Exploring efficient imperative handover mechanisms for heterogeneous wireless networks. In *Network-Based Information Systems, 2009. NBIS '09. International Conference on*, pages 286–291, Aug 2009. doi: 10.1109/NBiS.2009.95.

[18] Fatema Sabeen Shaikh. *Intelligent proactive handover and QoS management using TBVH in heterogeneous networks*. PhD thesis, Middlesex University, 2010.

[19] Osman Khalid, Samee U Khan, Sajjad A Madani, Khizar Hayat, Majid I Khan, Nasro Min-Allah, Joanna Kolodziej, Lizhe Wang, Sherali Zeadally, and Dan Chen. Comparative study of trust and reputation systems for wireless sensor networks. *Security and Communication Networks*, 6(6):669–688, 2013.

[20] Haris Pervaiz, Leila Musavian, and Qiang Ni. Joint user association and energy-efficient resource allocation with minimum-rate constraints in two-tier hetnets. In *Proc. IEEE PIMRC 2013*, pages 1634–1639, London, UK, Sept. 2013.

[21] Charilaos C Zarakovitis and Qiang Ni. A performance comparative study on the implementation methods for ofdma cross-layer optimization. *Future Generation Computer Systems*, 28(6):923–929, 2012.

[22] Kun Yang, S. Ou, K. Guild, and Hsiao-Hwa Chen. Convergence of ethernet pon and ieee 802.16 broadband access networks and its qos-aware dynamic bandwidth allocation scheme. *Selected Areas in Communications, IEEE Journal on*, 27(2): 101–116, February 2009. ISSN 0733-8716. doi: 10.1109/JSAC.2009.090202.

[23] Guopeng Zhang, Kun Yang, Peng Liu, Enjie Ding, and Yali Zhong. Joint channel bandwidth and power allocation game for selfish cooperative relaying networks. *Vehicular Technology, IEEE Transactions on*, 61(9):4142–4156, Nov 2012. ISSN 0018-9545. doi: 10.1109/TVT.2012.2211389.

[24] Thomas L Saaty. How to make a decision: the analytic hierarchy process. *European journal of operational research*, 48(1):9–26, 1990.

[25] Tansir Ahmed, Kyandoghere Kyamakya, Markus Ludwig, KR Anne, J Schroeder, S Galler, K Kyamakya, K Jobmann, Stefan Rass, Johann Eder, et al. A context-aware vertical handover decision algorithm for multimode mobile terminals and its performance. Proceedings of the IEEE/ACM Euro American Conference on Telematics and Information Systems (EATIS 2006), pp. 19-28, ISBN. 958-8166-36-5, February 7-10, 2006, Santa Marta, Colombia., 2006.

[26] Thomas L Saaty. Consistency. Technical report, Turku Polytechnic, School of Telecommunications and e-Business, Finland. Available online at http://www.brahmatwinn.unijena.de

[27] Haris Pervaiz and John Bigham. Game theoretical formulation of network selection in competing wireless networks: an analytic hierarchy process model. In *Next Generation Mobile Applications, Services and Technologies, 2009. NGMAST'09. Third International Conference on*, pages 292–297. IEEE, 2009.

[28] Peng Jiang, J. Bigham, and Jiayi Wu. Cooperative geographic load balancing in hybrid cellular networks. In *Signal Processing, Communications and Networking, 2008. ICSCN '08. International Conference on*, pages 288–294, Jan 2008. doi: 10.1109/ICSCN.2008.4447206.

[29] Takafumi Kanazawa, Toshimitsu Ushio, and Tatsushi Yamasaki. Replicator dynamics of evolutionary hypergames. *Systems, Man and Cybernetics, Part A: Systems and Humans, IEEE Transactions on*, 37(1):132–138, 2007.

[30] C. Mohanram and S. Bhashyam. Joint subcarrier and power allocation in channel-aware queue-aware scheduling for multiuser OFDM. *IEEE Trans. Wireless Comm.*, 6(9):3208–3213, Sept 2007.

[31] A. M. El-Hajj, E. Yaacoub, and Z. Dawy. On uplink OFDMA resource allocation with ergodic sum-rate maximization. In *Proc. IEEE PIMRC 2009*, pages 276–280, Tokyo, Japan, Sept. 2009.

[32] Y. Han K. Kim and S-L Kim. Joint subcarrier and power allocation in uplink OFDMA systems. *IEEE Comm. Letters*, pages 526–528, June 2005.

[33] C. Ng and C. Sung. Low complexity subcarrier and power allocation for utility maximization in uplink OFDMA systems. *IEEE Trans. Wireless Comm.*, 7(5): 1667–1675, June 2008.

[34] A. M. El-Hajj, Z. Dawy, and W.Saad. A stable matching game for joint uplink/-downlink resource allocation in OFDMA wireless networks. In *Proc. IEEE ICC 2012*, pages 6876–6881, Ottawa, Canada, June. 2012.

[35] G. W. Miao, N. Himayat, G. Y. Li, and D. Bormann. Energy-efficient design in wireless OFDMA. In *Proc. IEEE ICC 2008*, pages 3307–3312, Beijing, China, May. 2008.

[36] G. W. Miao, N. Himayat, and G. Y. Li. Energy-efficient transmission in frequency-selective channels. In *Proc. IEEE GLOBECOM 2008*, pages 1–5, New Orleans, LA, USA, Nov. 2008.

[37] A. Akbari, R.Hoshyar, and R.Tafazolli. Energy-efficient resource allocation in wireless OFDMA systems. In *Proc. IEEE PIMRC 2010*, pages 1731–1735, Istanbul, Turkey, Sept. 2010.

[38] S. Khakurel, L. Musavian, and T. Le-Ngoc. Trade-off between spectral and energy efficiencies in a fading communication link. In *Proc. IEEE Vehicu. Tech. Conf. (VTC-Spring),To appear*, Dresden, Germany, Jun. 2013.

[39] D. Fooladivanda, A. Al Daoud, and C. Rosenberg. Joint channel allocation and user association for heterogeneous wireless cellular networks. In *Proc. IEEE PIMRC 2011*, pages 384–390, Toronto,Canada, Sept. 2011.

[40] Dan Wu, Jinlong Wang, R.Q. Hu, Yueming Cai, and Liang Zhou. Energy-efficient resource sharing for mobile device-to-device multimedia communications. *IEEE Transactions on Vehicular Technology*, 63(5):2093–2103, Jun 2014. ISSN 0018-9545. doi: 10.1109/TVT.2014.2311580.

[41] Qiaoyang Ye, Beiyu Rong, Yudong Chen, M. Al-Shalash, C. Caramanis, and J.G. Andrews. User association for load balancing in heterogeneous cellular networks. *IEEE Trans. on Wireless Commu.*, 12(6):2706–2716, June 2013. ISSN 1536-1276. doi: 10.1109/TWC.2013.040413.120676.

[42] D. Fooladivanda and C. Rosenberg. Joint resource allocation and user association for heterogeneous wireless cellular networks. *IEEE Trans. Wireless Comm.*, 2012.

[43] Chia-Hao Yu, Klaus Doppler, Cassio B Ribeiro, and Olav Tirkkonen. Resource sharing optimization for device-to-device communication underlaying cellular networks. *IEEE Transactions on Wireless Communications*, 10(8):2752–2763, 2011.

[44] Klaus Doppler, Chia-Hao Yu, Cassio B Ribeiro, and Pekka Janis. Mode selection for device-to-device communication underlaying an lte-advanced network. In *IEEE Wireless Communications and Networking Conference (WCNC)*, pages 1–6, 2010.

[45] Shahid Mumtaz, Kazi Mohammed Saidul Huq, Ayman Radwan, Jonathan Rodriguez, and Rui L Aguiar. Energy efficient interference-aware resource allocation in lte-d2d communication. In *IEEE International Conference on Communications (ICC)*, pages 282–287, 2014.

[46] M.N. Tehrani, M. Uysal, and H. Yanikomeroglu. Device-to-device communication in 5G cellular networks: challenges, solutions, and future directions. *IEEE Communications Magazine*, 52(5):86–92, May 2014. ISSN 0163-6804. doi: 10.1109/MCOM.2014.6815897.

[47] Guanding Yu, Lukai Xu, Daquan Feng, Rui Yin, G.Y. Li, and Yuhuan Jiang. Joint mode selection and resource allocation for device-to-device communications. *IEEE Transactions on Communications*, 62(11):3814–3824, Nov 2014. ISSN 0090-6778. doi: 10.1109/TCOMM.2014.2363092.

[48] Monowar Hasan and Ekram Hossain. Distributed resource allocation in d2d-enabled multi-tier cellular networks: An auction approach. In *IEEE International Conference on Communications (ICC)*, June 2015.

[49] F. Vzquez-Gallego, J. Alonso-Zarate, L. Alonso, and M. Dohler. Analysis of energy efficient distributed neighbour discovery mechanisms for machine-to-machine networks. *Ad Hoc Networks*, 18(0):40 – 54, 2014. ISSN 1570-8705. doi: http://dx.doi.org/10.1016/j.adhoc.2013.03.006. URL http://www.sciencedirect.com/science/article/pii/S1570870513000383.

[50] Mojdeh Amani, Toktam Mahmoodi, Mallikarjun Tatipamula, and Hamid Aghvami. SDN-based data offloading for 5G mobile networks. *ZTE Communications*, 2:009, 2014.

[51] H. ElSawy, E. Hossain, and M.-S. Alouini. Analytical modeling of mode selection and power control for underlay D2D communication in cellular networks. *IEEE Transactions on Communications*, 62(11):4147–4161, Nov 2014. ISSN 0090-6778. doi: 10.1109/TCOMM.2014.2363849.

[52] Stephen Boyd and Lieven Vandenberghe. Convex optimization. *Cambridge University Press, Cambridge, UK*, 2004.

[53] H. Tabassum, M.Z. Shakir, and M. Alouini. Area green efficiency (age) of two tier heterogeneous cellular networks. In *IEEE Globecom Workshops (GC Wkshps)*, pages 529–534, Dec 2012. doi: 10.1109/GLOCOMW.2012.6477629.

[54] R. Hernandez-Aquino, D. McLernon, M. Ghogho, and S.A.R. Zaidi. Energy efficiency in MIMO large scale two-tier networks with beamforming and adaptive modulation. In *Proc. 21st European Signal Processing Conference (EUSIPCO)*, pages 1–5, Sept 2013.

[55] Chunlong He, G.Y. Li, Fu-Chun Zheng, and Xiaohu You. Energy-efficient resource allocation in OFDM systems with distributed antennas. *IEEE Trans. on Veh. Technol.*, 63(3):1223–1231, March 2014. ISSN 0018-9545. doi: 10.1109/TVT.2013.2282373.

[56] Zhanyang Ren, Shanzhi Chen, Bo Hu, and Weiguo Ma. Energy-efficient resource allocation in downlink ofdm wireless systems with proportional rate constraints. *IEEE Trans. on Veh. Technol.*, 63(5):2139–2150, Jun 2014. ISSN 0018-9545. doi: 10.1109/TVT.2014.2311235.

[57] Z. Song, Q. Ni, K. Navaie, S. Hou, and S. Wu. Energy and spectral efficiency tradeoff with α-fairness in downlink OFDMA systems. *IEEE Commun. Lett.*, 19(7): 1265–1268, July 2015. ISSN 1089-7798. doi: 10.1109/LCOMM.2015.2427275.

[58] C.C. Zarakovitis and Q. Ni. Maximising energy efficiency in multiuser multicarrier broadband wireless systems: Convex relaxation and global optimisation techniques. *IEEE Trans. on Vehicu. Tech.*, July 2015,DOI: 10.1109/TVT.2015.2455536.

[59] Y.A. Sambo, M.Z. Shakir, K.A. Qaraqe, E. Serpedin, M.A. Imran, and B. Ahmed. Energy efficiency improvements in HetNets by exploiting device-to-device communications. In *Proc. 22nd European Signal Processing Conference (EUSIPCO)*, pages 151–155, Sept 2014.

[60] K.M.S. Huq, S. Mumtaz, J. Bachmatiuk, J. Rodriguez, X. Wang, and R.L. Aguiar. Green HetNet CoMP: Energy efficiency analysis and optimization. *IEEE Trans. on Veh. Technol.*, PP(99):1–1, Nov. 2014. ISSN 0018-9545. doi: 10.1109/TVT.2014.2371331.

[61] P. Monti, S. Tombaz, L. Wosinska, and J. Zander. Mobile backhaul in heterogeneous network deployments: Technology options and power consumption. In *Proc. 14th Int. Conf. on Transparent Optical Networks (ICTON)*, pages 1–7, July 2012. doi: 10.1109/ICTON.2012.6253839.

[62] S. Tombaz, P. Monti, Kun Wang, A. Vastberg, M. Forzati, and J. Zander. Impact of backhauling power consumption on the deployment of heterogeneous mobile networks. In *Proc. IEEE Global Telecommunications Conference (GLOBECOM 2011)*, pages 1–5, Dec 2011. doi: 10.1109/GLOCOM.2011.6133999.

[63] R Timothy Marler and Jasbir S Arora. Survey of multi-objective optimization methods for engineering. *Structural and multidisciplinary optimization*, 26(6): 369–395, 2004.

[64] Daniel Pérez Palomar and Mung Chiang. A tutorial on decomposition methods for network utility maximization. *IEEE J. on Sel. Areas in Commun.*, 24(8):1439–1451, 2006.

[65] Wei Yu and R. Lui. Dual methods for nonconvex spectrum optimization of multicarrier systems. *Communications, IEEE Transactions on*, 54(7):1310–1322, July 2006. ISSN 0090-6778. doi: 10.1109/TCOMM.2006.877962.

[66] Yanjie Dong, Min Sheng, Shun Zhang, and Chungang Yang. Coalition based interference mitigation in femtocell networks with multi-resource allocation. In

Proc. IEEE ICC 2014, pages 2695–2700, Sydney, Australia, June 2014. doi: 10.1109/ICC.2014.6883731.

[67] C.C. Zarakovitis and Q. Ni. Maximising energy efficiency in multiuser multicarrier broadband wireless systems: Convex relaxation and global optimisation techniques. *IEEE Trans. on Vehicu. Tech.*, 2015, DOI: 10.1109/TVT.2015.2455536.

[68] Xiaohu Ge, Bin Yang, Junliang Ye, Guoqiang Mao, Cheng-Xiang Wang, and Tao Han. Spatial spectrum and energy efficiency of random cellular networks. *IEEE Trans. on Commun.*, 63(3):1019–1030, 2015.

[69] Guowang Miao, Nageen Himayat, Geoffrey Ye Li, and Shilpa Talwar. Low-complexity energy-efficient scheduling for uplink OFDMA. *Communications, IEEE Transactions on*, 60(1):112–120, 2012.

[70] F. Haider, Cheng-Xiang Wang, H. Haas, E. Hepsaydir, and Xiaohu Ge. Energy-efficient subcarrier-and-bit allocation in multi-user ofdma systems. In *Proc. IEEE VTC 2012 Spring*, pages 1–5, Yokohama, Japan, May 2012. doi: 10.1109/VETECS.2012.6240331.

[71] L. Musavian and Q. Ni. Effective capacity maximization with statistical delay and effective energy efficiency requirements. *IEEE Trans. on Wireless Commun.*, 14 (7):3824–3835, July 2015. ISSN 1536-1276. doi: 10.1109/TWC.2015.2412542.

[72] C.C. Zarakovitis and Qiang Ni. Energy efficient designs for communication systems: Resolutions on inverse resource allocation principles. *IEEE Commun. Lett.*, 17(12):2264–2267, December 2013. ISSN 1089-7798. doi: 10.1109/LCOMM.2013.101813.131660.

[73] Suman Khakurel, Leila Musavian, and Tho Le-Ngoc. Trade-off between spectral and energy efficiencies in a fading communication link. In *Proc. IEEE VTC 2013 Spring*, pages 1–5, Dresden, Germany, May 2013.

[74] Lei Deng, Yun Rui, Peng Cheng, Jun Zhang, QT Zhang, and Mingqi Li. A unified energy efficiency and spectral efficiency tradeoff metric in wireless networks. *Communications Letters, IEEE*, 17(1):55–58, 2013.

[75] Jie Tang, Daniel KC So, Emad Alsusa, Khairi Hamdi, et al. Resource efficiency: A new paradigm on energy efficiency and spectral efficiency tradeoff. *IEEE Trans. on Wireless Commun.*, 13(8):4656–4669, 2014.

[76] Cong Xiong, Geoffrey Ye Li, Shunqing Zhang, Yan Chen, and Shugong Xu. Energy-and spectral-efficiency tradeoff in downlink OFDMA networks. *IEEE Trans. on Wireless Commun.*, 10(11):3874–3886, 2011.

[77] L. Xu, G. Yu, and Y. Jiang. Energy-efficient resource allocation in single-cell ofdma systems: Multi-objective approach. *IEEE Trans. on Wireless Commun.*, PP (99):1–1, 2015. ISSN 1536-1276. doi: 10.1109/TWC.2015.2443104.

[78] X Ge, T Han, Yan Zhang, G Mao, C Wang, and J Zhang. Spectrum and energy efficiency evaluation of two-tier femtocell networks with partially open channels. *IEEE Trans. on Veh. Technol.*, 63(3), 2014.

[79] Giacomo Bacci, Elena-Veronica Belmega, Panayotis Mertikopoulos, and Luca Sanguinetti. Energy-aware competitive power allocation in heterogeneous networks with QoS constraints. *IEEE Trans. on Wireless Commun.*, PP(99), Apr. 2015. doi: 10.1109/TWC.2015.2425397.

[80] G. Yu, Y. Jiang, L. Xu, and G.Y. Li. Multi-objective energy-efficient resource allocation for multi-RAT heterogeneous networks. *IEEE J. on Sel. Areas in Commun.*, PP(99):1–1, 2015. ISSN 0733-8716. doi: 10.1109/JSAC.2015.2435374.

[81] Gubong Lim, Cong Xiong, Leonard J Cimini, and Geoffrey Ye Li. Energy-efficient resource allocation for OFDMA-based multi-RAT networks. *IEEE Trans. on Wireless Commun.*, 13(5):2696–2705, 2014.

[82] J. Tang, D.K.C. So, E. Alsusa, K.A. Hamdi, and A. Shojaeifard. Resource allocation for energy efficiency optimization in heterogeneous networks. *IEEE J. on Sel. Areas in Commun.*, 33(10), Oct. 2015.

[83] Haijun Zhang, Chunxiao Jiang, N.C. Beaulieu, Xiaoli Chu, Xianbin Wang, and T.Q.S. Quek. Resource allocation for cognitive small cell networks: A cooperative bargaining game theoretic approach. *IEEE Trans. on Wireless Commun.*, 14(6): 3481–3493, June 2015. ISSN 1536-1276. doi: 10.1109/TWC.2015.2407355.

[84] Olga Galinina, Sergey Andreev, Andrey Turlikov, and Yevgeni Koucheryavy. Optimizing energy efficiency of a multi-radio mobile device in heterogeneous beyond-4G networks. *Elsevier Journal of Performance Evaluation*, 78:18–41, Aug. 2014. ISSN 0166-5316. doi: http://dx.doi.org/10.1016/j.peva.2014.06.002. URL http://www.sciencedirect.com/science/article/pii/S016653161400056X.

[85] M. Ismail, A.T. Gamage, Weihua Zhuang, and X.S. Shen. Energy efficient uplink resource allocation in a heterogeneous wireless medium. In *Proc. IEEE ICC 2014*, pages 5275–5280, Sydney, Australia, June 2014. doi: 10.1109/ICC.2014.6884159.

[86] Li Ping Qian, Cheng Qian, Yuan Wu, and Qingzhang Chen. Power controlled system revenue maximization in large-scale heterogeneous cellular networks. In *Proc. IEEE ICC 2014*, pages 5269–5274, Sydney, Australia, June 2014.

[87] S. Samarakoon, M. Bennis, W. Saad, and M. Latva-aho. Opportunistic sleep mode strategies in wireless small cell networks. In *Proc. IEEE ICC 2014*, pages 2707–2712, Sydney, Australia, June 2014. doi: 10.1109/ICC.2014.6883733.

[88] Francesco Pantisano, Mehdi Bennis, Walid Saad, and Mérouane Debbah. Spectrum leasing as an incentive towards uplink macrocell and femtocell cooperation. *IEEE J. on Sel. Areas in Commun.*, 30(3):617–630, 2012.

[89] M.Z. Shakir, K.A. Qaraqe, H. Tabassum, M.-s. Alouini, E. Serpedin, and M.A. Imran. Green heterogeneous small-cell networks: toward reducing the CO2 emissions of mobile communications industry using uplink power adaptation. *IEEE Commun. Mag.*, 51(6):52–61, June 2013. ISSN 0163-6804. doi: 10.1109/MCOM.2013.6525595.

[90] Amr Abdelnasser, Ekram Hossain, and Dong In Kim. Tier-aware resource allocation in ofdma macrocell-small cell networks. *IEEE Trans. on Commun.*, 63(3): 695–710, Mar. 2015.

[91] Kyuho Son, Soohwan Lee, Yung Yi, and Song Chong. REFIM: A practical interference management in heterogeneous wireless access networks. *IEEE J. on Sel. Areas in Commun.*, 29(6):1260–1272, June 2011. ISSN 0733-8716. doi: 10.1109/JSAC.2011.110613.

[92] Michael Emmerich and André Deutz. Multicriteria optimization and decision making. *LIACS. Leiden university, NL*, 2006.

[93] D.W.K. Ng, E.S. Lo, and R. Schober. Energy-efficient resource allocation in OFDMA systems with large numbers of base station antennas. *IEEE Trans. on Wireless Commun.*, 11(9):3292–3304, September 2012. ISSN 1536-1276. doi: 10.1109/TWC.2012.072512.111850.

[94] Werner Dinkelbach. On nonlinear fractional programming. *Management Science*, 13(7):pp. 492–498, 1967. ISSN 00251909. URL http://www.jstor.org/stable/2627691.

[95] Wei Yu and Raymond Lui. Dual methods for nonconvex spectrum optimization of multicarrier systems. *IEEE Trans. on Commun.*, 54(7):1310–1322, 2006.

[96] Kibeom Seong, Mehdi Mohseni, and John M Cioffi. Optimal resource allocation for OFDMA downlink systems. In *Proc. IEEE Int. Symp. of Information Theory 2006*, pages 1394–1398, Seattle, WA, USA, July 2006.

[97] Ekram Hossain, Long Bao Le, and Dusit Niyato. *Radio resource management in multi-tier cellular wireless networks*. John Wiley & Sons, 2013.

[98] Yaniv Azar, George N Wong, Kangping Wang, Rimma Mayzus, Jocelyn K Schulz, Hang Zhao, Felix Gutierrez, DuckDong Hwang, and Theodore S Rappaport. 28 ghz propagation measurements for outdoor cellular communications using steerable beam antennas in new york city. In *Communications (ICC), 2013 IEEE International Conference on*, pages 5143–5147. IEEE, 2013.

[99] T. S. Rappaport, E. Ben-Dor, J. N. Murdock, and Y. Qiao. 38 ghz and 60 ghz angle-dependent propagation for cellular amp; peer-to-peer wireless communications. In *Communications (ICC), 2012 IEEE International Conference on*, pages 4568–4573, June 2012. doi: 10.1109/ICC.2012.6363891.

[100] Theodore S Rappaport, Robert W Heath Jr, Robert C Daniels, and James N Murdock. *Millimeter wave wireless communications*. Pearson Education, 2014.

[101] Theodore S Rappaport, Shu Sun, Rimma Mayzus, Hang Zhao, Yaniv Azar, Kangping Wang, George N Wong, Jocelyn K Schulz, Mathew Samimi, and Felix Gutierrez. Millimeter wave mobile communications for 5g cellular: It will work! *IEEE Access*, 1:335–349, 2013.